Catalysis with Cobalt Porphyrins: Solution and Mechanochemistry

by

Heinrich Laker

Thesis presented in partial fulfilment of the requirements for the degree of Master of Science

at

Stellenbosch University

Supervisor: Prof. Delia A. Haynes
Faculty of Science
Department of Chemistry and Polymer Science

March 2021

Declaration

By submitting this thesis/dissertation electronically, I declare that the entirety of the work contained therein is my own, original work, that I am the sole author thereof (save to the extent explicitly otherwise stated), that reproduction and publication thereof by Stellenbosch University will not infringe any third party rights and that I have not previously in its entirety or in part submitted it for obtaining any qualification.

March 2021

Abstract

In this study, cobalt metalloporphyrins (Co-porphyrins) were investigated for their potential to catalyze the oxidation of benzyl alcohol in solution, and also by mechanochemistry as a non-classical solid-state method.

A newly-discovered coordination polymer (CP) from our group, comprised of cobalt(II) *meso*-tetraphenylporphyrin (CoTPP) and 4-(4'-pyridyl)-1,2,3,5-dithiadiazolyl (pyrDTDA) as a bridging ligand, was previously shown to catalyze the oxidation of benzyl alcohol. The aim of this study was to compare the performance of CoTPP derivatives bearing different axial ligands to the CP in order to assess what effect the DTDA ligand has on the catalytic reaction. However, obtaining good yields of the CP was challenging. Perplexed by this, we investigated the synthesis and structure of the pyrDTDA radical, confirming the existence of both neutral and charged pyrDTDA radicals that form during the synthetic procedure. The two different pyrDTDA radicals were separated and purified, and their nature was confirmed using various analytical techniques. After using the two pyrDTDA radicals in separate synthetic procedures of the CP, surprisingly no significant difference in yields was observed.

Three additional CoTPP derivatives were used in the oxidation of benzyl alcohol to compare to the CP: CoTPP with no axial ligand, 3,5-lutidine as axial ligand (CoTPP-Lut), and chloride as axial ligand (CoTPP-Cl). The catalysts showed moderate activity in the presence of *tert*-butyl hydroperoxide (TBHP), all achieving above 70% conversion. A steady increase in conversion of benzyl alcohol was observed as the catalyst concentration increased, except for the CP where the opposite was observed. A possible explanation is the tendency of porphyrins to aggregate in solution at certain concentrations. As the conversion of benzyl alcohol increased, more over-oxidation to benzoic acid was observed. Overall, the CP and CoTPP-Cl, in which the cobalt metal center is in +3 oxidation state, achieved the highest conversions of 84% and 86% respectively. The axial ligands in CP and CoTPP-Cl are potentially prolonging the lifetime of these catalysts during the reaction.

These catalysts were also used to oxidize benzyl alcohol mechanochemically, using urea-hydrogen peroxide (UHP) as a safer oxidant. In comparison to the absence of catalyst, the Co-porphyrin catalysts did not increase the conversion, however over-oxidation of the benzaldehyde to benzoic acid was observed. Interestingly, for CoTPP, benzoic acid was observed at 1.0 mol% and 1.5 mol%, whereas benzoic acid was only observed for CoTPP-Cl at

1.5 mol%. This seemed different from solution, where CoTPP-Cl was the more active catalyst. The nature of mechanochemical reactions could allow a greater probability for peroxide to bind CoTPP due to more accessible sites, which could explain the higher activity of CoTPP than CoTPP-Cl by mechanochemistry.

Overall, this study provided insight into the catalytic potential of metalloporphyrins. Catalysis by these compounds under mechanochemical conditions shows some promise, and this remains open for exploration.

Uittreksel

In hierdie studie is kobalt metaalporfyriene (Co-porfyriene) ondersoek vir hul potensiaal om die oksidasie van bensielalkohol te kataliseer in oplossing, en ook deur meganochemie as 'n nie-klassieke vastestof-toestand metode.

‘n Koördinasie polimeer (KP) wat in ons groep geïdentifiseer is, wat bestaan uit kobalt (II) *meso*-tetrafenielporfyrien (CoTPP) en 4-(4'-piridyl)-1,2,3,5-ditiadiazolyl (pyrDTDA) as ‘n oorbruggende ligand, het reeds voorheen getoon dat dit die oksidasie van bensielalkohol kan kataliseer. Die doel van die huidige studie was om die katalitiese aktiwiteit van soortgelyke CoTPP verbindings, wat verskillende aksiale ligande bevat, te vergelyk met dié van CP om die effek van die DTDA ligand te bepaal. Dit was egter uitdagend om goeie obrengste van die CP te bereik. Verbysterd hieroor het ons besluit om die sintese en struktuur van die pyrDTDA radikale te ondersoek, en is die vorming van beide neutrale en gelaaide pyrDTDA radikale bevestig. Die twee verskillende pyrDTDA radikale is geskei en gesuiwer, en die aard van hul strukture is bevestig met behulp van verskeie analitiese tegnieke. Na afloop van die gebruik van die twee pyrDTDA radikale in afsonderlike sinteses van die CP, is daar verbasend genoeg geen noemenswaardige verskil in opbrengste waargeneem nie.

Drie addisionele CoTPP verbindings is gebruik in die oksidasie van bensielalkohol om met die katalitiese aktiwiteit van die CP te vergelyk: CoTPP met geen aksiale ligand, 3,5-lutidien as aksiale ligand (CoTPP-Lut), en chloried as aksiale ligand (CoTPP-Cl). Al die katalisators het matige aktiwiteit getoon in die teenwoordigheid van *ters*-butiel hidroperoksied (TBHP) en het ‘n omskakeling van meer as 70 % behaal. ‘n Bestendige toename in die omskakeling van bensielalkohol is waargeneem namate die katalisator konsentrasie toegeneem het, behalwe vir die CP waar die teenoorgestelde waargeneem is. ‘n Moontlike verklaring hiervoor is die geneigdheid van porfyriene om saam te pak in oplossing by sekere konsentrasies. Namate die omskakeling van bensielalkohol toegeneem het, is meer oor-oksidasie na bensoësuur waargeneem. Oor die algemeen het die CP en CoTPP-Cl, waarin die kobalt metaal sentrum in die +3 oksidasietoestand is, die hoogste omskakelings behaal van onderskeidelik 84% en 86%. Dit is moontlik dat die aksiale ligand die lewensduur van die CP en CoTPP-Cl help verleng tydens die katalitiese reaksie.

Hierdie katalisators is ook gebruik om bensielalkohol meganochemies te oksideer met ureum-waterstofperoksied (UHP) as ‘n veiliger oksidant. In vergelyking met die afwesigheid van

katalisator het die Co-porfyrien katalisators nie die omskakeling van bensielalkohol bevorder nie, maar die oor-oksidasie van bensaldehied na bensoësuur is waargeneem. Interessant genoeg is bensoësuur waargneem vir CoTPP in katalisator konsentrasies van 1.0 mol% en 1.5 mol%, terwyl bensoësuur slegs waargeneem is vir CoTPP-Cl by ‘n katalisator konsetrasie van 1.5 mol%. Dit is teëstrydig met die geval in oplossing waar CoTPP-Cl die meer aktiewe katalisator is. Die aard van meganochemiese reaksies kan die hoër aktiwiteit van CoTPP in vergelyking met CoTPP-Cl verklaar deurdat meer toeganklike bindingsplekke die waarskynlikheid vir peroksied om te bind aan CoTPP verhoog.

Saamgevat bied hierdie studie insig oor die katalitiese potensiaal van metaalporfyriene. Katalise deur hierdie verbindings onder meganochemiese toestande is belowend, en dit bly oop vir verkenning.

Acknowledgements

First and foremost, I want to extend my sincere gratitude and appreciation to my supervisor, Prof Delia Haynes. Thank you for giving me the opportunity to explore chemistry under your guidance. Your endless positivity and support carried me through. Please do not stop spreading that around, it works!

Secondly, to Emile Maggot and Dr Leigh Loots, huge thank you for your mentorship and scientific support. To Emile for constantly dealing with my catalysis issues all the way through and always keen to help, you are an incredible human being and researcher and I cannot wait for you to get the Dr – good luck for the last bit. To Leigh, for dealing with all my random questions since Honours, and always having an answer ready, but also all the mechanochemistry issues. You are an amazing colleague, not only to me but to the whole Supramolecular Chemistry group, and we are lucky to have you.

To the Supramolecular Chemistry group, thank you so much for all the support and fun times. In particular to Dewald van Heerden and Alan Eaby for all the fruitful discussions about science and research in general, thank you for always being willing to listen, keen to go for a coffee and for lunch, it was very much appreciated. Huge thank you to Dr Marike du Plessis and Lisa van Wyk for showing me around the instruments and having patience with all my questions. A huge thank you must also go to Dr Jeanie Lombard, Marisa Strydom and Sam Le Roux for support during group meetings and making the lab a fun and productive environment – you will be missed.

I would also like to extend my appreciation to the support staff for their service in and around the labs. A huge thanks also to CAF for a carrying out the MS and CHNS analyses.

Finally, to my family, Jacques, Chrina and Suzanne, thank you for your patience and understanding during the course of this project. Thank you for dealing with my moods and keeping me fed, it did not go unnoticed. Most importantly, thank you for letting me do what I love.

Lastly, I would like to thank Stellenbosch University for the facilities and Sasol and the NRF for funding.

List of Abbreviations

a_N	-	Hyperfine coupling constant
BuLi	-	*n*-Butyllithium
CoTPP	-	Cobalt(II) *meso*-tetraphenylporphyrin
CoTPP-Cl	-	Cobalt(III) *meso*-tetraphenylporphyrin chloride
CoTPP-Lut	-	3,5-dimethylpyridine cobalt (II) *meso*-tetraphenylporphyrin
CP	-	Coordination polymer
CSD	-	Cambridge Structural Database
DCM	-	Dichloromethane
DMF	-	*N*,*N*-dimethylformamide
DTDA	-	Dithiadiazolyl
EPR	-	Electron Paramagnetic Resonance
EtO_2	-	Diethyl ether
G	-	Gauss
HCl	-	Hydrochloric acid
H-DTDA	-	1,2,3,5-dithiadiazolyl
HMDS	-	Hexamethyldisilazane
IR	-	Infrared
IUPAC	-	International Union of Pure and Applied Chemistry
K	-	Kelvin
LAG	-	Liquid-assisted grinding
MeCN	-	Acetonitrile

MS	-	Mass spectrometry
$NaBH_4$	-	Sodium borohydride
NEt_3	-	Triethylamine
NMR	-	Nuclear Magnetic Resonance
Ph-DTDA	-	4-phenyl-1,2,3,5-dithiadiazolyl
PXRD	-	Powder X-ray Diffraction
pyrDTDA	-	4-(4'-pyridyl)-1,2,3,5-dithiadiazolyl
$SbPh_3$	-	Triphenylantimony
SCl_2	-	Sulfur dichloride
SC-XRD	-	Single-crystal X-ray diffraction
SOMO	-	Singly occupied molecular orbital
TBHP	-	*tert*-butyl hydroperoxide
TEMPO	-	2,2,6,6-tetramethylpiperidin-1-yl-oxy
TPP	-	*meso*-Tetraphenylporphyrin
THF	-	Tetrahydrofuran
UV-Vis	-	Ultraviolet-Visible
Zn/Cu	-	Zinc-copper couple
ZrO_2	-	Zirconium oxide

Table of contents

Chapter 1

Introduction

1.1 General introduction

Porphyrins and their metallated analogs are a class of pyrrole-derived macrocyclic compounds that occur naturally, and are all derivatives of the simplest porphyrin – called porphin – that possess the fundamental ring system with 18 π-electrons, as illustrated in Figure 1.1a.[1–5] The central pair of hydrogens are basic in nature, and can be replaced by a variety of metal ions to yield a metalloporphyrin, as shown in Figure 1.1b (or in its simplest form, a metalloporphin).[2-4] The IUPAC ring numbering system is illustrated in Figure 1.1b, which shows the pyrrolic *β*-positions and methine carbon atoms (numbers 5, 10, 15 and 20).[1,3,6] Alternatively, the Fischer notation can also be used, which designates the numbering of the pyrrolic *β*-positions from 1 - 8, and labels the methine carbon atoms as positions α, β, γ and δ.[1,3,4,6] These are also referred to as the *meso* positions.[3,6]

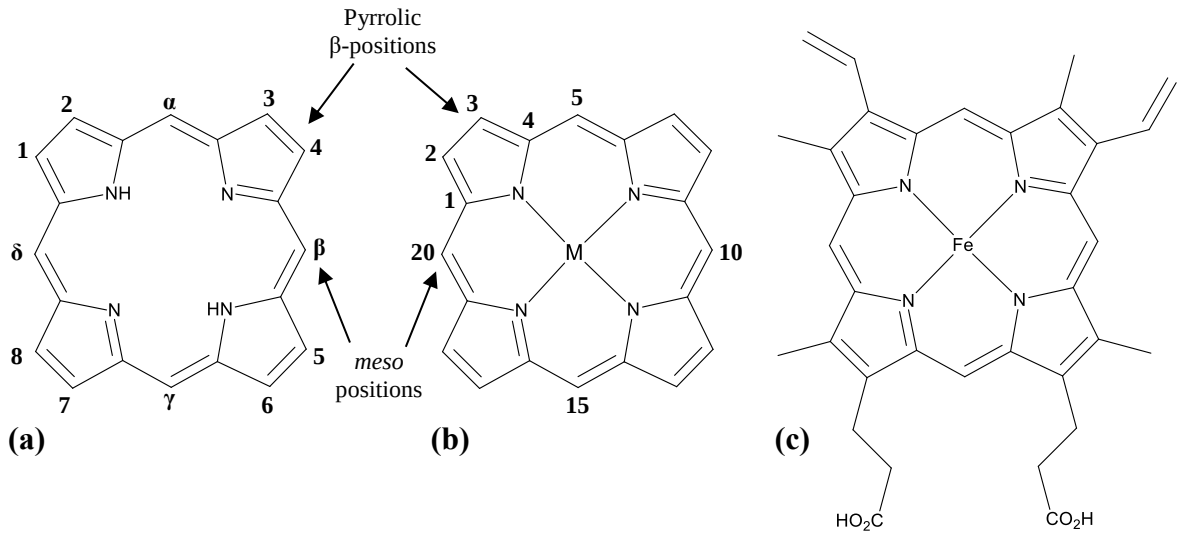

Figure 1.1: (a) The simplest porphyrin, called porphin. (b) Core structure of a metalloporphyrin. M represents a metal ion. (c) Structure of the iron-porphyrin complex of the heme group.

The first synthetic porphyrin – with methyl groups at the α, β, γ and δ positions (Figure 1.1a) called α,β,γ,δ-tetramethylporphyrin – was prepared by Rothemund in 1935.[7] The porphyrin used commonly in biomimetic studies is α,β,γ,δ-tetraphenylporphyrin,[3,5,8] which has phenyl

groups instead of methyl groups at the *meso* positions, also synthesized for the first time by Rothemund and Menotti in 1941.[9]

Metalloporphyrins are of great interest by virtue of their involvement in very complicated, but essential, biological processes, such as the transfer of oxygen, photosynthesis and as catalysts for biological redox reactions.[2,4,10] One such example is an iron-porphyrin complex (Figure 1.1c) that serves as the non-amino acid component for heme, which in turn forms part of a large network of hemoproteins, found in our blood.[1,4,5,8,10]

When research reached a point that it allowed scientists to understand these complex processes, it was realized just how extraordinarily versatile and efficient these systems are. Biomimetic chemists were hard at work, trying to obtain synthetic equivalents that could mimic natural systems, and hopefully utilize these as catalysts in synthetic organic chemistry. The work described in this study investigated the catalytic potential of Co-porphyrins in the oxidation of benzyl alcohol in solution, but also by mechanochemistry.

1.1.1 *meso*-Tetraphenylporphyrins (TPP)

1.1.1.1 Structure and synthesis

The basic porphyrin skeleton consists of the characteristic ring system (Figure 1.1a) with methine-carbon bridges at positions α – δ.[1–4] In the porphin structure, these carbons are substituted with hydrogen atoms. The molecule is called a porphyrin upon the substitution of one or more of these hydrogens.[4] In the context of this study, the compound of interest is *meso*-tetraphenylporphyrin (TPP), in which the hydrogen atoms on the *meso* positions are replaced by phenyl groups.

Even though Rothemund and Menotti were the first to synthesize TPP, their method had drawbacks, including low yields and long reactions times.[8,9] Consequently, Adler and co-workers determined that the yield and rate is quite dependent on certain reaction parameters – like the type of solvent and availability of oxygen – and reported an improved synthetic procedure in 1967 in which pyrrole and benzaldehyde are refluxed in propionic acid, as depicted in Figure 1.2.[11]

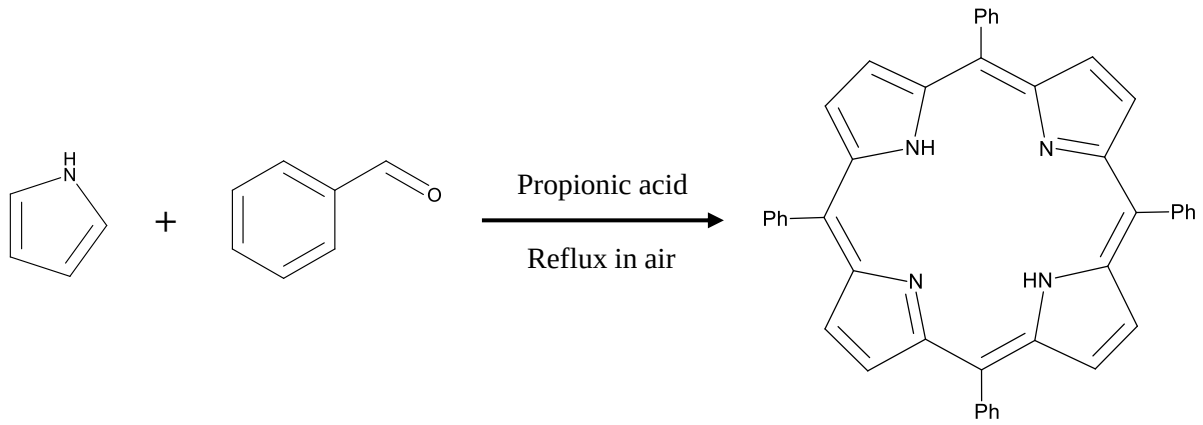

Figure 1.2: Synthetic scheme for the preparation of TPP.[11]

1.1.1.2 Structural modifications

The *meso*-tetraphenylporphyrin scaffold can be modified and categorized into one of three generations of ligands (I, II and III).[12,13] Generation I porphyrin ligands comprise either no or at most one substituent on the phenyl ring in the para position (denoted **X** in Figure 1.3).[12,13] The same synthetic procedure developed by Adler *et al* can be followed to make generation I porphyrins (Section 1.1.1.1),[11] provided that the appropriate aldehyde is used. For instance, to prepare *meso*-tetrakis(4-chlorophenyl)porphyrin that bears a chloro substituent in the *para* position, 4-chlorobenzaldehyde would be used in the synthetic procedure.

When TPP has substituents on at least two positions of the phenyl ring (denoted in Figure 1.3 as **X**, **Y** and **Z** for *para*, *meta* and *ortho* respectively), it is considered as a generation II ligand.[12,13] The synthesis requires a slight modification from the Adler method, owing to the harsh reaction conditions needed for the Adler route (refluxing in propionic acid), which some complex and sensitive aldehydes cannot survive. Developed by Linday *et al*, the procedure entails an acid-catalyzed condensation between pyrrole and the appropriate aldehyde under N_2 at room temperature.[14] This first yields a reduced porphyrin, called a porphyrinogen, which is then oxidized to the porphyrin using quinone as an oxidant.[14] In this way, sensitive synthetic transformations can be achieved under milder reaction conditions, lessening the manipulations that are needed on the porphyrin itself, and making it possible to obtain more complex porphyrin scaffolds that cannot be obtained by the original Adler method.[14]

Lastly, generation III porphyrin ligands bear substituents on both the phenyl rings and pyrrolic *β*-positions (shown in Figure 1.3, denoted as **R**).[12,13] Generally, this involves the incorporation of chlorine, fluorine and bromine atoms in the pyrrolic *β*-positions, and the synthetic procedure entails the perhalogenation of generation I and II porphyrin ligands.[13,15] All the above

porphyrins can be metallated by the method of Adler with the appropriate metal salt,[16] as will be discussed in the next section.

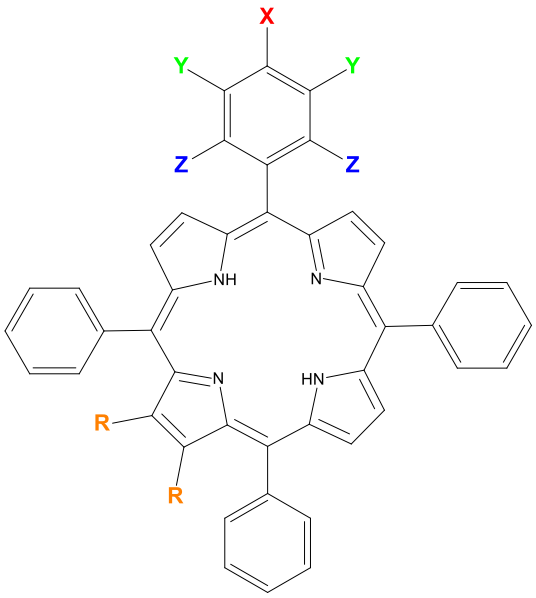

Figure 1.3: Derivatives of *meso*-tetraphenylporphyrin with different substituents on the phenyl ring (X – Z) and pyrrole positions (R). Substituents X – Z are only shown on one ring for simplicity, but apply to the remaining phenyl rings as well.

1.1.2 Metalloporphyrins

1.1.2.1 Structure and synthesis

The inner hydrogen atoms of the porphyrin are quite susceptible to replacement by a single metal cation, in which case the metal atom will be complexed by all four nitrogen atoms, as illustrated in Figure 1.1b.[3,4] In most metalloporphyrins, the metal ion coordinates in the plane of the nitrogen atoms, giving rise to a four-coordinate square planar geometry. However, with the incorporation of additional ligands, five- and six-coordinate structures are also possible, resulting in square pyramidal and distorted octahedral geometries, respectively.[3]

Metallated porphyrins were initially prepared by Rothemund and Menotti as well,[17] but the syntheses were also limited by slow reaction rates, low yields and tedious purification procedures.[16] Once more, Adler and co-workers were able to optimize the procedure to give higher yields and shorter reaction times. Their method involves refluxing the porphyrin with a metal salt in *N*,*N*-dimethylformamide (DMF), as presented in Figure 1.4.[16] As with the synthetic procedure for TPP from Adler, this method is also still widely used today.

In the context of this thesis, we are interested in the cobalt-metallated tetraphenylporphyrin (CoTPP). To make this material, the metal salt cobalt acetate tetrahydrate is refluxed together with TPP in DMF.

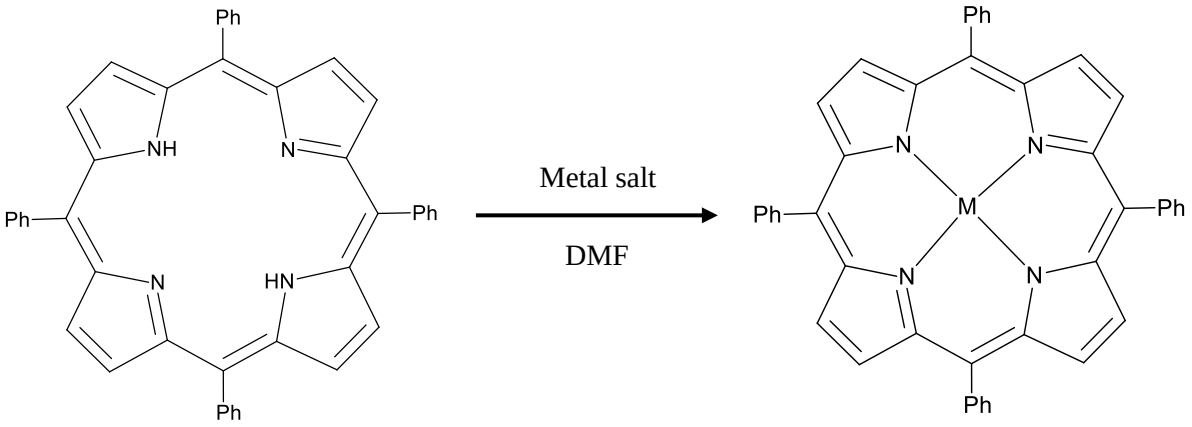

Figure 1.4: Synthetic scheme for the preparation of metalloporphyrins.[16]

1.1.2.2 Ultraviolet-Visible (UV-Vis) spectra

Porphyrins possess a striking purple colour due to the high degree of conjugation in their structures, and they absorb light in the UV-Vis region, which can be very useful in characterizing these compounds.[2,18–20] A spectrum of TPP is presented in Figure 1.5. A very intense band is found at approximately 417 nm, called the Soret band, whilst in the range 500-700 nm there are 4 less intense bands, called the Q bands.[2]

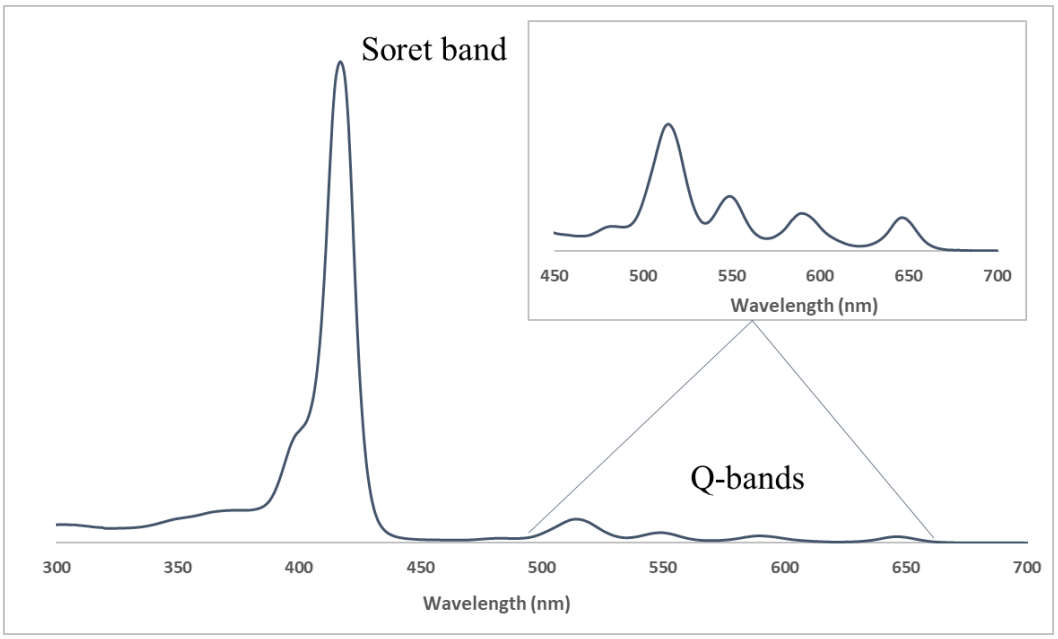

Figure 1.5: UV-Vis spectrum of TPP between 300-700 nm. Spectrum from this work.

Spectroscopic changes occur when a metal is substituted into the porphyrin core due to a change in symmetry, and this is useful in providing evidence of the success of the metalation reaction.[2,18,20,21] Figure 1.6 presents spectra of CoTPP (a) and a comparison with the free base TPP (b). Two very clear changes transpire upon metalation: the Soret band shifts, and the Q-bands collapse, also accompanied by a shift in wavelength.[2] These distinctive absorbance

bands are a result of transitions from different highest occupied molecular orbitals (HOMO) of the porphyrin to the lowest unoccupied molecular orbital (LUMO) of the porphyrin.[22] The HOMOs and LUMOs are altered with changes in metal and substituents on the porphyrin and this results in the bands shifting and changing intensity.[2] In the case of CoTPP, the Soret band shifts to 410 nm from 417 nm (Figure 1.6). Furthermore, the Q-bands undergo a much more significant change, collapsing from 4 bands to 2, accompanied by a shift in wavelength (Figure 1.6). In addition, when a ligand coordinates to the metalloporphyrin, the Soret band and Q-bands could shift in either direction, which is dependent on the nature of the ligand and how strongly it binds to the metal.[18] For instance, when a chloride coordinates to CoTPP to form cobalt(III) tetraphenylporphyrin chloride (CoTPP-Cl), the Soret band shifts to 406 nm and the one Q-band is observed at 543 nm.[23]

In this work, UV-Vis spectroscopy was extensively used to characterize these compounds and confirm the success of the metalation of CoTPP.

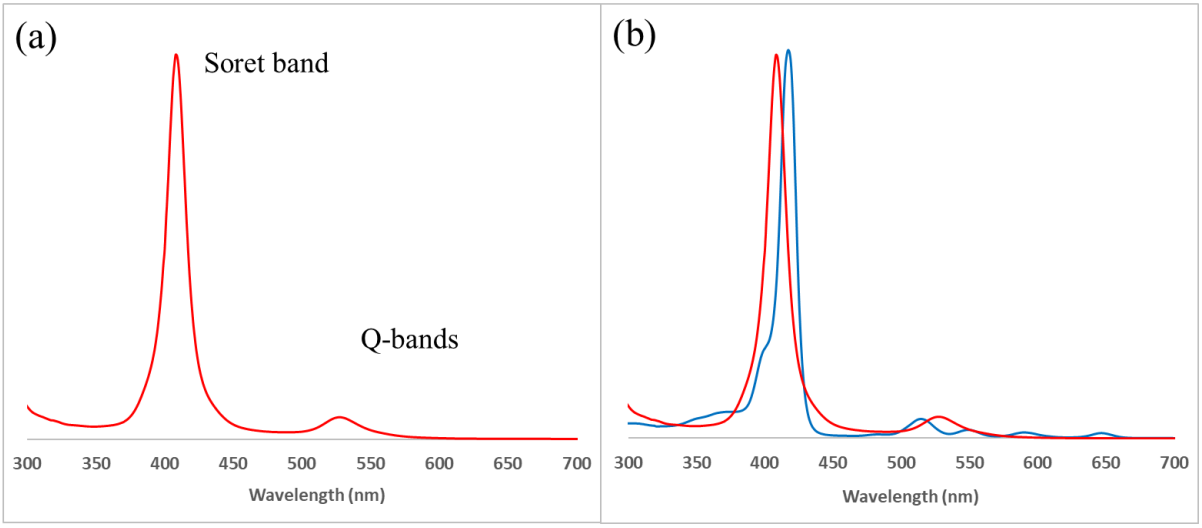

Figure 1.6: (a) UV-Vis spectrum of CoTPP between 300-700 nm. (b) UV-Vis spectra of TPP (blue) and CoTPP (red). Spectra from this work.

1.1.2.3 Coordination chemistry

The interest in the coordination chemistry of metalloporphyrins commenced after the discovery that some proteins consist of a metalloporphyrin core system that is able to bind and activate molecular oxygen, amongst other small molecules.[24] After the incorporation of the metal into the porphyrin scaffold, axial coordination sites above and below the plane of the porphyrin are available for additional ligands to coordinate,[24] as shown in Figure 1.7. The coordination chemistry of metalloporphyrins is well understood, and has been reviewed by Dolphin and co-workers in the context of carbon, nitrogen and oxygen donors.[24]

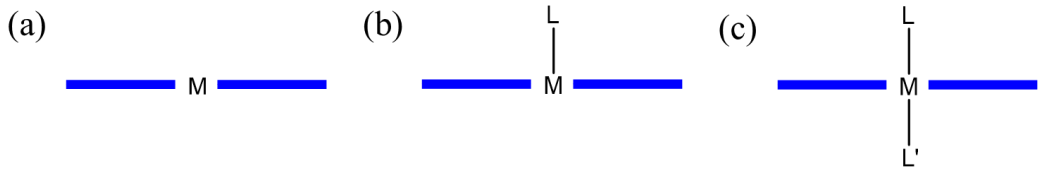

Figure 1.7: Axial ligand binding in metalloporphyrins. (a) Metalloporphyrins with no axial ligands adopt a square planar geometry, while (b) one axial ligand results in a square pyramidal geometry. (c) Axial ligands on both axial sites will result in an octahedral geometry. This image was reproduced from reference 24.

Reports of the coordination of oxygen donors to metalloporphyrins have become quite ubiquitous in the literature, especially molecular oxygen (O_2) and to a lesser extent peroxides (ROOH). This is a result of the desire to unravel how biological systems utilize oxygen in order to develop efficient catalysts for oxidation reactions.[24]

In the context of this thesis, the coordination chemistry of Co-porphyrins is of particular interest. Initially, when a cobalt cation is inserted into the porphyrin scaffold, it generally exists in the +2 oxidation state, but can change to the +3 oxidation state upon the coordination of ligands like molecular oxygen,[25] peroxide[26,27] or halogens,[28,29] forming a monoaxial 5-coordinate complex.[24,25,27,30] In general, however, the change in oxidation state and the metal's ability to bind other ligands, such as O_2, is quite dependent on the nature of the solvent, the structural modifications on the macrocycle, the presence of other ligands such as amines, and also external factors like temperature and inert atmospheres.[30] It is well known that amines can coordinate effectively to Co-porphyrins,[31] and together with the nature of the solvent, this has been shown to have an effect on the reversible binding of molecular oxygen.[32] Stynes and Ibers reported that the affinity of a Co-porphyrin for molecular oxygen increases as the basicity of the axial ligand increases, *i.e.* the Co-porphyrin binds oxygen more readily when 1-methylimidazole is an axial ligand, as opposed to pyridine.[32] Furthermore, the degree of oxygenation is also greater in more polar solvents, *i.e.* more oxygenation is observed in DMF as opposed to toluene.[32] Walker reported using EPR spectroscopy to study coordination of amines to the 5th and 6th positions of a Co-porphyrin.[33] She noticed that the presence of air in the solvent had an effect on which complex formed: in the absence of air, a 5-coordinate Co-porphyrin complex forms with the weaker basic amines, whereas strong basic amines form 6-coordinate complexes. However, in the presence of air, a Co-porphyrin complex with an amine in the 5th position and an oxygen in the 6th position forms, with the ease of formation dependent on the base strength of the amine: weaker basic amines require higher air pressures to form the complex.[33]

Tezuka *et al* reported on how the substituents on the porphyrin macrocycle affect the redox properties of the Co-porphyrin complex, which ultimately affects how it binds and activates

molecular oxygen.[34] Due to the resonance interactions taking place on the porphyrin ring, electron-donating groups (like CH_3) increases the electron density on the central metal atom, promoting the binding and activation of molecular oxygen.[34]

Collectively, the factors discussed above influence the electron density on the central metal atom, and can result in a change in the oxidation state, which in turn has an effect on the catalytic capabilities and properties of the metalloporphyrin.

1.1.2.4 Application as catalysts

There is a high demand for catalysts that can achieve the oxidation of organic compounds under mild reaction conditions. Metalloporphyrins have been used as models for biomimetic studies, especially since the discovery of cytochrome P-450 monooxygenases that are able to oxidize almost any organic substrate, including unreactive alkanes.[8,35] With metalloporphyrins being able to undergo valency changes and ligand exchanges, it makes them suitable to catalyze a variety of redox reactions.[36] Being able to efficiently incorporate oxygen, metalloporphyrins have been extensively involved in autoxidation processes, which have been comprehensively reviewed by Mlodnicka.[36] Meunier also reviewed metalloporphyrins as being '*versatile catalysts for oxidation reactions'*, with an additional section on how metalloporphyrins have been involved in oxidative DNA cleavage.[12]

Again, in the context of this thesis, the interest lies in particular with the catalytic capabilities of Co-porphyrins. Co-porphyrins have been used as catalysts in many oxidation reactions, which include the oxidation of alkanes,[13,37,38] alcohols,[39] alkenes,[40] aldehydes[41,42] and a variety of other organic substrates.[43,44]

A recent study by Pamin *et al* regarding oxidation catalysis by Co-porphyrins is very intriguing.[13] They describe the potential of Co-porphyrins to oxidize three cycloalkanes (Figure 1.8) by comparing the three different ligand generation systems, as discussed in Section 1.1.1.2.

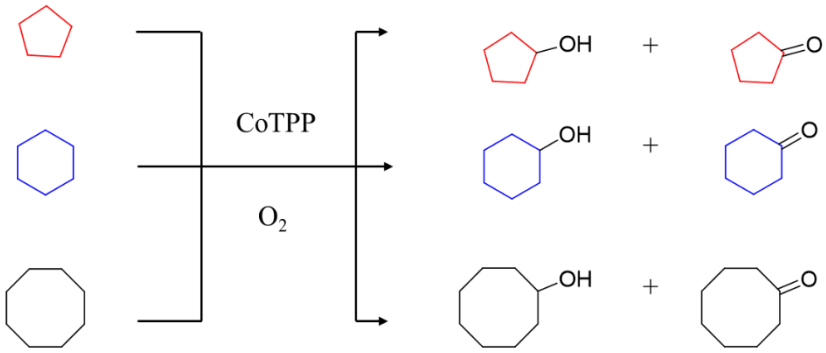

Figure 1.8: Oxidation of cycloalkanes: cyclopentane (red), cyclohexane (blue) and cyclooctane (black) in the presence of CoTPP and molecular oxygen. Figure reproduced from reference 13.

They used nine catalytic systems, three in each generation series (I – III), by varying the substituents on the phenyl ring and pyrrolic *β*-positions to include methyl groups, nitro groups and halogens.[13] These catalysts were then employed in cycloalkane oxidation, which yielded cycloalcohols and cycloketones, as shown in Figure 1.8. They reported that all the catalysts were active in the oxidation of cycloalkanes, and surprisingly, generation II catalysts were more active than the rest, resulting in yields of 68.8% of cyclooctanone as opposed to generation III catalysts with yields of approximately 56% of cyclooctanone.[13] It was shown that the substituents on the phenyl and pyrrolic *β*-positions have a major influence on the products of the catalytic reaction, with both electron-donating and -withdrawing group increasing the yields of oxygenates.[13]

Several other reviews and reports of different metalloporphyrins that catalyze reactions have appeared,[5,45–47] and the abilities of these complexes are renowned. The question is, however, will metalloporphyrins be able to mimic this type of activity in the solid state using mechanochemistry?

1.2 Mechanochemistry

1.2.1 Brief historical outline

Going back in history, when and where the first mechanochemical reactions were carried out still remains conjecture. Mechanochemistry generally refers to a process occurring in the solid state by some kind of mechanical treatment, such as grinding, impacting, shearing, shaking, friction and compression; indeed mechanochemistry actually dates back to prehistoric times when these methods were used to prepare food, medicines, process minerals and to generate fires.[48–51] According to Takacs,[52] the reduction of mercury sulfide (cinnabar) to elementary mercury by grinding in a copper mortar and pestle in the presence of acetic acid is the earliest existing record (~ 315 B.C.) of a mechanochemical reaction.[48,49,52–54] For the next couple of

thousand years, nothing definitive was published about the use of mechanochemistry, which could suggest that mechanochemistry was practiced inadvertently, and therefore was not recorded often.[49] Nevertheless, we do know that grinding and milling were still frequently utilized in human activity, and with the mortar and pestle being a typical laboratory instrument of the early chemist, chemical transformations by grinding were bound to be realized, even if they were unplanned.[48,49,51]

The first comprehensive study regarding the effect of mechanical force on chemical reactions was carried out at the end of the 19th century by Matthew Carey Lea.[48,49,51,55] Not only did he show that mechanical action was capable of causing a chemical change, but his experiments were also the first to discriminate between the effects of heat and mechanical action.[48–51,53,55] The most important findings were from the decomposition studies of mercury chloride and silver chloride: he observed that both these compounds decompose upon grinding in a mortar, however when heated, they sublime and melt, respectively, without decomposing. He realized the significance of these results: the ability to obtain a different chemical outcome in the same system as a result of applying heat versus a mechanical action (thermal versus mechanical energy), which makes him the true founding father of mechanochemistry.[48–51,53,55] After the tremendous efforts of Carey Lea (and others), research into mechanochemistry and solid-state reactions commenced in the first half of the 20th century.[49] For example, the use of polymers became popular around the 1920s, which prompted an investigation into how these macromolecules would behave under mechanical action.[48,49] Smekal made the interesting discovery of mechanical activation, and described it as a process that improves the reactivity of solids as a result of multiple lattice defects after mechanical deformation.[48–50,54,56] A few other areas of research that could also be credited with playing an essential role in the more recent history of mechanochemistry are mechanical alloying,[57] mechanically induced self-sustaining reactions (MSR),[58] mechanochemistry using the atomic force microscope (AFM)[59,60] and organic mechanochemistry.[49,50,53]

Nowadays, mechanochemistry has found application in different scientific disciplines that include not only chemists, but also engineers, physicists, geologists and materials scientists.[49] The potential of mechanochemistry to produce new and useful materials provides good rationale for further research, especially if this could be achieved in a greener and more efficient manner.[49]

1.2.2 Equipment and techniques

Very soon in mechanochemistry research, it was realized that the nature and procedures of mechanochemical reactions differ significantly from their conventional solution-based counterparts. If one is carrying out a mechanochemical reaction, it implies that the chemical transformation was achieved by absorbing mechanical energy,[61] which somehow needs to be incorporated when the reaction commences.[53] Therefore, suitable equipment is required to accomplish this, and so heater-stirrers, flasks and beakers will not suffice.[62]

The input of mechanical energy is usually achieved through grinding, which is the universal term used for the application of some mechanical treatment to solids, and could refer to manual or automated methods.[53] For a very long time, the traditional method employed for manual grinding has been the mortar and pestle (Figure 1.9a).[49,53,62–66] This is by far the simplest and most affordable method to initiate reactions mechanically, however the limitations to this method outweigh its advantages.[62–64] Seeing that this is a manual method, several operators in a laboratory could use it, and apply a force that will differ in strength across the group.[63] As a result, different levels of energy will be supplied to the system that is almost impossible to quantify, and will significantly vary as the reaction time becomes longer, after which it becomes dependent on the stamina of the operator.[49,63,66] Furthermore, controlling and defining reaction conditions – such as humidity and exposure to air – is an enormous challenge, which severely compromises the reproducibility and robustness of the method.[62,64,65] Nevertheless, it can still be utilized in qualitative explorations, but nowadays automated ball mills (Figure 1.9b and c) are dominating research in mechanochemistry.[49,53,54,57,62–67]

Figure 1.9b and c are an illustration of the most common type of ball mill, better known as shaker or mixer mills[49,57] which are routinely used as benchtop instruments in a laboratory with reaction scales ranging from milligrams to grams.[57,62–67] Another common instrument includes the planetary ball mill, which allow scales ranging from grams to kilograms.[57,65,67] The vials are mounted onto a spinning disk, called the ‘sun wheel’, and spins in an opposite direction to the sun wheel, creating shear forces.[57,66] While the shaker and planetary mills are limited to batch reactions, mechanochemistry as a continuous process can be achieved via twin screw extrusion.[65,67,68] The procedure entails transferring the solid reactants through a barrel while counter-rotating screws apply compression and shear forces, possibly obtaining kilograms of material by the hour.[65,67,68] Planetary ball mills and twin screw extrusion will not be discussed further, but the shaker mills will be elaborated on, since these were used during the course of this study.

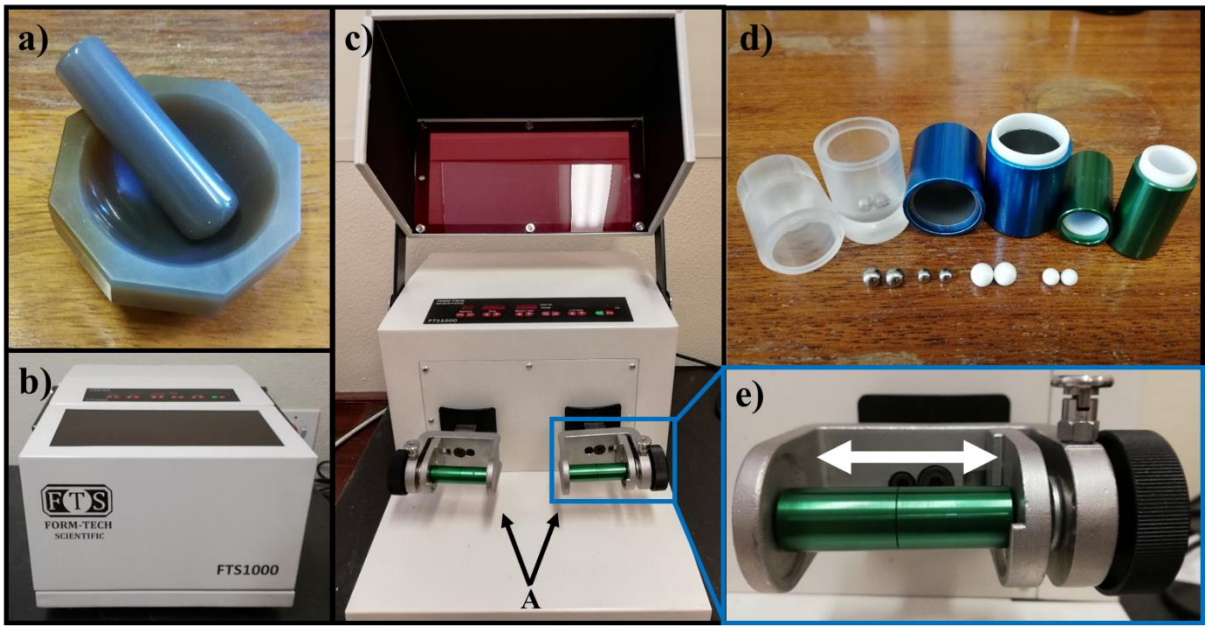

Figure 1.9: Typical equipment in a mechanochemistry laboratory. a) Mortar and pestle, b) and c) FTS 1000 shaker mill (lid on and off), d) grinding jars and grinding balls and e) close-up of a clamped jar.

The operational procedure of the shaker mill entails loading the sample and grinding balls into a vial, fixing it onto a clamp (denoted A in Figure 1.9c and a close-up in Figure 1.9e) and then shaking it back-and-forth several thousand times per minute. [57,66,67] The milling and mixing of the sample is happening continuously with every shake as the balls apply an impact force against the end of the vial and the sample itself.[57,66]

As with any reaction, understanding the different reaction parameters or variables is crucial in achieving optimum reactivity, and some are more controllable than others.[57,66] In short, these can be divided into technological, process and chemical parameters.[63,69] As alluded to above, the choice of what type of ball mill to use falls under the technological category, but the material you are milling in, as well as the material, number and size of the milling balls can also be varied (Figure 1.9d).[57,62,63,69] For instance, materials that are commonly used for grinding in mechanochemistry are stainless steel, zirconium oxide (ZrO_2), Teflon and tungsten carbide (WC), all with different densities that can provide different degrees of impact to the reaction.[62] Furthermore, changing the number and size of balls also can have a pronounced influence, and the rule that is frequently followed is that fewer balls of larger size provides higher impact, whereas using more balls of smaller size could enhance the mixing that occurs between the reactants, but also promotes more friction and the accompanied increase in temperature of the reaction.[62]

The process parameters refer to the control of how efficiently the kinetic energy can enter the system and subsequently be transferred to the reagents during the reaction.[57,63,66,69] This is quite

easily regulated by adjusting the frequency of milling and time of the reaction.[63,66] Lastly, chemical parameters are also commonly found within conventional solution-based methods such as the type of chemical reaction taking place, the kind of substrates, the presence of a catalyst (or some other additive) and the ratio between these.[63] Another important chemical parameter, unique to mechanochemical reactions, is the possibility of grinding with a small amount of solvent in a technique called liquid-assisted grinding (LAG).[65,70–72]

Mechanochemistry in its simplest form involves grinding the reactants neat, *i.e.* the reactants are ground together without any added solvent (or other liquids that might act as a solvent).[70] As soon as solvent is added intentionally, it is termed LAG, which has become a powerful technique to control reactivity in mechanochemistry by either speeding up reactions, or facilitating reactions that do not proceed via neat grinding.[70–72] This effect was first noticed by the Jones group, who observed that the rate of co-crystal formation improves upon the addition of a 'small amount' of suitable solvent.[73] Following this, the same group also reported how LAG can assist in polymorph control of single- and multicomponent crystals,[74,75] and also how it can aid in the screening of crystalline salts.[76]

In earlier descriptions of LAG, researchers would use terms like adding '*a few drops*' or a '*small amount*' of solvent to a reaction, which sounds quite perplexing and may not be very helpful in attempts to reproduce certain reactions. This led to Jones and Friščić coming up with a way to express LAG quantitatively, and in 2009 they introduced the parameter η which is defined as the ratio of the volume of added solvent (in μL) to weight of reactants (in mg).[62,65,71,77] With this emperical definition, LAG reactions can now be characterized and compared. For more information on this topic, see Chapter 4.

1.2.3 Catalysis

Mechanochemistry has become an effective and versatile method for catalytic transformations in the solid state. Since mechanistic insights into mechanochemistry are still lacking, chemical reactivity under mechanochemical conditions cannot always be predicted. This means that sometimes the only way to know whether a reaction will work is to simply carry it out and apply a trial-and-error based approach, although in general solid reactants that have poor solubility in common organic solvents and reactions that require hazardous solvents could possibly be good candidates for mechanochemistry.[66]

Furthermore, even though numerous reactions have been catalyzed by mechanochemistry, a question that often arises is why do we want to catalyze reactions by mechanochemistry; or

alternatively, what advantages does it offer over its solution-based counterparts? One advantage is reaction discovery, *i.e.* the potential to achieve products that are not possible from solution-based methods, but also, reactions usually happens faster under mechanochemical conditions and selectivity is simultaneously improved as well.[66,71] Perhaps the most important advantage of mechanochemistry is that it makes chemical transformations greener.[62,71,78] This means that chemical reactions are carried out in a cleaner and safer manner than the ones currently in use. This is achieved through milling without the use of large amounts of toxic and/or volatile solvents, which is quite appealing considering our efforts in developing environmentally benign methods.[62,71,78]

In the following subsections, a few examples regarding redox reactions and metal-catalyzed reactions carried out mechanochemically will be highlighted within the context of this thesis.

1.2.3.1 Oxidation and reduction

Oxidation and reduction reactions are essential chemical transformations in organic chemistry, which provides enough reason to investigate their use under mechanochemical conditions, especially with many solid oxidizing and reducing agents available.[69,79]

One of the first oxidation reactions that was carried out in the solid state was reported by Toda *et al*. They were able to oxidize several ketones to esters in the presence of *meta*-chloroperbenzoic acid.[80] The reactants were either ground in an agate mortar and pestle or stirred at room temperature in chloroform.[80] The results from grinding showed an improvement in yield over the reactions in chloroform, especially in the case of benzophenone, where a yield of 85% was obtained by grinding, in comparison to 13% in solution during the same reaction time of 24 hours.[80] Since then, other oxidation reactions have been reported that include the oxidation of anilines,[81] thioethers and thiophenes,[82] methoxylated aromatics[37] and alcohols.[83–85] The oxidation of alcohols is of particular interest since the resulting carbonyl compounds are of industrial value, but also in the context of this thesis, where it is the oxidation of benzyl alcohol that is under investigation. The Mal group have reported twice on the oxidation of aromatic alcohols.[83,84] In the first example, they were able to oxidize various aromatic alcohols in the presence of 2-iodoxybenzoic acid (1.1 equivalents) with the longest reaction time being 3 hours, achieving high selectivity towards the aldehyde (~ 99%) (Scheme 1.1).[83] Perhaps more interesting, the waste product after oxidation (2-iodosobenzoic acid) was recycled for subsequent oxidation reactions with Oxone® through an *in situ* oxidative regeneration up to 15 times with minimal loss in activity.[83]

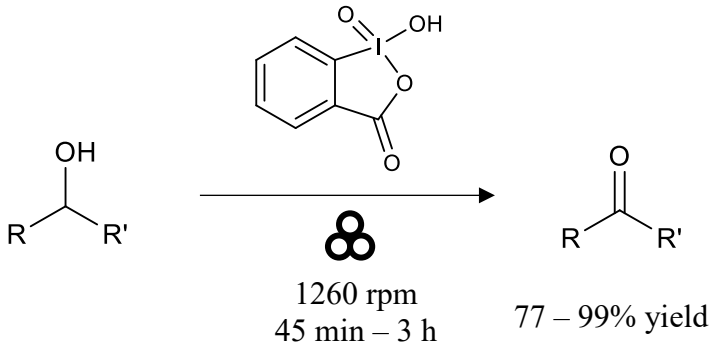

Scheme 1.1: Oxidation of alcohols to carbonyls by mechanochemistry using 2-iodoxybenzoic acid as oxidant. Scheme reproduced from reference 83.

The second report involves the oxidation of alcohols as a first step in the Biginelli reaction, in which they utilized 2-iodoxybenzoic acid again, but also *N*-bromosuccinimide and a combination of potassium bromide, Oxone® and 2,2,6,6-tetramethylpiperidin-1-yl-oxy (TEMPO) radical.[84] An article published by Zhang *et al* also reported on the oxidation of benzyl alcohol by ferrate (VI), commonly in the form K_2FeO_4, with iron in a high oxidation state of +6, bearing very strong oxidizing potential.[86] After 30 minutes, more than 80% of the alcohol has been converted, with over-oxidation starting to occur, and at the end of 3 hours, essentially all the alcohol has been converted to benzoic acid, with trace amounts of benzaldehyde present.[86]

With regards to reduction by mechanochemistry, Toda *et al* reported that the reduction of ketones proceeds in the solid state with sodium borohydride ($NaBH_4$) by using a mortar and pestle, which took between 1 – 5 days .[87] Similarly, the Mack group also reported the reduction of aldehydes and ketones with $NaBH_4$, but instead applied a high-speed ball milling approach, and were able to obtain alcohols at higher rate of between 1 and 6 hours, with conversions greater than 95%.[88] Moreover, even though $NaBH_4$ is not normally used for the reduction of esters, they were able to achieve the reduction of esters to alcohols with a combination of $NaBH_4$ and lithium chloride, supposedly forming the more reactive lithium borohydride *in situ*, to promote the reduction.[88,89]

In other reactions, Wang and co-workers described using the reductant Hantzsch 1,4-dihydropyridine for the first time in mechanochemical organic synthesis.[90] Previously used in the reduction of α,β-unsaturated aldehydes,[91] it was shown that the aldehyde is not reduced in these reactions, but rather the reaction is selective for reductive benzylization of malononitrile and 4-methylaniline to form benzylated products in good to excellent yields of 62% – 98% within 90 minutes.[90] Even though the reaction system shows quite a substituent

effect, it was very selective for benzylization since other functional groups like cyano and nitro groups were not reduced during the reaction.[90]

1.2.3.2 Metal-catalyzed reactions

Various metal-catalyzed reactions have been carried out under mechanochemical conditions, and in most cases, catalysts designed for solution-based catalysis can be used without any modifications.[71] In addition, it has been shown that catalysts can be prepared by mechanochemical methods, and subsequently be used in catalysis as well. For instance, Hernández and Bolm reported the mechanosynthesis of a rhodium complex – $[Cp^*RhCl_2]_2$ – and subsequently used it in the activation of C–H bonds.[92] Utilizing the LAG technique (Section 1.2.2), they were able to prepare the metal complex in good yields at room temperature by milling for 3 hours, which turned out to be better than the solution-based procedure which requires the reaction to be refluxed for several hours.[92] Subsequently, the complex was able to catalyze the halogenation of 2-phenylpyridine in more than 80% yield within 3 hours of milling.[92]

Numerous other organic named reactions have also been carried out mechanochemically. These include the Heck,[93] Sonogashira,[94] and Suzuki-Miyaura[95,96] reactions which are all palladium-based catalytic systems, but also the Huisgen cycloaddition[97] and Glaser coupling[98] reactions that incorporate copper catalysts. Other metals include manganese that is involved in cross-coupling reactions,[99] iridium in C–H bond amidation reactions,[100] iron in Diels-Alder reactions[101] and cobalt in the allylation and amidation of indoles.[102,103]

Metals have also been involved in oxidation reactions, which in the context of this thesis is particularly important. More specifically, the oxidation of alcohols has been achieved by Porcheddu *et al* using Stahl's catalyst, a Cu^I/TEMPO system, under mechanochemical conditions, originally used in a solution-based procedure (Scheme 1.2).[104]

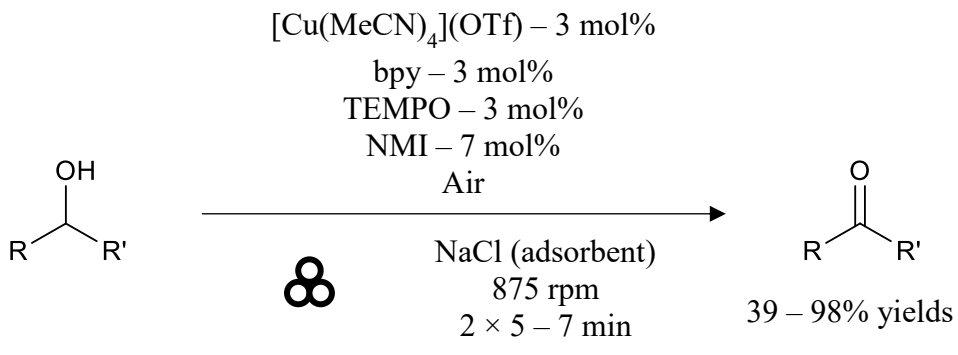

Scheme 1.2: Oxidation of alcohols with Cu^I/TEMPO-based catalyst, developed by Stahl, under mechanochemical conditions. Scheme reproduced from reference 104.

They were able to obtain conversions of above 90% for a variety of primary and secondary alcohols in under 15 minutes, with only aldehyde/ketone products and no trace of over-oxidation.[104] This reaction was much faster than the solution-based protocol, which is quite a remarkable achievement, and once again shows the versatility of mechanochemical reactions with regards to selectivity and reaction rate.

Mechanochemistry can also offer the option of using the reaction environment that is available as means to achieve chemical transformations, *i.e.* utilizing bulk metal surfaces, including the milling vessel, to achieve catalytic transformations.[62,71,72] For example, the Mack group reported the synthesis of triazoles via the cycloaddition reaction of azides and alkynes in a copper vial and using a copper grinding ball.[105] They obtained triazoles in very high yields (> 95%) in only 15 minutes of grinding, showing how metal surfaces can replace the traditional powdered catalysts, and in addition, simplifying the recyclability of the catalyst. In another example, the same group reported the use of metallic silver-foil (Ag) as a catalyst for the cyclopropanation of alkenes.[106] The procedure simply entails grinding the silver foil together with the reactants in a stainless steel jar with a stainless steel ball, with the Ag foil effectively acting as a heterogeneous catalyst.[106] Nearly quantitative yields were obtained (96%) with high diastereomeric ratio within 16 hours of milling.[106]

1.3 Project aims

The general aim of this project was to become familiar with inert synthesis using classical Schlenk line techniques, general synthetic procedures in air or under nitrogen atmosphere and also carrying out catalytic reactions in solution and in the solid state by mechanochemistry and subsequently analyzing the reaction products accurately.

Secondly, the project was focused on catalysis. Specifically, it has previously been shown that a newly-discovered coordination polymer (CP) from our group, consisting of cobalt (II) *meso*-tetraphenylporphyrin and 4-(4'-pyridyl)-1,2,3,5-dithiadiazolyl radical (pyrDTDA),[107,108] catalyzes the oxidation of benzyl alcohol.[109] We speculated whether the axial radical ligand is important in the catalytic reaction. The initial aims of this project were thus to synthesize and characterize similar Co-porphyrin derivatives with different axial ligands, including a 3,5-lutidine axial ligand and a chloride axial ligand. Following this, we aimed to assess whether the axial DTDA ligand has an effect on the catalytic reaction, and concurrently probing what the role of the oxidation state of the metal is by using the catalysts in the oxidation of benzyl alcohol and comparing the results. Since Co-porphyrins have not been explored as catalysts in mechanochemical reactions, the final aim of the project was to optimize and develop a suitable

reaction protocol for mechanochemical catalysis using Co-porphyrins, also using the oxidation of benzyl alcohol as the model reaction.

1.4 Thesis outline

Chapter 1 provides an overview on *meso*-tetraphenylporphyrins and their metallated analogues with respect to their structure, synthesis and coordination chemistry. In addition, applications of these compounds in catalysis is highlighted. Furthermore, the field of mechanochemistry is introduced with a brief historical outline. Following this, the equipment and techniques used in mechanochemical reactions are summarized, as well as catalytic applications with respect to redox and metal-catalyzed reactions.

Chapter 2 describes a synthetic investigation into the pyrDTDA radicals. It is a challenge to prepare bulk CP, and during our efforts to optimise the preparation of CP, a paper appeared reporting how pyrDTDA synthesis produces two different forms of the radical. It was then decided to investigate the synthesis of these two forms further, and assess the effect this might have on the synthesis of the CP.

Chapter 3 covers the assessment of the catalytic results obtained for the oxidation of benzyl alcohol by Co-porphyrins in solution. This chapter describes how the conversions and selectivity compare to one another with respect to different axial ligands and oxidation state.

Chapter 4 covers the evaluation of the oxidation of benzyl alcohol by mechanochemistry, how the mechanochemical conditions were optimized using urea-hydrogen peroxide and what effect the Co-porphyrins had on the yield and selectivity of the reaction.

Chapter 5 comprises an all-round summary of the most important results obtained in this study and the implications of these. In addition, recommendations for future work are given should this study advance beyond the current point.

Appendix A contains all the general and relevant information regarding chemicals, reactions and instrumentation used during the course of this project.

Appendix B contains experimental data such as IR spectra, ^{1}H NMR spectra, UV-Vis spectra and MS spectra of the relevant compounds pertaining to their characterization. Furthermore, catalytic results are presented here.

1.5 References

1 P. Rothemund, *J. Am. Chem. Soc.*, 1936, **58**, 625–627.

2 M. Gouterman, *J. Mol. Spectrosc.*, 1961, **6**, 138–163.

3 E. B. Fleischer, *Acc. Chem. Res.*, 1970, **3**, 105–112.

4 J. L. Hoard, *Science*, 1971, **174**, 1295–1302.

5 J. C. Barona-Castaño, C. C. Carmona-Vargas, T. J. Brocksom and K. T. De Oliveira, *Molecules*, 2016, **21**, 1–27.

6 M. G. H. Vicente and K. M. Smith, *Curr. Org. Chem.*, 2000, **4**, 139–174.

7 P. Rothemund, *J. Am. Chem. Soc.*, 1935, **57**, 2010–2011.

8 D. Dolphin, T. G. Traylor and L. Y. Xie, *Acc. Chem. Res.*, 1997, **30**, 251–259.

9 P. Rothemund and A. R. Menotti, *J. Am. Chem. Soc.*, 1941, **63**, 267–270.

10 I. Beletskaya, V. S. Tyurin, A. Y. Tsivadze, R. Guilard and C. Stern, *Chem. Rev.*, 2009, **109**, 1659–1713.

11 A. D. Adler, F. R. Longo, J. D. Finarelli, J. Goldmacher, J. Assour and L. Korsakoff, *J. Org. Chem.*, 1967, **32**, 476.

12 B. Meunier, *Chem. Rev.*, 1992, **92**, 1411–1456.

13 K. Pamin, E. Tabor, S. Górecka, W. W. Kubiak, D. Rutkowska-Zbik and J. Połtowicz, *ChemSusChem*, 2019, **12**, 684–691.

14 J. S. Lindsey, I. C. Schreiman, H. C. Hsu, P. C. Kearney and A. M. Marguerettaz, *J. Org. Chem.*, 1987, **52**, 827–836.

15 M. W. Grinstaff, M. G. Hill, J. A. Labinger and H. B. Gray, *Science*, 1994, **264**, 1311–1313.

16 A. D. Adler, F. R. Longo, F. Kampas and J. Kim, *J. Inorg. Nucl. Chem.*, 1970, **32**, 2443–2445.

17 P. Rothemund and A. R. Menotti, *J. Am. Chem. Soc.*, 1948, **70**, 1808–1812.

18 V. M. Albers and H. V. Knorr, *J. Chem. Phys.*, 1936, **4**, 422–425.

19 V. M. Albers and H. V. Knorr, *J. Chem. Phys.*, 1941, **9**, 497–502.

20 A. H. Corwin, A. B. Chivvis, R. W. Poor, D. G. Whitten and E. W. Baker, *J. Am. Chem. Soc.*, 1968, **90**, 6577–6583.

21 G. D. Dorough, J. R. Miller and F. M. Huennekens, *J. Am. Chem. Soc.*, 1951, **73**, 4315–4320.

22 H. C. Longuet-Higgins, C. W. Rector and J. R. Platt, *J. Chem. Phys.*, 1950, **18**, 1174–1181.

23 W. Xia, S. I. Vagin and B. Rieger, *Chem. Eur. J.*, 2014, **20**, 15499–15504.

24 P. D. Smith, B. R. James and D. H. Dolphin, *Coord. Chem. Rev.*, 1981, **39**, 31–75.

25 D. A. Summerville, R. D. Jones, B. M. Hoffman and F. Basolo, *J. Chem. Educ.*, 1979, **56**, 157–162.

26 T. Yamada and Y. Kamiya, *Bull. Chem. Soc. Jpn.*, 1980, **53**, 1077–1080.

27 G. M. Mamardashvili, O. R. Simonova, N. V. Chizhova and N. Z. Mamardashvili, *Russ. J. Gen. Chem.*, 2018, **88**, 1154–1163.

28 M. N. Dufour, A. L. Crumbliss, G. Johnston and A. Gaudemer, *J. Mol. Catal.*, 1980, **7**, 277–287.

29 J. Huet, A. Gaudemer, C. Boucly-Goester and P. Boucly, *Inorg. Chem.*, 1982, **21**, 3413–3419.

30 G. Mamardashvili, E. Kaigorodova, O. Simonova and N. Mamardashvili, *J. Coord. Chem.*, 2018, **71**, 4194–4209.

31 F. A. Walker, *J. Am. Chem. Soc.*, 1973, **95**, 1150–1153.

32 H. C. Stynes and J. A. Ibers, *J. Am. Chem. Soc.*, 1972, **94**, 5125–5127.

33 F. A. Walker, *J. Am. Chem. Soc.*, 1970, **92**, 4235–4244.

34 M. Tezuka, Y. Ohkatsu and T. Osa, *Bull. Chem. Soc. Jpn.*, 1976, **49**, 1435–1436.

35 D. Mansuy, *C. R. Chim.*, 2007, **10**, 392–413.

36 T. Mlodnicka, *J. Mol. Catal.*, 1986, **36**, 205–242.

37 S. L. Collom, P. T. Anastas, E. S. Beach, R. H. Crabtree, N. Hazari and T. J. Sommer, *Tetrahedron Lett.*, 2013, **54**, 2344–2347.

38 X. T. Zhou, H. Y. Chen, Q. Han, M. Lv and H. B. Ji, *New J. Chem.*, 2020, **44**, 10286–10291.

39 X. Zhou and H. Ji, *Chinese J. Catal.*, 2012, **33**, 1906–1912.

40 H. Kameyama, F. Narumi, T. Hattori and H. Kameyama, *J. Mol. Catal. A Chem.*, 2006, **258**, 172–177.

41 Y. Ohkatsu and T. Osa, *Bull. Chem. Soc. Jpn.*, 1977, **50**, 2945–2949.

42 Y. Ohkatsu, O. Sekiguchi and T. Osa, *Bull. Chem. Soc. Jpn.*, 1977, **50**, 701–705.

43 A. K. Mandal, V. Khanna and J. Iqbal, *Tetrahedron Lett.*, 1996, **37**, 3769–3772.

44 A. K. Mandal and J. Iqbal, *Tetrahedron*, 1997, **53**, 7641–7648.

45 C. M. Che and J. S. Huang, *Chem. Commun.*, 2009, 3996–4015.

46 M. Costas, *Coord. Chem. Rev.*, 2011, **255**, 2912–2932.

47 M. J. F. Calvete, M. Piñeiro, L. D. Dias and M. M. Pereira, *ChemCatChem*, 2018, **10**, 1–25.

48 V. V. Boldyrev and K. Tkáčová, *J. Mater. Synth. Process.*, 2000, **8**, 121–132.

49 L. Takacs, *Chem. Soc. Rev.*, 2013, **42**, 7649–7659.

50 E. Boldyreva, *Chem. Soc. Rev.*, 2013, **42**, 7719–7738.

51 L. Takacs, *J. Mater. Sci.*, 2018, **53**, 13324–13330.

52 L. Takacs, *Jom*, 2000, **52**, 12–13.

53 S. L. James, C. J. Adams, C. Bolm, D. Braga, P. Collier, T. Friščic, F. Grepioni, K. D. M. Harris, G. Hyett, W. Jones, A. Krebs, J. Mack, L. Maini, A. G. Orpen, I. P. Parkin, W. C. Shearouse, J. W. Steed and D. C. Waddell, *Chem. Soc. Rev.*, 2012, **41**, 413–447.

54 P. Baláž, M. Achimovicová, M. Baláž, P. Billik, C. Z. Zara, J. M. Criado, F. Delogu, E. Dutková, E. Gaffet, F. J. Gotor, R. Kumar, I. Mitov, T. Rojac, M. Senna, A. Streletskii and W. C. Krystyna, *Chem. Soc. Rev.*, 2013, **42**, 7571–7637.

55 L. Takacs, *J. Mater. Sci.*, 2004, **39**, 4987–4993.

56 V. V Boldyrev, *Russ. Chem. Rev.*, 2006, **75**, 177–189.

57 C. Suryanarayana, *Prog. Mater. Sci.*, 2001, **46**, 1–184.

58 L. Takacs, *Prog. Mater. Sci.*, 2002, **47**, 355–414.

59 G. Binnig, C. F. Quate and C. Gerber, *Phys. Rev. Lett.*, 1986, **56**, 930–933.

60 M. K. Beyer and H. Clausen-Schaumann, *Chem. Rev.*, 2005, **105**, 2921–2948.

61 A. D. McNaught and A. Wilkinson, *IUPAC Compendium of Chemical Terminology*, Blackwell Scientific Publications, Oxford, 1997.

62 J. L. Do and T. Friščić, *Synlett*, 2017, **28**, 2066–2092.

63 A. Stolle, R. Schmidt and K. Jacob, *Faraday Discuss.*, 2014, **170**, 267–286.

64 J. G. Hernández and T. Friščić, *Tetrahedron Lett.*, 2015, **56**, 4253–4265.

65 D. Tan and T. Friščić, *European J. Org. Chem.*, 2018, **2018**, 18–33.

66 J. L. Howard, Q. Cao and D. L. Browne, *Chem. Sci.*, 2018, **9**, 3080–3094.

67 J. Andersen and J. Mack, *Green Chem.*, 2018, **20**, 1435–1443.

68 D. E. Crawford, C. K. G. Miskimmin, A. B. Albadarin, G. Walker and S. L. James, *Green Chem.*, 2017, **19**, 1507–1518.

69 A. Stolle, T. Szuppa, S. E. S. Leonhardt and B. Ondruschka, *Chem. Soc. Rev.*, 2011, **40**, 2317–2329.

70 G. A. Bowmaker, *Chem. Commun.*, 2013, **49**, 334–348.

71 J. Do and T. Friščić, *ACS Cent. Sci.*, 2017, **3**, 13–19.

72 C. Mottillo and H. M. Titi, *Angew. Chemie - Int. Ed.*, 2020, **59**, 1018–1029.

73 N. Shan, F. Toda and W. Jones, *Chem. Commun.*, 2002, **2**, 2372–2373.

74 A. V Trask, N. Shan, W. D. S. Motherwell, W. Jones, S. Feng, R. B. H. Tan and K. J. Carpenter, *Chem. Commun.*, 2005, 880–882.

75 A. V. Trask, W. D. S. Motherwell and W. Jones, *Chem. Commun.*, 2004, 890–891.

76 A. V. Trask, D. A. Haynes, W. D. S. Motherwell and W. Jones, *Chem. Commun.*, 2006, 51–53.

77 T. Friščić, S. L. Childs, S. A. A. Rizvi and W. Jones, *CrystEngComm*, 2009, **11**, 418–426.

78 R. B. N. Baig and R. S. Varma, *Chem. Soc. Rev.*, 2012, **41**, 1559–1584.

79 G. Cravotto and E. C. Gaudino, *RSC Green Chem.*, 2015, **2015**, 58–80.

80 F. Toda, M. Yagi and K. Kiyoshige, *J. Chem. Soc. Chem. Commun.*, 1988, 958–959.

81 R. Thorwirth, F. Bernhardt, A. Stolle, B. Ondruschka and J. Asghari, *Chem. Eur. J.*, 2010, **16**, 13236–13242.

82 G. Cravotto, D. Garella, D. Carnaroglio, E. C. Gaudino and O. Rosati, *Chem. Commun.*, 2012, **48**, 11632–11634.

83 T. K. Achar, S. Maiti and P. Mal, *RSC Adv.*, 2014, **4**, 12834–12839.

84 P. K. Sahoo, A. Bose and P. Mal, *European J. Org. Chem.*, 2015, **2015**, 6994–6998.

85 A. Porcheddu, F. Delogu, L. De Luca, C. Fattuoni and E. Colacino, *Beilstein J. Org. Chem.*, 2019, **15**, 1786–1794.

86 Z. Y. Zhang, D. Ji, W. Mao, Y. Cui, Q. Wang, L. Han, H. Zhong, Z. Wei, Y. Zhao, K. Nørgaard and T. Li, *Angew. Chemie - Int. Ed.*, 2018, **57**, 10949–10953.

87 F. Toda, K. Kiyoshige and M. Yagi, *Angew. Chemie Int. Ed. English*, 1989, **28**, 320–321.

88 J. Mack, D. Fulmer, S. Stofel and N. Santos, *Green Chem.*, 2007, **9**, 1041–1043.

89 G. Wang, *Chem. Soc. Rev.*, 2013, **42**, 7668–7700.

90 Z. Zhang, J. Gao, J. J. Xia and G. W. Wang, *Org. Biomol. Chem.*, 2005, **3**, 1617–1619.

91 S. G. Ouellet, J. B. Tuttle and D. W. C. MacMillan, *J. Am. Chem. Soc.*, 2005, **127**, 32–33.

92 J. G. Hernández and C. Bolm, *Chem. Commun.*, 2015, **51**, 12582–12584.

93 E. Tullberg, D. Peters and T. Frejd, *J. Organomet. Chem.*, 2004, **689**, 3778–3781.

94 D. A. Fulmer, W. C. Shearouse, S. T. Medonza and J. Mack, *Green Chem.*, 2009, **11**, 1821–1825.

95 F. Schneider, A. Stolle, B. Ondruschka and H. Hopf, *Org. Process Res. Dev.*, 2009, **13**, 44–48.

96 Z. J. Jiang, Z. H. Li, J. B. Yu and W. K. Su, *J. Org. Chem.*, 2016, **81**, 10049–10055.

97 R. Thorwirth, A. Stolle, B. Ondruschka, A. Wild and U. S. Schubert, *Chem. Commun.*, 2011, **47**, 4370–4372.

98 R. Schmidt, R. Thorwirth, T. Szuppa, A. Stolle, B. Ondruschka and H. Hopf, *Chem. Eur. J.*, 2011, **17**, 8129–8138.

99 L. Li, J. J. Wang and G. W. Wang, *J. Org. Chem.*, 2016, **81**, 5433–5439.

100 G. N. Hermann, P. Becker and C. Bolm, *Angew. Chemie - Int. Ed.*, 2016, **55**, 3781–3784.

101 Y. J. Tan, Z. Zhang, F. J. Wang, H. H. Wu and Q. H. Li, *RSC Adv.*, 2014, **4**, 35635–35638.

102 X. Jiang, J. Chen, W. Zhu, K. Cheng, Y. Liu, W. K. Su and C. Yu, *J. Org. Chem.*, 2017, **82**, 10665–10672.

103 H. Cheng, J. G. Hernández and C. Bolm, *Adv. Synth. Catal.*, 2018, **360**, 1800–1804.

104 A. Porcheddu, E. Colacino, G. Cravotto, F. Delogu and L. De Luca, *Beilstein J. Org. Chem.*, 2017, **13**, 2049–2055.

105 T. L. Cook, J. A. Walker and J. Mack, *Green Chem.*, 2013, **15**, 617–619.

106 L. Chen, M. O. Bovee, B. E. Lemma, K. S. M. Keithley, S. L. Pilson, M. G. Coleman and J. Mack, *Angew. Chemie - Int. Ed.*, 2015, **54**, 11084–11087.

107 L. J. van Laeren, Investigation of thiazyl radical-metalloporphyrin complexes, Stellenbosch University, 2017.

108 D. A. Haynes, L. J. Van Laeren and O. Q. Munro, *J. Am. Chem. Soc.*, 2017, **139**, 14620–14637.

109 N. Chaudhary and D. A. Haynes, *Unpublished work*.

Chapter 2

Synthetic investigation into 4-(4'-pyridyl)-1,2,3,5-dithiadiazolyl

2.1 Introduction

Dithiadiazolyl (DTDA) radicals are a class of organic free radicals that contain the unsaturated thiazyl (—S=N—) unit combined with carbon to form a heterocyclic structure.[1,2] There are four possible isomers, of which only two have been isolated to date, and one is shown in Figure 2.1, the 1,2,3,5-dithiadiazolyl radical.[3] The origin of DTDA radicals can be traced back to the discovery of poly(sulfur-nitride), which is often referred to as the first *organic metal* since it exhibits conducting behavior at approximately 0.3 K.[3–5] Following several investigations, it was determined that the conductive properties of poly(sulfur-nitride) are due to the high mobility of π-electrons along the polymeric SN chain.[4,5] This was an extraordinary discovery that showed that the properties of the material are directly related to its solid-state structure. This captivated solid-state chemists and ushered in a resurrection of sulfur-nitrogen chemistry. Subsequent research on poly(sulfur-nitride) focused on exploring its properties through tweaking of the backbone, and incorporation of carbon unexpectedly resulted in C/N/S heterocycle-containing compounds, of which the DTDA radical is an example.[4]

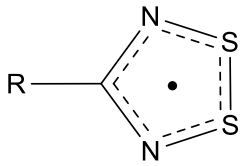

Figure 2.1: Structure of the 1,2,3,5-dithiadiazolyl radical where R represents any substituent.

Since their discovery, DTDA radicals have been widely studied, and their chemistry is well established from both a fundamental and materials point of view.[1,3,4,6–11] This can be attributed to their relative ease of synthesis, stability in the solid state (in the absence of oxygen) and also their high thermal stability. More captivating is their fascinating electronic structure: the SN moiety has high spin density (possessing a three-electron π-bond) and bears no substituents, which means that the nitrogen and sulfur atoms are able to participate in supramolecular

contacts.[3,7,9–11] Furthermore, the unpaired electron resides in an π-antibonding molecular orbital, the singly occupied molecular orbital (SOMO), which presents a nodal plane at the lone carbon of the heterocyclic ring.[12–14] As a result, the spin density is confined to the heterocyclic ring and no resonance interactions can occur between the R-group and the heterocyclic ring.[3,15,16] This means that the electronic properties of the ring will remain largely unaffected, irrespective of the identity of the R-group. Taken together, a fundamental understanding of their electronic structure is essential in utilizing DTDA radicals in crystal engineering studies.[3] For instance, as mentioned before, the nitrogen and sulfur atoms of the heterocyclic ring are available to engage in intermolecular interactions by virtue of the SN bond being polar.[4] Furthermore, the carbon-nodal SOMO allows for the incorporation of additional supramolecular synthons in the R-group, such as a phenyl ring with a cyano group that could also take part in electrostatic intermolecular interactions.[4]

In order to exploit the useful properties, such as conductivity and magnetism, that could arise in these compounds, an exchange pathway between the unpaired spins is required.[1,3,4,7,9,11] This, in turn, is completely dependent on the molecular arrangement, which is complicated by the tendency of DTDA radicals to dimerize in the solid state.[1,3,4,11] Dimerization involves a bonding interaction between the SOMOs, which means that the unpaired electrons are paired up, leaving the material diamagnetic and resulting in the concomitant loss of magnetic and conducting properties.[1,3,7,11] For this reason, there is a need for the development of design strategies that will enable control over the arrangement of molecules in the solid state.

Another strategy that has received more attention recently is the use of DTDA radicals as spin-bearing ligands in metal complexes.[7,10] The advantage of using DTDA radicals is that there are two atoms on the heterocyclic ring that could coordinate to a metal center.[7,10] Whereas early examples showed zero-valent metals complexing with DTDA radicals through the sulfur atoms, often resulting in the breakage of the S−S bond,[13,17–22] coordination through the nitrogen has been accomplished with divalent metals in more recent investigations.[23–26] Moreover, with an appropriate R-group, such as a pyridyl group, it is possible for DTDA radicals to coordinate through both the DTDA ring and the pyridyl nitrogen atom and actually bridge two metal centers.[27–29] Not only can this help to overcome dimerization, but DTDA radicals could form the basis of a coupled network wherein unpaired electrons can exchange between paramagnetic metal centers, resulting in organometallic magnets.[7]

Furthermore, these radicals are also capable of behaving as redox non-innocent ligands when coordinated to an appropriate metal atom (or ion).[7] Redox transformations can then occur

between the radical and the metal, allowing the radical, as a neutral 7 π system, to convert to either a cationic 6 π (oxidation) or anionic 8 π system (reduction).[7,30,31] This has potential significance in bioinorganic chemistry, because the resulting complexes can be utilized as model systems to study biochemical processes wherein metalloproteins bear radical ligands.[7,32] In addition, the performance of a metal complex during catalytic reactions could be modified by virtue of a synergistic cooperativity between the radical and the metal center, unlocking new reactivity.[30]

In view of controlling the solid-state arrangement of DTDA radicals, one strategy in our group involves the interactions of DTDA radicals with metalloporphyrins, which have commonly been used to tailor a range of supramolecular architectures.[33] Unfortunately, obtaining solid material of the resulting complexes is problematic, and our efforts have diverted to a solution-state investigation.[34] However, crystalline material of a particular DTDA-metalloporphyrin complex was obtained: the reaction of 4-(4'-pyridyl)-1,2,3,5-dithiadiazolyl radical (pyrDTDA) with the Co(II) complex of 5,10,15,20-tetraphenylporphyrin (CoTPP) resulted in a coordination polymer (CP) in which the pyrDTDA bridges two cobalt ions as shown in Figure 2.2.[29,34] Investigation of this coordination polymer in the solid and solution states is ongoing.

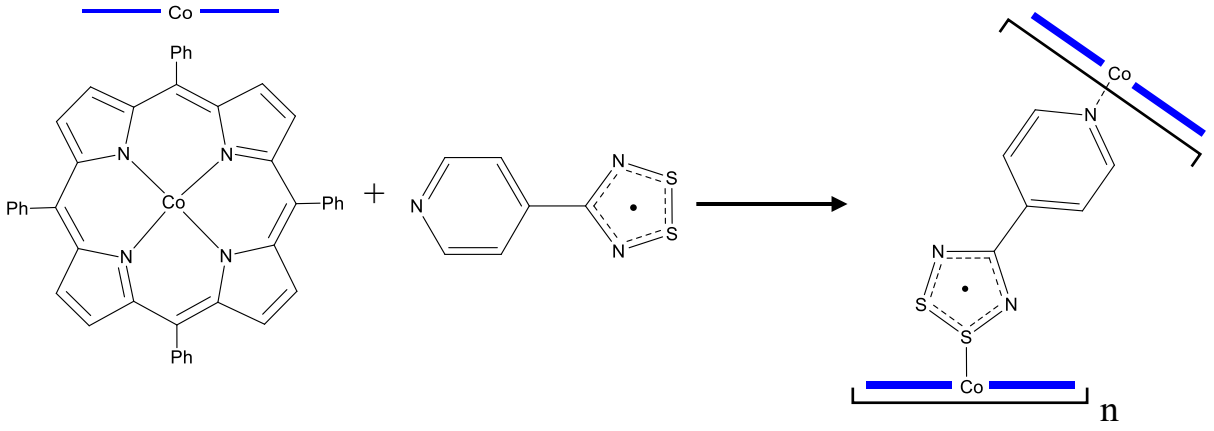

Figure 2.2: Compound structures for the formation of the CP.

Since metalloporphyrins can act as catalysts,[35–38] we investigated whether the CP could also effectively act as a catalyst and, furthermore, what the influence of the redox non-innocent DTDA radical ligand is on the catalytic activity. Preliminary work carried out by Dr Chaudhary in our group showed that the CP effectively catalyzed the oxidation of benzyl alcohol to the corresponding carbonyl compounds. The reaction was carried out in acetonitrile for 16 hours at 70 °C using *tert*-butyl hydroperoxide (TBHP) as oxidant.[39]

The initial focus of the current study was to repeat the catalytic reactions with the CP, and to compare its catalytic activity to other CoTPP derivatives. Unfortunately, preparing bulk material of the CP was challenging and impeded the progress in the early stages of this investigation. Recently, a new publication appeared from the Oakley group,[40] which revealed that there might be some issues with the synthetic method we were using for the pyrDTDA radical. We therefore decided to investigate the synthesis of the pyrDTDA radical in more detail, and our efforts are outlined in this chapter.

2.2 Preparation of 4-(4'-pyridyl)-1,2,3,5-dithiadiazolyl radical

Research from the Oakley group[40] has revealed structural changes of pyrDTDA during the synthesis that could ultimately have an effect on the preparation of bulk CP. They propose the formation of a charged pyrDTDA radical with a protonated pyridine, which then requires an extra deprotonation step with base to obtain the neutral radical (Figure 2.3).[40] If this is correct, it means that if the deprotonation step is not included, a charged pyrDTDA radical is obtained. This could mean poor (or no) coordination to the metal and may be an explanation for why such low yields of the CP are obtained.

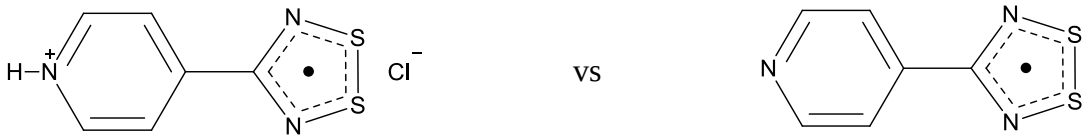

Figure 2.3: The two pyrDTDA radicals that forms, proposed by Oakley and coworkers.[40]

In this work, we decided to investigate the synthesis and assess the structural changes as reported by the Oakley group.[40] Specifically, is it possible to prepare the charged and neutral pyrDTDA radicals separately, and if so, are we able to distinguish between them based on characterization with various analytical techniques? In addition, if we were to use them separately in CP synthesis, will the yields be different?

2.2.1 General synthetic route towards the pyrDTDA radical

The pyrDTDA radical was synthesized for the first time in 2000 by Wong and coworkers.[22] Initially, our synthesis of the pyrDTDA radical followed a similar route, based on known literature procedures[1,41] with minimal modifications (depicted in Figure 2.4).

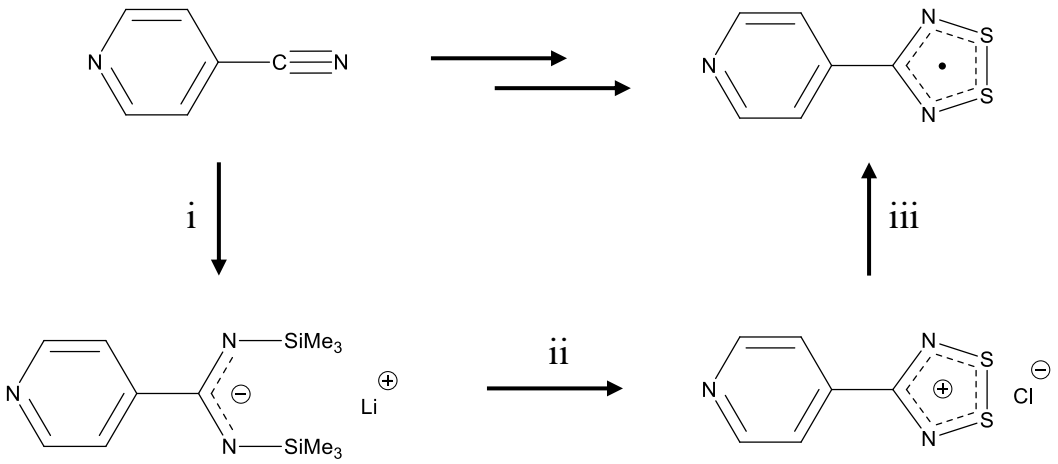

Figure 2.4: Typical synthetic route towards the pyrDTDA. Reagents and reaction conditions: i) BuLi, HMDS, EtO_2. ii) SCl_2, 0 °C. iii) $SbPh_3$ or Zn/Cu, THF.

The synthesis involves the addition of 4-pyridinecarbonitrile to a lithium bis (trimethylsilyl)amide generated *in situ* (step i), forming the lithiated amidinate, followed by a condensation reaction with SCl_2 to form the dithiadiazolyl chloride salt (step ii).[1,41] The radical is then obtained by reduction of the salt with either $SbPh_3$ in the melt or Zn/Cu couple in dry THF (step iii), and subsequently purified by vacuum sublimation.

This procedure is routinely used in the synthesis of related DTDA radical compounds. According to Oakley, however, because of the basic nature of the pyridyl nitrogen, synthetic adjustments are required to obtain the neutral pyrDTDA radical,[40] as will be elaborated on in Section 2.2.2.

2.2.2 Synthetic adjustments towards the synthesis of the pyrDTDA radical

The consequence of the basic properties of the pyridyl nitrogen is that an additional step must be added to the synthetic procedure to ensure a neutral radical is obtained as the product. In Figure 2.5, the left-hand side illustrates the usual procedure as described above (Figure 2.4), denoted pathway A, and the right-hand side shows pathway B, the modified pathway with an additional step at the end.

Following from the lithiated amidinate **2**, step i is the same for both pathways, however the intermediate dithiadiazolylium salt structures are different. The Oakley group proposes the formation of a dithiadiazolylium double salt **3b** in which the nitrogen of the pyridyl group is protonated after the addition of SCl_2.[40] Consequently, the reduction step ii generates the charged pyrDTDA radical **4** instead of the neutral radical **5**, which can only be obtained from **4** after treatment with base.[40]

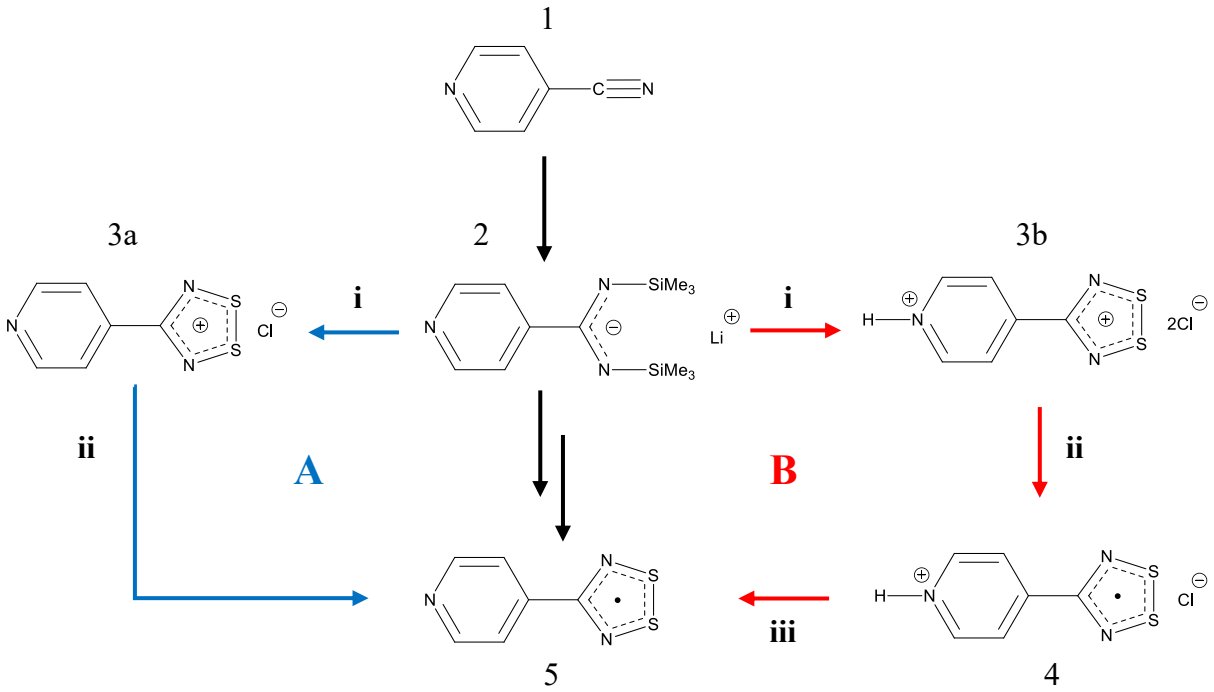

Figure 2.5: Typical synthetic route **A** and proposed synthetic route **B** yielding pyrDTDA. Reagents and reaction conditions: i) SCl_2, 0 °C. ii) $SbPh_3$ or Zn/Cu, THF. iii) NEt_3, MeCN.

The formation of the double salt with the protonated nitrogen is practically feasible due to the possibility of the SCl_2 being hydrolysed. SCl_2 reacts with water to form hydrochloric acid (and other products), which implies that moisture from the air or wet solvent could result in the formation of HCl,[40,42,43] which could protonate the pyridyl nitrogen. Since standard Schlenk techniques are employed, and solvents are dried prior to synthesis, a minimum amount of water could be available, and it is very likely that both radicals **4** and **5** are formed when the general synthetic pathway A is followed. Nevertheless, the challenge emerging from this is to separate them from each other and to distinguish between them based on the characterization with various analytical techniques.

Generally, striking colour changes occur during the synthetic procedure of DTDA radicals: the lithiated amidinate **2** is a pale yellow solution, which changes to an ochre-coloured solid (the dithiadiazolylium salt **3a** and **3b**) after condensation with SCl_2, followed by reduction and deprotonation that results in a dark purple crude solid (radical **4** and **5**) which sublimes as either dark purple or black powders. Relying on colour changes to distinguish **4** and **5** from one another is therefore not reliable since the same changes are observed for both and the purified solids could either have a dark purple or black colour. Fortunately, a specific physical property of these two pyrDTDA radicals allows differentiation between them – the temperature at which they sublime. During the purification step by sublimation, the charged pyrDTDA radical **4**

sublimes at temperatures above 140 °C up to 170 °C, whereas the neutral radical **5** starts to sublime at 90 °C ranging up to 140 °C.

These observations are in agreement with what the Oakley group reported, with a slight difference in the sublimation temperature of the neutral pyrDTDA radical **5**.[40] In our work, the colour of the crude solids are both dark purple, consistent with what Oakley observed, whereas the sublimed solids varied between dark purple and black powders. Oakley *et al* did not attempt to purify and isolate the charged radical **4**, but they report a lower sublimation temperature for the neutral pyrDTDA radical **5** between 50 – 100 °C.[40] Even though the study of the Oakley group did not focus on characterizing pyrDTDA radicals **4** and **5** separately, they did employ infrared spectroscopy to track the structural changes.[40]

After incorporating the synthetic adjustments proposed by Oakely, we were able to prepare pyrDTDA radical **4** via pathway B (by stopping after step ii) and pyrDTDA radical **5** also via pathway B (stopping after step iii) in two separate synthetic procedures. This was confirmed by extensive characterization, which is described in Section 2.3. We started with electron paramagnetic resonance spectroscopy (EPR) because we first wanted to confirm the presence of a DTDA radical species.

2.3 Characterization

2.3.1 Electron Paramagnetic Resonance Spectroscopy

EPR spectroscopy remains an essential technique when it comes to the characterization of DTDA radicals.[12,44] The EPR spectra in this study were obtained at room temperature, and these are presented in Figure 2.6.

The distinctive 1:2:3:2:1 pentet confirms the presence of the DTDA radical in both cases, whilst the g-factor values fall in the region of the free electron, and are similar to those reported for other DTDA radicals.[1] In addition, the hyperfine coupling constants (a_N) also compare well to those reported in the literature, with a_N = 5.10 and 5.01 G for **4** and **5**, respectively.

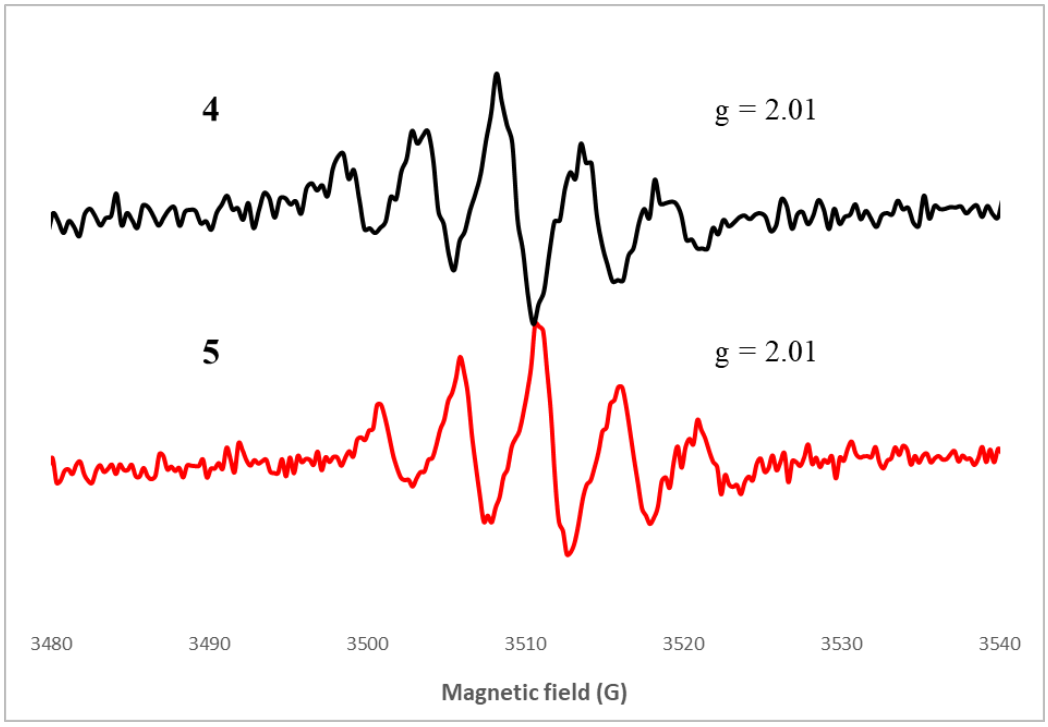

Figure 2.6: EPR spectra of the proposed pyrDTDA radicals **4** and **5** in DCM at room temperature. A high signal-to-noise ratio is observed due to poor solubility of the radicals.

Even though the pyrDTDA radical has not received much attention in the literature, the appearance of these spectra were anticipated due to the nature of the SOMO: since the unpaired electron remains on the heterocyclic ring, it couples to two equivalent nitrogen nuclei (I = 1) to give rise to the characteristic pentet pattern.[1,3,4,6,11] Coupling to the sulfur atoms occurs as well, however due to the low natural abundance of ^{33}S, it is usually not detected.[1] This phenomenon has been confirmed by several EPR studies.[1,2,16,33,38] The g-factor values of the pyrDTDA radicals in this study match well with examples from the literature,[22,29,40] but this implies EPR spectroscopy cannot be exploited to distinguish between radicals **4** and **5**. Infrared (IR) spectroscopy was consequently used as characterization technique; since all the intermediary products are first obtained as dry solids, measuring their IR spectra is straightforward and can serve as a convenient method to correlate the structural differences to differences in their IR spectra.[40]

2.3.2 Infrared Spectroscopy

IR spectroscopy data for substituted DTDA radicals are not generally relied upon for characterization purposes due to the complexity of the major peaks in the fingerprint region (400 – 1600 cm^{-1}), and therefore are not frequently reported in literature. One particular case is of interest: the work done by the Rawson group after the discovery of the very first solid-state paramagnetic DTDA radical, and the realization that it can be prepared as two different polymorphs.[45,46] The group conducted some thermal and magnetic studies to examine the

interconversion between the two phases α and β, but also attempted to distinguish between the two polymorph structures spectroscopically.[47] They found that the fingerprint region is extremely sensitive to the nature of the polymorph present, and consequently were able to differentiate between the two polymorphs based on the IR spectra.[47] This suggests that in the case of the two proposed pyrDTDA radical structures **4** and **5**, the differences in the IR spectra should be even more apparent, since we are working with different molecules as opposed to different polymorphs.

The group of Cordes *et al* studied the simplest DTDA radical (R=H, H-DTDA) and they were able to obtain the IR spectra of the discrete radical and the dimer (from the gas and solid phase, respectively).[14] Moreover, they were able to qualitatively assign the bands of the dimer from the spectrum obtained experimentally to the spectrum that was simulated theoretically.[14] Only a handful of bands are noted for H-DTDA between 250 – 1600 cm^{-1},[14] but upon the substitution of a phenyl (R-) group (Figure 2.7 – **Ph-DTDA)**, for instance, the interpretation can become more challenging due to bands arising from =C–H bending and C=C ring stretches in the fingerprint region.[48,49]

Nevertheless, several bands can still be assigned, as will be discussed with reference to Figure 2.7, and to reported and calculated IR data from the literature.[22,29,40] The few bands that are quite easily discernible appear in the range 500 – 920 cm^{-1}, and are characteristic of the heterocyclic ring.[14,29,48] One band at around 830 cm^{-1} also indicates the substitution of the phenyl group (or pyridyl R-group).[48]

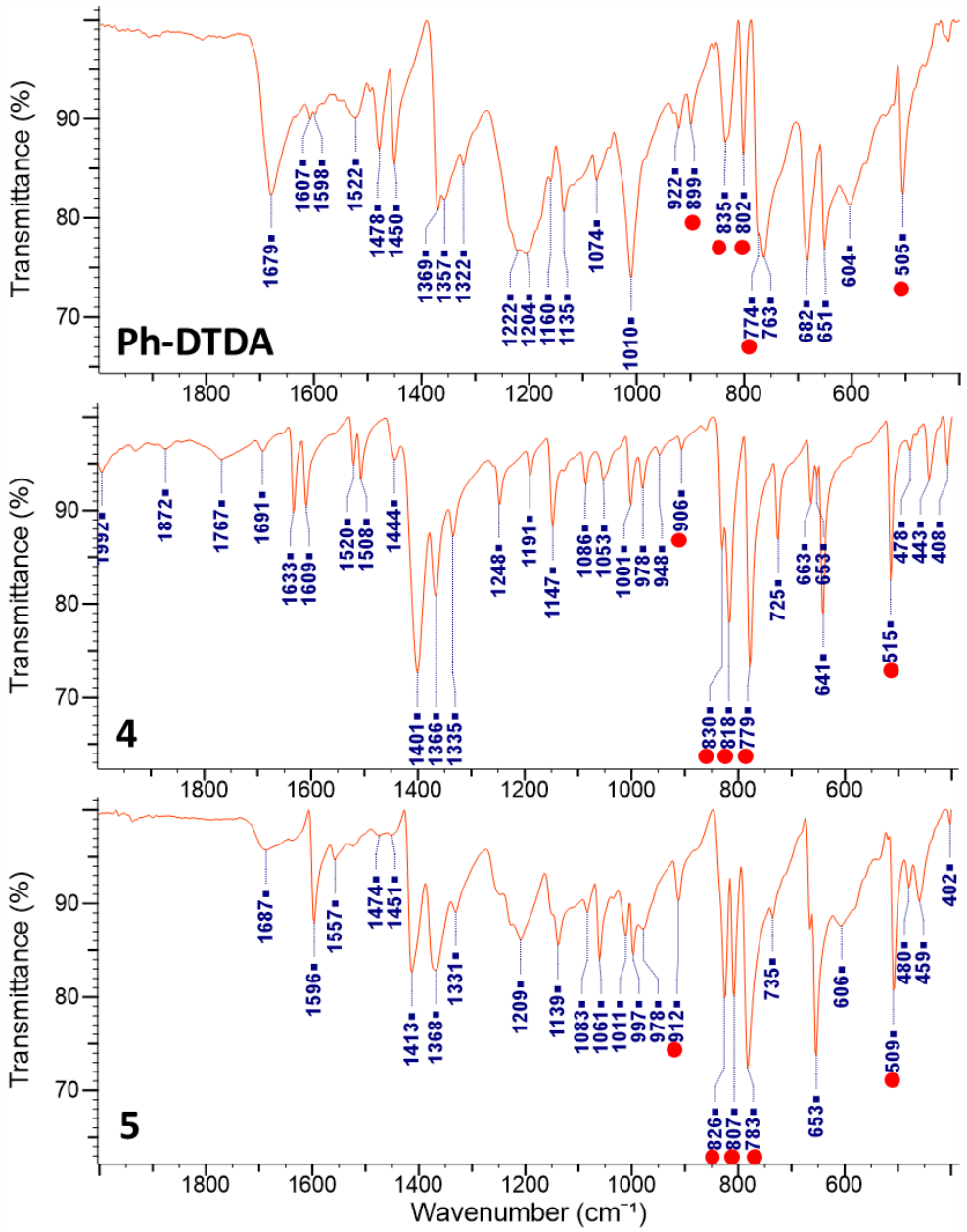

Figure 2.7: IR spectra (fingerprint region) of the 4-phenyl-1,2,3,5-dithiadiazolyl radical **Ph-DTDA**, the charged pyrDTDA radical **4** and the neutral pyrDTDA radical **5**. Red dots show common peaks of the heterocyclic ring.

These bands could shift, depending on the substituent, but are easy to identify, as shown in Figure 2.7 for the Ph-DTDA and pyrDTDA radicals **4** and **5** (red dots), and are also found in related DTDA radical compounds containing aryl substituents.[14,22–24,26,29,40,47,48,50–53]

In addition to just routine characterization, IR spectroscopy can be utilized to monitor and track the synthesis of DTDA radicals, as shown by Oakley and coworkers.[40] The IR spectra of the double salt **3b** and the two radicals **4** and **5** are illustrated in Figure 2.8.

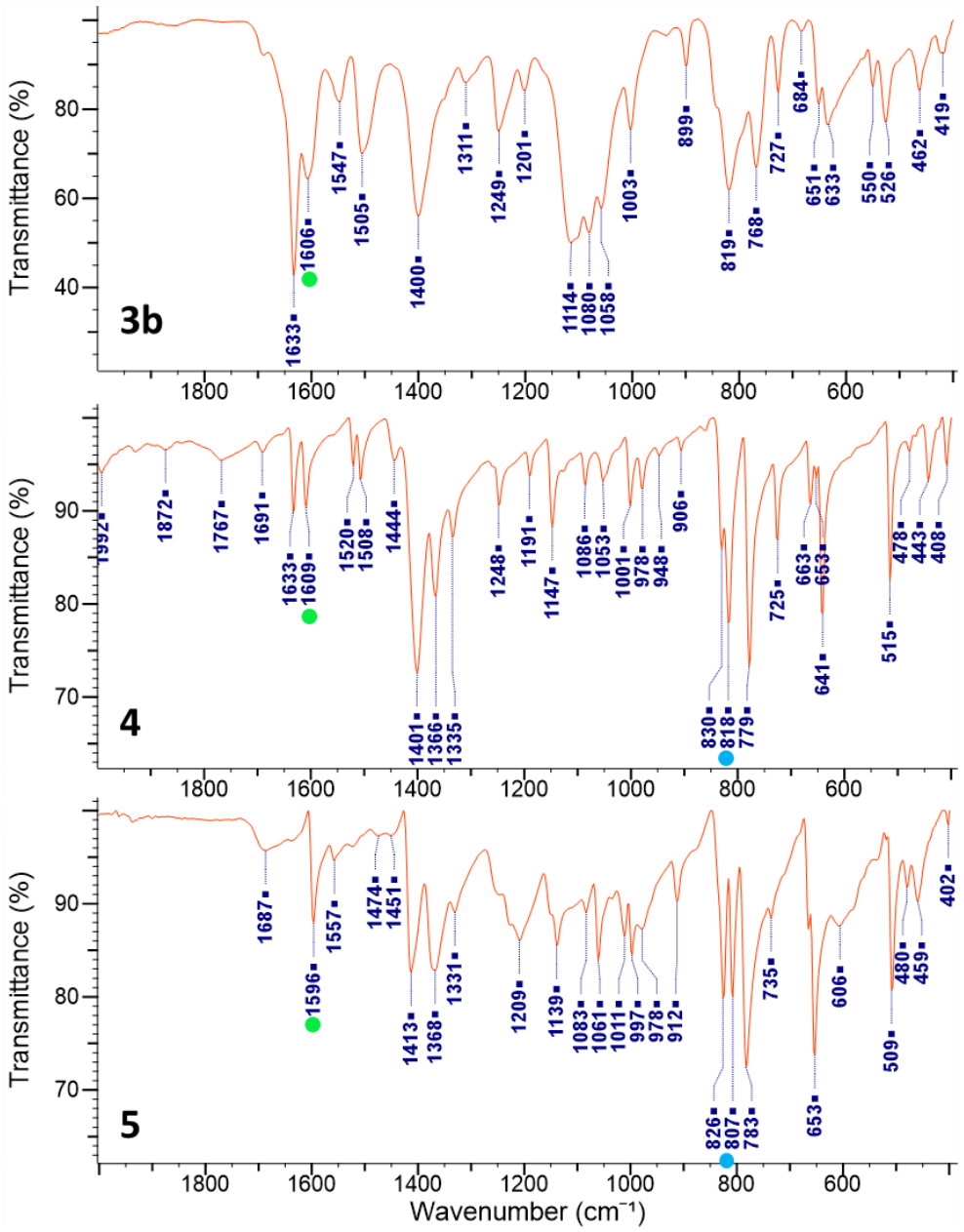

Figure 2.8: IR spectra (fingerprint region) of the dithiadiazolylium double salt **3b**, the charged pyrDTDA radical **4** and the neutral pyrDTDA **5**.

From Figure 2.8, the spectral changes between the salt and the radicals are quite clear, since it is not a radical, some of the characteristic heterocyclic ring bands are absent. More important, though, are the subtle changes between the two radicals **4** and **5**. Firstly, the characteristic bands of the heterocyclic ring, as mentioned above, are present in both spectra, but at slightly different wavenumbers (red dots - Figure 2.7). For instance, the antisymmetric stretching vibration of the N–S bond for the DTDA ring has been calculated by Munro and Haynes to be at 814 cm^{-1}, which they reported at 816 cm^{-1},[29] similar to what we found at 818 cm^{-1} for the charged pyrDTDA radical **4**, and observed at 807 cm^{-1} for the neutral pyrDTDA **5** (blue dots - Figure 2.8)**.** This also corresponds well to what Oakley measured, at 807 cm^{-1}.[40] Furthermore, since the nitrogen on the pyridyl group is protonated, differences in the vibrational frequencies in the

surrounding bonds should also be apparent in the fingerprint region. For example, Munro and Haynes calculated that the C=N_{py} bond has a stretching vibrational frequency at 1585 cm^{-1}, which they reported at 1608 cm^{-1}.[29] Seeing that the nitrogen is protonated after the addition of SCl_2, one would expect this band to be present in the salt **3b** as well. Indeed, this band is present in the salt and charged pyrDTDA radical in almost an identical position at 1606 and 1609 cm^{-1}, respectively (green dots - Figure 2.8). As soon as the hydrogen is removed, the band shifts closer to the calculated value at 1596 cm^{-1} (green dot - Figure 2.8), also correlating well with what Oakley reported for the neutral pyrDTDA at 1597 cm^{-1}.[40]

Additionally, noticeable differences in the functional group region give an indication of different structures as well (Figure 2.9).

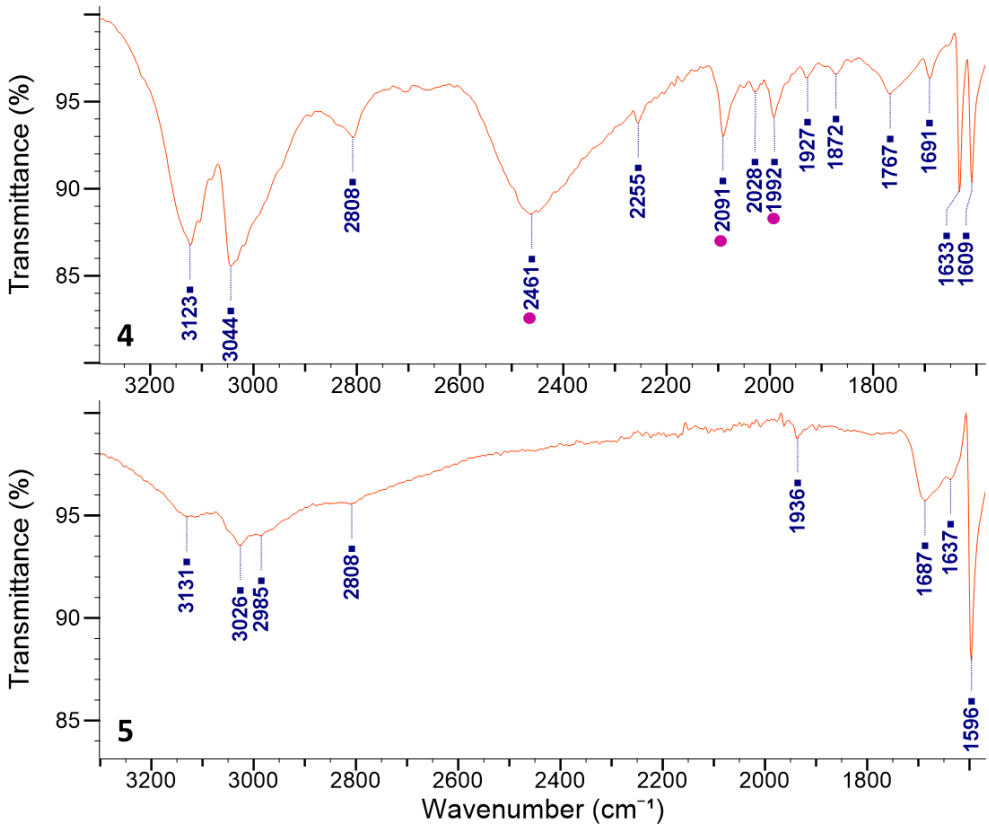

Figure 2.9: IR spectra (functional group region) of the charged pyrDTDA radical **4** and neutral pyrDTDA radical **5**.

In particular, a very broad band at approximately 2461 cm^{-1} and two smaller bands at 2091 and 1992 cm^{-1} completely vanish going from the charged pyrDTDA radical **4** to the neutral pyrDTDA radical **5** (purple dots – Figure 2.9). Even though the IR spectrum in this region is not reported by Oakley,[40] the same differences are found in experimental IR spectra measured of pyridine and pyridine hydrochloride (purple dots – Figure 2.10, see Appendix B for full spectra).

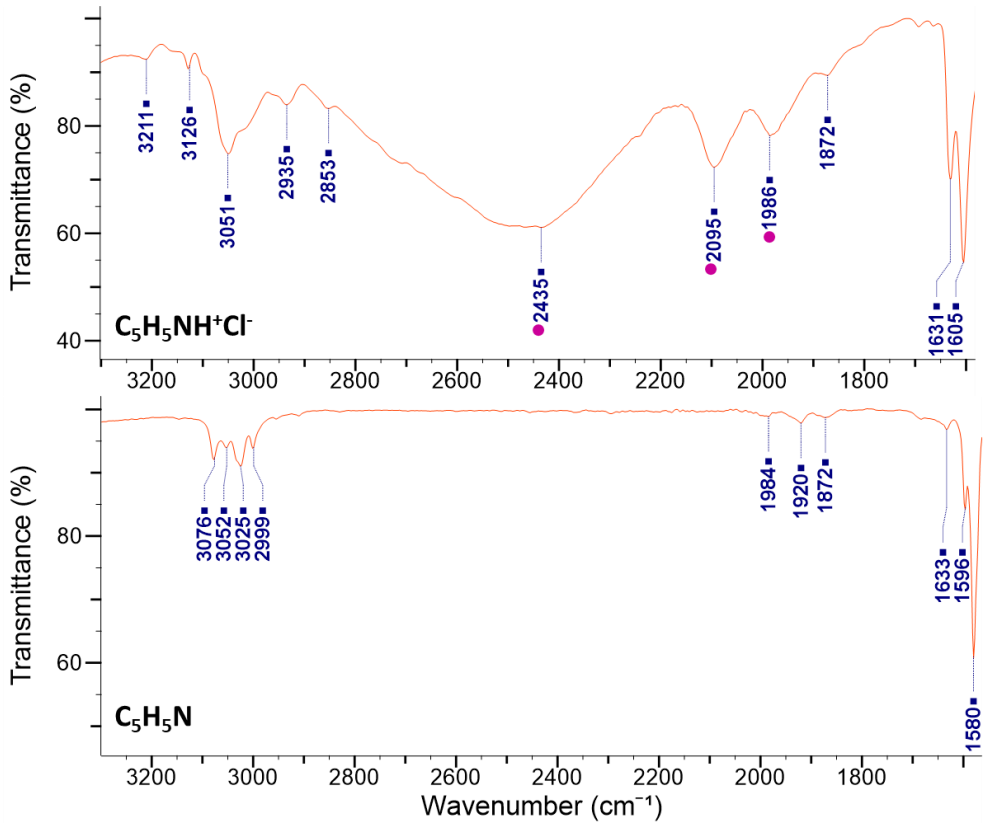

Figure 2.10: IR spectra (functional group region) of pyridine hydrochloride ($C_5H_5H^+Cl^-$) and pyridine (C_5H_5N).

According to Cook, the band at 2435 cm^{-1} arises due to the N-H stretching vibration, which is in agreement with what he reports at 2439 cm^{-1} for pyridine hydrochloride.[54] The broadness and intensity is due to an interaction between the chloride anion and the hydrogen on the pyridyl nitrogen, which could vary dependent on the anion.[54] Therefore, one would not expect to see this band in the IR spectrum of pyridine. Similarly, the broad band at 2461 cm^{-1} (Figure 2.9) for the charged pyrDTDA radical **4** could also be due to the chloride and hydrogen interacting, and is therefore not seen in the IR spectrum of the neutral pyrDTDA radical **5**.

2.3.3 Powder X-Ray Diffraction

Powder X-ray diffraction (PXRD) is a technique that is routinely used to analyze crystalline powdered samples. The resulting powder patterns can then be compared to a calculated pattern obtained from a crystal structure, confirming the correct compound has been prepared. We employed PXRD analysis in an attempt to confirm that the pyrDTDA radicals **4** and **5** as isolated are distinct materials.

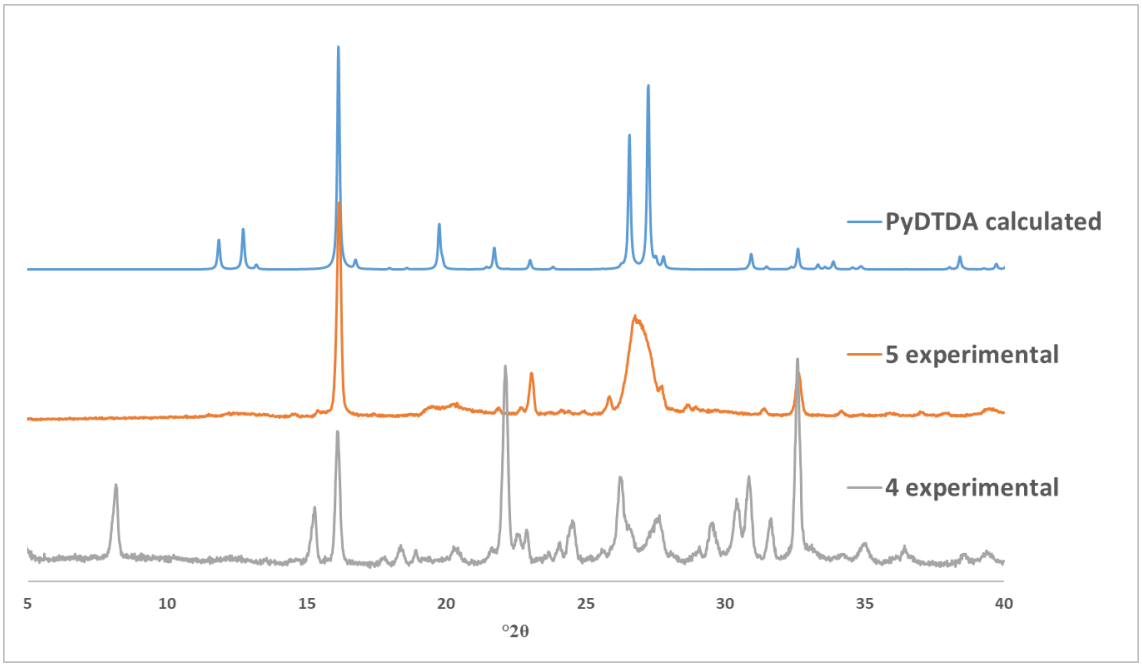

Figure 2.11: Comparison of the PXRD patterns of the two proposed pyrDTDA radicals with the calculated pattern from the CSD - TINQEP.[40]

Generally, when DTDA radicals are purified by sublimation, good quality crystals grow on the cold finger that are suitable for single-crystal X-ray diffraction (SC-XRD). Unfortunately, both pyrDTDA radicals **4** and **5** sublime as crystalline powders, with crystals usually not big enough for SC-XRD. Nevertheless, reproducible powder patterns were obtained, which are illustrated in Figure 2.11.

The Oakley group did not report the PXRD pattern of the charged pyrDTDA radical **4**, but it differs quite significantly from the pattern of the neutral pyrDTDA **5**, with a few peaks in common with the calculated pattern (TINQEP).[40] Radical **4** also has more distinct sharp peaks, as opposed to radical **5** which gave rise to broader peaks and a few 'humps', that could indicate the presence of a disarrayed nanocrystalline phase.[40,55,56]

Due to few differences seen in the diffractograms of **4** and **5**, one can conclude that they are not the same compound, however it is very possible that the bulk material of **4** could contain a mixture of the two radicals.

2.3.4 Other analysis

2.3.4.1 Solid-state UV-Visible Spectroscopy

Solution UV-Vis spectra of several dithiadiazolylium salts have been reported[57–59] since they tend to be brightly coloured, such as orange and yellow. However, reports of solution UV-Vis spectra on DTDA radicals remain limited and even fewer in the case of solid-state UV-Vis spectra. The pyrDTDA radicals **4** and **5** in this work varied between being dark purple and black, which prompted us to measure and evaluate their UV-Vis spectra. In Figure 2.12, the solid-state UV-Vis spectra of pyrDTDA radicals **4** and **5** are illustrated. For neutral pyrDTDA radical **5**, the absorbance range seems to span from approximately 550 nm to 830 nm, whereas in the case of the charged pyrDTDA radical **4**, this range is extended to 930 nm, confirming two different compounds. Attempts were made to record the solution UV-Vis spectra of these compounds as well, but these failed to give any meaningful signal due to the poor solubility of these radicals in common organic solvents.

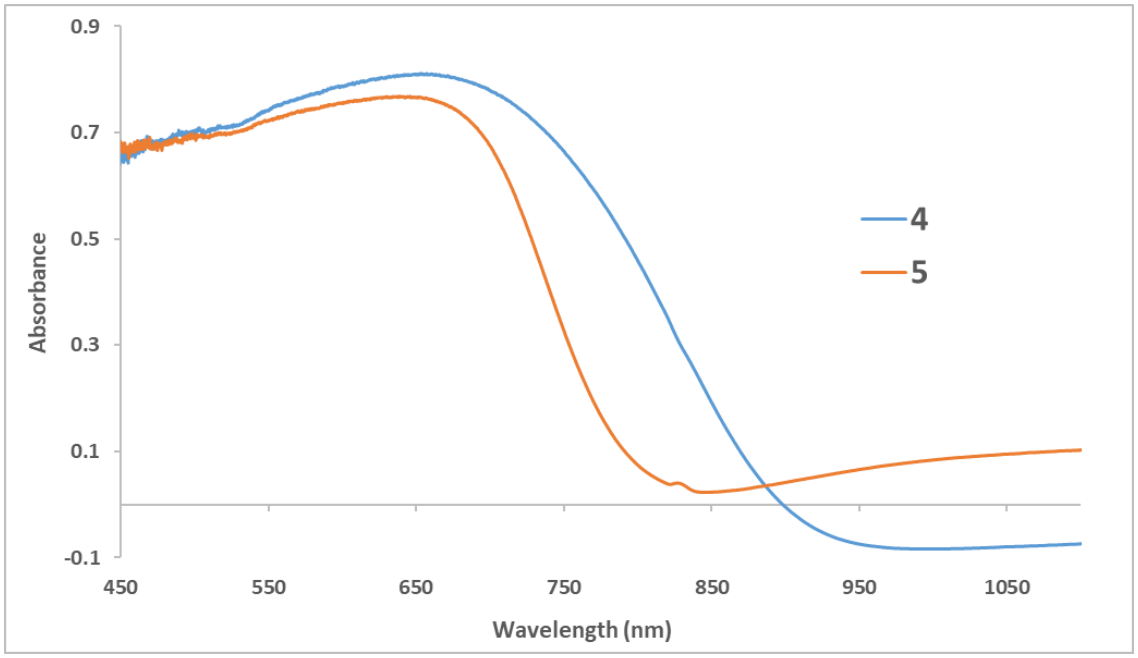

Figure 2.12: Solid-state UV-Vis spectrum, utilizing an integrating sphere of charged pyrDTDA radical **4** and neutral pyrDTDA radical **5**.

2.3.4.2 Elemental analysis

Analysis of the total carbon, nitrogen, hydrogen and sulfur (CHNS) elemental composition of a compound could aid in confirming the correct compound, as well as its purity. In this work, the charged pyrDTDA radical **4** contains a chloride and an additional hydrogen atom, so the elemental composition is different in comparison to the neutral pyrDTDA radical **5**. Table 2.1 contains the calculated percentage elemental composition, as well as the analyzed percentage elemental composition of the pyrDTDA radicals **4** and **5**, which was measured in triplicate for both radicals from the same respective batches (denoted in brackets as 1, 2 and 3). The calculated and analyzed elemental compositions for both pyrDTDA radicals **4** and **5** do not agree. The differences range between 3 – 5% for both radicals, which may be due to the decomposition of the radical samples before analysis. For **5** successive analyzed compositions deviate from the expected values, but match each other quite well, indicating that the sample is pure. It is possible that this sample contains traces of the charged pyrDTDA radical, in addition to the neutral pyrDTDA radical.

Table 2.1: Elemental analysis data for the pyrDTDA radicals **4** and **5**.

	Charged pyrDTDA radical **4**				Neutral pyrDTDA radical **5**			
M_r (g/mol)	218.17				182.25			
Formula	$C_6H_5N_3S_2Cl$				$C_6H_4N_3S_2$			
	C	H	N	S	C	H	N	S
% Element (calculated)	32.95	2.30	19.21	29.32	39.54	2.21	23.06	35.19
% Element (analyzed) (1)	28.40	1.93	19.01	30.47	34.52	2.33	20.36	39.19
% Element (analyzed) (2)	32.57	2.77	20.53	31.61	34.91	2.97	20.75	33.90
% Element (analyzed) (3)	29.94	3.05	19.58	31.54	34.61	3.04	20.54	35.64

2.3.4.3 Mass spectrometry

Mass spectrometry (MS) was also employed to confirm the structures of the pyrDTDA radicals. Illustrated in Figure 2.13 and Figure 2.14 are the single-mass spectra of pyrDTDA radicals **4** and **5**, respectively. It was found that the molecular ion peak $[M + H]^+$ appeared at around 182.993 m/z for both, which matches well with the calculated m/z of 182.9925. This confirms that both materials contain the pyridyl-DTDA unit. Tandem mass analysis (MS/MS) was also carried out with both pyrDTDA radicals, which resulted in the same fragmentation pattern for both materials (see Appendix B).

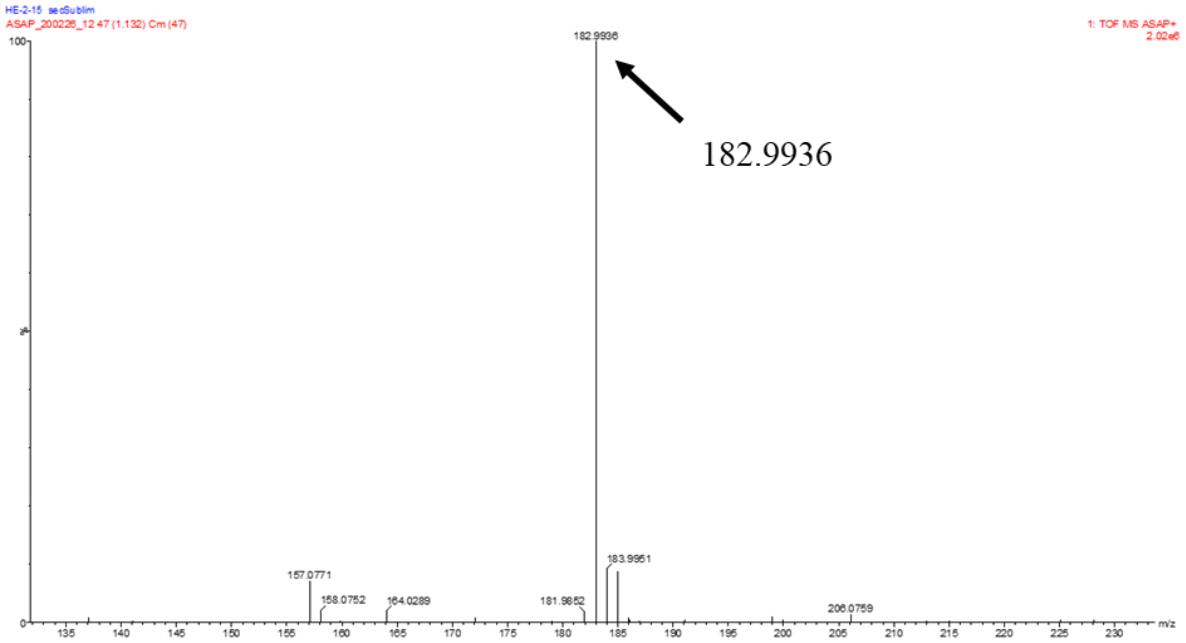

Figure 2.13: Single-mass analysis of the charged pyrDTDA radical **4**.

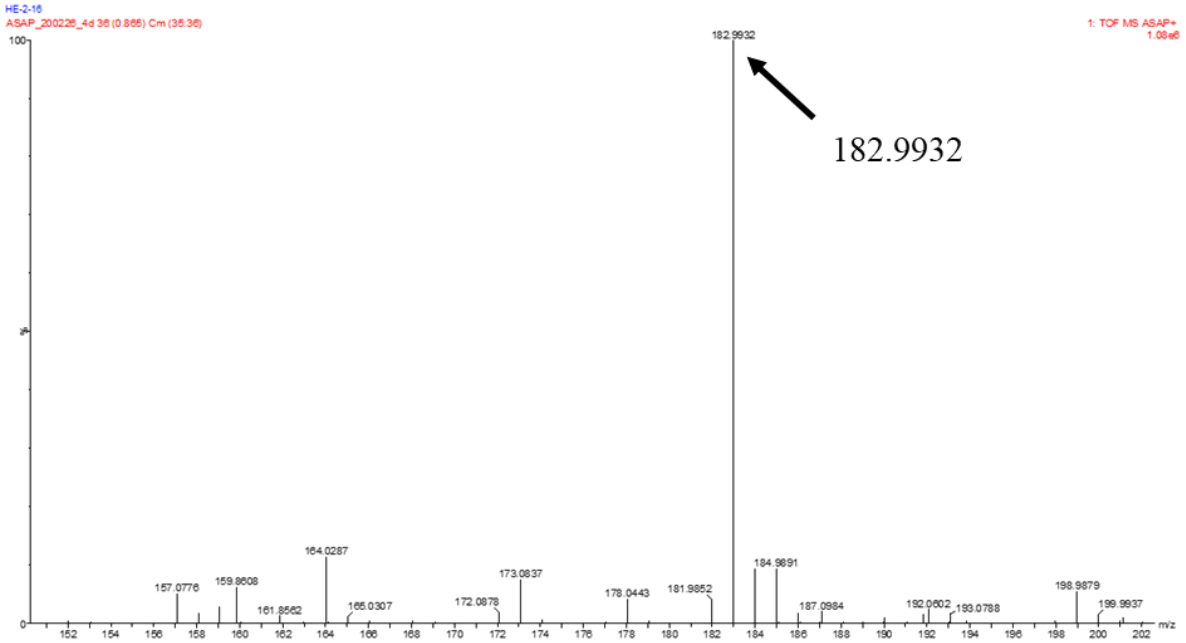

Figure 2.14: Single-mass analysis of the neutral pyrDTDA radical **5**.

2.4 Effect on CP synthesis

Obtaining good quality crystals and bulk material of the CP was a challenge in the initial stages of this investigation, when only a few milligrams could be isolated from each synthesis.[29,34] The use of different solvents (DCM and toluene) and different crystallization techniques was unsuccessful – only solvent layering yielded suitable crystals for SC-XRD.[34] Moderate yields were obtained once the reaction conditions were optimized;[39] generally between 28 to 40 mg per synthesis (44 – 63% yield, based on the CP monomer unit).[39] The optimized reaction conditions involved dissolving CoTPP in dry, degassed THF at 40 °C. After dissolution, excess radical was added and the reaction mixture gently stirred for 2 hours. The resulting suspension was left to stand overnight and precipitated with dry *n*-hexane the next day (Scheme 2.1).[39]

We speculated that if the charged pyrDTDA radical were used in CP synthesis, it would result in lower yields in comparison to using the neutral pyrDTDA. To an extent, this is what we saw when using pure **4** and **5** in synthesis: when the charged pyrDTDA radical **4** was used in CP synthesis, approximately 33 mg (52% yield, based on the monomer unit) was obtained, in line with what was previously obtained with the optimized reaction conditions, whereas the neutral pyrDTDA radical **5** only yielded a few milligrams more with approximately 37 mg (58% yield, based on the monomer unit).

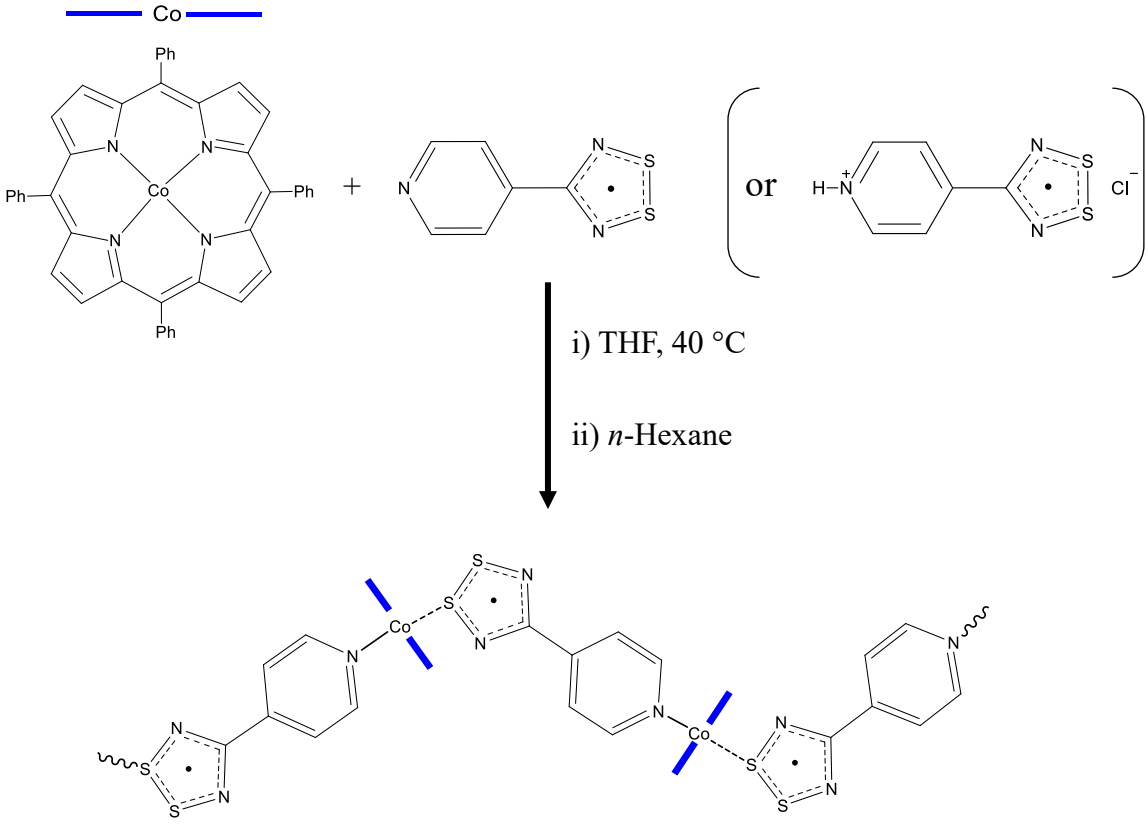

Scheme 2.1: Optimized synthetic procedure for the CP.

This is quite a surprising result, and raises more questions than answers. If the nitrogen of the pyridine ring in radical **4** is protonated, how does it coordinate to the metal and result in comparable yields to the neutral radical **5**? Nonetheless, this remains an interesting result, and implies that the neutral pyrDTDA radical **5** is not necessarily required when synthesizing the CP. IR and UV-Vis data for the two CPs synthesized from the two pyrDTDA radicals are virtually identical (see Appendix B), however, there seem to be subtle differences in the Nuclear Magnetic Resonance (NMR) spectroscopy and MS data (see Appendix B), and investigations are underway to evaluate the significance of this.

2.5 Concluding remarks

In this chapter, the synthesis of a newly discovered coordination polymer – consisting of the 4-(4'-pyridyl)-1,2,3,5-dithiadiazolyl radical and a Co(II) complex of 5,10,15,20-tetraphenylporphyrin (CoTPP) – has been described, with a focus on the coordinated pyrDTDA radical ligand. When the Oakley group proposed the formation of an unprecedented charged radical – protonated at the nitrogen of the pyridine ring – that requires an extra step in the synthesis in order to yield the neutral radical, we speculated whether this was the cause of the low-moderate yields of CP. We extended our investigation, with the aim of acquiring sufficient evidence based on various analytical techniques to comprehensively characterize the charged and neutral pyrDTDA radicals separately, thereby confirming the existence of both. The analytical techniques utilized in this study include EPR spectroscopy, IR spectroscopy, PXRD, solid-state UV-Vis spectroscopy, CHNS analysis and MS. After being able to prepare and characterize them separately, pyrDTDA radicals **4** and **5** were used in CP synthesis, in which no real significant difference in the yields were obtained, which was a surprising result. The IR and UV-Vis data are identical for the two CPs, however subtle differences in NMR and MS have been observed.

2.6 Experimental details

Details of chemicals and instrumentation that were used are provided in Appendix A.

2.6.1 Synthesis of 4-(4'-pyridyl)-1,2,3,5-dithiadiazolyl radical (pyrDTDA)

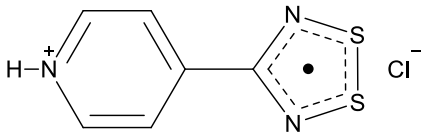

pyrDTDA
4

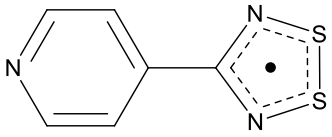

pyrDTDA
5

The radical was synthesized utilizing classical Schlenk techniques. Dry diethyl ether (20 – 30 mL) was added to a nitrogen-filled Schlenk tube. The flask was then cooled down to -78 °C using a dry ice-acetone bath after which hexamethyldisilazane (2.0 mL, 9.54 mmol) and *n*-butyl lithium (7.2 mL, 11.52 mmol) were added slowly by syringe while stirring. The bath was removed and the reaction mixture allowed to warm up to room temperature, noting the colour change of the solution from milky white to clear. 4-pyridinecarbonitrile (1.002 g, 9.62 mmol) was subsequently added, yielding a pale yellow solution, which was allowed to stir overnight. The following day, the solution was a darker pale yellow or ochre colour. The solution was cooled to 0 °C in an ice bath before adding SCl_2 (1.2 mL, 18.9 mmol) dropwise with vigorous stirring. An immediate ochre-coloured precipitate formed. The reaction mixture was allowed to warm to room temperature and stirred for a further 2 – 3 hours. The stirring was stopped and the precipitate allowed to settle. The solid was filtered by cannula filtration, washed with dry diethyl ether (3 × 15 mL) and dried *in vacuo*, yielding a yellow to light orange powder. Dry tetrahydrofuran (THF, 10 mL) was added to the crude double salt, together with Zn/Cu couple (0.462 g, 7.2 mmol). The solution was stirred overnight, or until a complete colour change from ochre to purple had occurred. Excess THF was then removed and the crude product dried *in vacuo*, yielding a purple solid. The solid was transferred to a clean, dry Schlenk tube and purified by sublimation onto a cold finger by heating to 140 – 170 °C under vacuum (1.5 mbar). Radical **4** was obtained as a black crystalline powder on the cold finger (238 mg, 1.09 mmol, 11.4% yield). (+)-ESI-MS: m/z 182.9936. EPR (9.854 GHz, CH_2Cl_2): 3510 G (pentet, a_n = 5.10 G), g = 2.0099. IR (cm^{-1}): 3123 (w) 3044 (s), 2808 (w), 2461 (b, s), 2091 (w), 1992 (w), 1767 (w), 1633 (w), 1609 (w), 1520 (w), 1508 (w), 1401 (s), 1366 (m), 1335 (w), 1248 (w), 1191 (w), 1147 (w), 1086 (w), 1053 (w), 1001 (w), 978, 830 (m), 818 (s), 779 (s), 725 (m), 663 (w), 641 (m), 515 (m), 443 (w), 408 (w).

The same procedure was followed for radical **5**. Once crude **4** was obtained, dry acetonitrile (20 mL) was added to the crude solid, together with excess triethylamine (NEt_3, 2.7 mL, 19.4 mmol). The mixture was allowed to stir for an hour. The resulting solid was filtered by cannula filtration, washed with dry acetonitrile (3 × 15 mL) and dried *in vacuo*, yielding a purple solid. The solid was then transferred to a clean, dry Schlenk and purified by sublimation onto a cold finger by heating to 90 – 140 °C under vacuum (1.5 mbar). Radical **5** was obtained as black blocks on the cold finger (0.159 g, 0.87 mmol, 9.1% yield). (+)-ESI-MS: m/z 182.9932. EPR (9.854 GHz, CH_2Cl_2): 3512 G (pentet, a_n = 5.01 G), g = 2.0098. IR (cm^{-1}): 3026 (b, w), 1687 (b, w), 1596 (w), 1413 (s), 1368 (m), 1331 (w) 1209 (b, m), 1139 (m) 1061 (m), 1011 (w), 997 (w), 912 (w), 826 (m), 807 (m), 653 (s), 509 (m), 480 (w), 459 (w).

2.6.2 Co(II) tetraphenylporphyrin – 4-(4'-pyridyl)-1,2,3,5-dithiadiazolyl radical coordination polymer (CP)

The optimized synthetic procedure for synthesis of the CP is given, using pyrDTDA radical **4** as an example.[39]

CoTPP (50 mg, 0.074 mmol) was dissolved in dry, degassed THF (20 mL). A few minutes was allowed for dissolution to occur, after which pyrDTDA radical **4** (34 mg, 0.155 mmol) was added under N_2 and the resulting dark red mixture was stirred gently at 40 °C for 2 hours. After the allotted time, stirring was stopped and the reaction mixture kept at room temperature overnight under N_2. The next day, dry *n*-hexane (40 mL) was added to precipitate the CP. The reaction mixture was filtered and dried in *vacuo* to yield CP as a brown powder (33 mg, 52% yield based on the monomer unit). UV-Vis (DMSO): 436 nm, 551 nm, 592 nm. IR (cm^{-1}): 3053 (b, w), 1693 (w) 1615 (w), 1532 (w), 1489 (w), 1442 (w), 1415 (w), 1351 (w), 1209 (w), 1178 (w), 1147 (w), 1116 (w), 1073 (w), 1009 (m), 842 (w), 795 (m), 752 (m), 702 (m), 665 (w), 589 (w), 525 (w), 470 (w), 449 (w).

The same procedure was followed for CP synthesis using neutral pyrDTDA radical **5**. IR and UV-Vis are identical, however subtle differences have been observed with the NMR and MS, which are not reported here, see Appendix B for spectra.

2.7 References

1 J. M. Rawson, A. J. Banister and I. Lavender, *Adv. Heterocycl. Chem.*, 1995, **62**, 137-247.

2 R. G. Hicks, *Stable radicals: Fundamentals and Applied Aspects of Odd-Electron*

compounds, John Wiley & Sons, Ltd, Chichester, West Sussex, 1st edn., 2010.

3 D. A. Haynes, *CrystEngComm*, 2011, **13**, 4793–4805.

4 J. M. Rawson, A. Alberola and A. Whalley, *J. Mater. Chem.*, 2006, **16**, 2560–2575.

5 M. M. Labes, P. Love and L. F. Nichols, *Chem. Rev.*, 1979, **79**, 1–15.

6 R. G. Hicks, *Org. Biomol. Chem.*, 2007, **5**, 1321–1338.

7 K. E. Preuss, *Dalt. Trans.*, 2007, 2357–2369.

8 O. A. Rakitin, *Russ. Chem. Rev.*, 2011, **80**, 647–659.

9 I. Ratera and J. Veciana, *Chem. Soc. Rev.*, 2012, **41**, 303–349.

10 K. E. Preuss, *Coord. Chem. Rev.*, 2015, **289**–**290**, 49–61.

11 C. P. Constantinides and P. A. Koutentis, *Stable N- and N/S-Rich Heterocyclic Radicals: Synthesis and Applications*, Elsevier Ltd, 2016, vol. 119.

12 R. T. Boere, R. T. Oakley, R. W. Reed and N. P. C. Westwood, *J. Am. Chem. Soc.*, 1989, **111**, 1180–1185.

13 A. J. Banister, I. B. Gorrell, W. Clegg and K. A. Jørgensen, *J. Chem. Soc. Dalt. Trans.*, 1991, **270**, 1105–1109.

14 A. W. Cordes, C. D. Bryan, W. M. Davis, R. H. de Laat, S. H. Glarum, J. D. Goddard, R. C. Haddon, R. G. Hicks, D. K. Kennepohl, R. T. Oakley, S. R. Scott and N. P. C. Westwood, *J. Am. Chem. Soc.*, 1993, **115**, 7232–7239.

15 P. J. Alsonso, G. Antorrena, J. I. Martinez, J. J. Novoa, F. Palacio, J. M. Rawson and J. N. B. Smith, *Appl. Magn. Reson.*, 2001, **20**, 231–247.

16 J. Luzon, J. Campo, F. Palacio, G. J. McIntyre, J. M. Rawson, R. J. Less, C. M. Pask, A. Alberola, R. D. Farley, D. M. Murphy and A. E. Goeta, *Phys. Rev. B*, 2010, **81**, 1–12.

17 A. J. Banister, I. B. Gorrell, W. Clegg and K. A. Jørgensen, *J. Chem. Soc. Dalt. Trans.*, 1989, 2229–2233.

18 A. J. Banister, I. B. Gorrell, S. E. Lawrence, C. W. Lehmann, I. May, G. Tate, A. J. Blake and J. M. Rawson, *J. Chem. Soc. Chem. Commun.*, 1994, 1779–1780.

19 R. T. Boeré, K. H. Moock, V. Klassen, J. Weaver, D. Lentz and H. Michael-Schulz, *Can. J. Chem.*, 1995, **73**, 1444–1453.

20 A. J. Banister, J. A. K. Howard, I. May and J. M. Rawson, *Chem. Commun.*, 1997, 1763–1764.

21 A. J. Banister, I. B. Gorrell, J. A. K. Howard, S. E. Lawrence, C. W. Lehman, I. May, J. M. Rawson, B. K. Tanner, C. I. Gregory, A. J. Blake and S. P. Fricker, *J. Chem. Soc. - Dalt. Trans.*, 1997, 377–384.

22 W.-K. Wong, C. Sun, W.-Y. Wong, D. W. J. Kwong and W.-T. Wong, *Eur. J. Inorg. Chem.*, 2000, **2**, 1045–1054.

23 N. G. R. Hearns, K. E. Preuss, J. F. Richardson and S. Bin-Salamon, *J. Am. Chem. Soc.*, 2004, **126**, 9942–9943.

24 M. Jennings, K. E. Preuss and J. Wu, *Chem. Commun.*, 2006, 341–343.

25 J. Britten, N. G. R. Hearns, K. E. Preuss, J. F. Richardson and S. Bin-Salamon, *Inorg. Chem.*, 2007, **46**, 3934–3945.

26 N. G. R. Hearns, R. Clérac, M. Jennings and K. E. Preuss, *Dalt. Trans.*, 2009, 3193–3203.

27 N. G. R. Hearns, K. D. Hesp, M. Jennings, J. L. Korčok, K. E. Preuss and C. S. Smithson, *Polyhedron*, 2007, **26**, 2047–2053.

28 E. M. Fatila, R. Clérac, M. Rouzières, D. V. Soldatov, M. Jennings and K. E. Preuss, *J. Am. Chem. Soc.*, 2013, **135**, 13298–13301.

29 D. A. Haynes, L. J. Van Laeren and O. Q. Munro, *J. Am. Chem. Soc.*, 2017, **139**, 14620–14637.

30 V. Lyaskovskyy and B. De Bruin, *ACS Catal.*, 2012, **2**, 270–279.

31 R. T. Boeré, K. H. Moock and M. Parvez, *Z. anorg. allg. Chem.*, 1994, **620**, 1589–1598.

32 J. A. Stubbe and W. A. Van Der Donk, *Chem. Rev.*, 1998, **98**, 705–762.

33 I. Beletskaya, V. S. Tyurin, A. Y. Tsivadze, R. Guilard and C. Stern, *Chem. Rev.*, 2009, **109**, 1659–1713.

34 L. J. van Laeren, Investigation of thiazyl radical-metalloporphyrin complexes, Stellenbosch University, 2017.

35 B. Meunier, *Chem. Rev.*, 1992, **92**, 1411–1456.

36 C. M. Che and J. S. Huang, *Chem. Commun.*, 2009, 3996–4015.

37 J. C. Barona-Castaño, C. C. Carmona-Vargas, T. J. Brocksom and K. T. De Oliveira, *Molecules*, 2016, **21**, 1–27.

38 M. J. F. Calvete, M. Piñeiro, L. D. Dias and M. M. Pereira, *ChemCatChem*, 2018, **10**, 1–25.

39 N. Chaudhary and D. A. Haynes, *Unpublished work*.

40 A. I. Taponen, J. W. L. Wong, K. Lekin, A. Assoud, C. M. Robertson, M. Lahtinen, R. Clérac, H. M. Tuononen, A. Mailman and R. T. Oakley, *Inorg. Chem.*, 2018, **57**, 13901–13911.

41 S. W. Robinson, D. A. Haynes and J. M. Rawson, *CrystEngComm*, 2013, **15**, 10205–10211.

42 H. L. Olin, *J. Am. Chem. Soc.*, 1926, **48**, 167–168.

43 B. Vasconcellos Da Silva, *Synlett*, 2008, 1265–1266.

44 S. A. Fairhurst, K. M. Johnson, L. H. Sutcliffe, K. F. Preston, A. J. Banister, Z. V. Hauptman and J. Passmore, *J. Chem. Soc. Dalt. Trans.*, 1986, 1465–1472.

45 A. J. Banister, N. Bricklebank, W. Clegg, M. R. J. Elsegood, C. I. Gregory, I. Lavender, J. M. Rawson and B. K. Tanner, *J. Chem. Soc. Chem. Commun.*, 1995, 679–680.

46 A. J. Banister, N. Bricklebank, I. Lavender, J. M. Rawson, C. I. Gregory, B. K. Tanner, W. Clegg, M. R. J. Elsegood and F. Palacio, *Angew. Chemie Int. Ed. English*, 1996, **35**, 2533–2535.

47 Y. Beldjoudi, A. Arauzo, F. Palacio, M. Pilkington and J. M. Rawson, *J. Am. Chem. Soc.*, 2016, **138**, 16779–16786.

48 A. J. Banister, N. R. M. Smith and R. G. Hey, *J. Chem. Soc. Perkin Trans. 1*, 1983, 1181–1186.

49 D. L. Pavia, G. M. Lampman and G. S. Kriz, *Introduction to Spectroscopy*, Thomson Brooks/Cole, Bellingham, 2001.

50 A. Alberola, E. Carter, C. P. Constantinides, D. J. Eisler, D. M. Murphy and J. M. Rawson, *Chem. Commun.*, 2011, **47**, 2532–2534.

51 C. P. Constantinides, D. J. Eisler, A. Alberola, E. Carter, D. M. Murphy and J. M. Rawson, *CrystEngComm*, 2014, **16**, 7298–7312.

52 C. P. Constantinides, E. Carter, D. Eisler, Y. Beldjoudi, D. M. Murphy and J. M. Rawson, *Cryst. Growth Des.*, 2017, **17**, 3017–3029.

53 L. Beer, A. W. Cordes, D. J. T. Myles, R. T. Oakley and N. J. Taylor, *CrystEngComm*, 2000, **2**, 109–114.

54 D. Cook, *Can. J. Chem.*, 1961, **39**, 2009–2024.

55 T. E. Gorelik, C. Czech, S. M. Hammer and M. U. Schmidt, *CrystEngComm*, 2016, **18**, 529–535.

56 K. Lekin, A. A. Leitch, A. Assoud, W. Yong, J. Desmarais, J. S. Tse, S. Desgreniers, R. A. Secco and R. T. Oakley, *Inorg. Chem.*, 2018, **57**, 4757–4770.

57 G. G. Alange, A. J. Banister, B. Bell and P. W. Millen, *J. Chem. Soc. Perkin Trans. 1*, 1979, 1192–1194.

58 T. Chivers, F. Edelmann, J. F. Richardson, N. R. M. Smith, O. Treu and M. Trsic, *Inorg. Chem.*, 1986, **25**, 2119–2125.

59 M. Amin and C. W. Rees, *J. Chem. Soc. Perkin Trans. 1*, 1989, 2495–2501.

Chapter 3

Catalysis in solution – Co-porphyrins as catalysts in the oxidation of benzyl alcohol

3.1 Introduction

Metalloporphyrins in catalysis have been the topic of a substantial amount of research since the discovery of cytochrome P-450, which at its centre, contains an iron porphyrin scaffold.[1-3] Cytochrome P-450 is an example of a hemoprotein within the human body that is able to efficiently catalyze oxidation reactions of substrates such as amines, sulfides, alcohols and even saturated hydrocarbons under mild reaction conditions.[1–3] Drawing inspiration from these systems, research has gone into developing synthetic models to mimic these reactions, which then in turn can be utilized in synthetic organic chemistry.[2] In 1979, the first synthetic metalloporphyrin was applied in epoxidation and hydroxylation reactions, developed by Groves and coworkers.[4] Since then, several reviews have been published on metalloporphyrins utilized in oxidation catalysis.[3,5–9] Among all the possible substrates for oxidation, the oxidation of alcohols is a particularly appealing chemical transformation in terms of fundamental research and in organic chemistry.[10,11] More specifically, the oxidation of benzyl alcohol is of great interest because the resulting carbonyl compound after oxidation can serve as a precursor for manufacturing purposes in the pharmaceutical and agricultural industries.[12]

In general, metalloporphyrin complexes of Fe(III), Mn(III) and Ru(II-VI) have provided the best catalytic results with regards to oxidation reactions to date, and reports involving these ions are therefore more prevalent in the literature, with fewer examples of Co(II/III) complexes being reported.

The structure of the porphyrin scaffold has a significant influence on the catalytic reaction, with specific reference to the *meso* positions: if no substituents are present on these positions, the metalloporphyrin catalyst is susceptible to degradation, resulting in a loss of catalytic activity.[1,5,7] The stability of the catalysts was improved by attaching phenyl (and related) groups to these positions.[1,5,7] Furthermore, additional substituents on the phenyl ring (*ortho*, *meta* and *para* to the porphyrin core structure) and pyrrolic β-positions led to the development of three

generations of catalyst, with each successive generation superior to its predecessor in terms of stability and catalytic activity.[1,5,7,9]

In addition to the porphyrin scaffold, axial ligation of other ligands to the metal center is also possible, generating 5- or 6-coordinate complexes.[13,14] Research into changing substituents on the porphyrin ligand and how it influences the catalytic activity and selectivity has been reported,[9,15] but fewer efforts have gone into probing the effect of the axial ligand. Nam and coworkers have shown for a Fe-porphyrin complex that the nature of the axial ligand has a remarkable effect on the hydroxylation of alkanes.[16] When the Fe-porphyrin bears an electron-donating ligand, such as a methoxy group (–OMe), hydrogen abstraction is enhanced and oxo-transfer happens more readily, thereby improving catalytic performance.[16] Considering these insights, we were curious to see how the newly-discovered coordination polymer (CP) (Chapter 2) would perform in oxidation catalysis.

This is a particularly interesting venture because of the structure of the CP: CoTPP scaffolds are bridged by pyrDTDA radicals to form a polymer in the solid state, which dissociates upon dissolution, yielding a Co(III)-containing monomer. The coordination of the pyridine nitrogen dominates in solution, and as a result, the catalytic species can be considered as the 5-coordinate species shown in Figure 3.1. In addition, studies on the catalytic capabilities of DTDA-metal complexes remain unexplored.

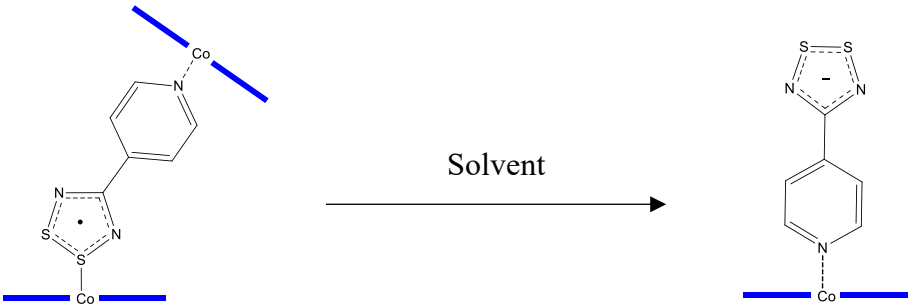

Figure 3.1: The CP dissociates into a 5-coordinate species when dissolved.

Preliminary work by Dr Chaudhary in our group investigated CP as a catalyst for the oxidation of benzyl alcohol to the corresponding carbonyl compounds (Figure 3.2), with promising results.[17] In order to probe the catalytic potential of CP, Dr Chaudhary carried out a series of reactions to optimize the catalytic reaction conditions. This was achieved in a systematic fashion, by varying one parameter at a time and keeping the other parameters constant in order to evaluate the effect each parameter has on the conversion of benzyl alcohol. This resulted in the following optimized reaction conditions: 0.5 mmol of benzyl alcohol was stirred in

acetonitrile at 70 °C for 16 hours, with addition of 1 mmol *tert*-butyl hydroperoxide (TBHP) and 1 mol% catalyst loading.[17] This was the starting point for the current study.

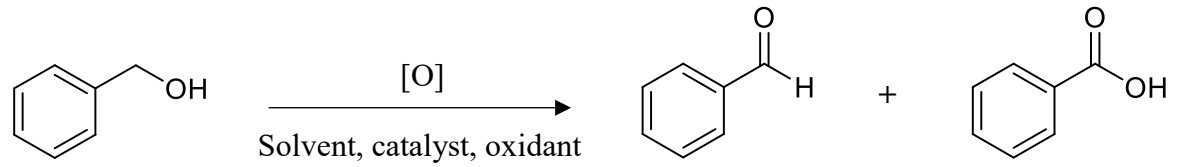

Figure 3.2: Conventional oxidation reaction of benzyl alcohol to the carbonyl compounds benzaldehyde and benzoic acid.

The apparent success of CP as an oxidation catalyst led us to extend the study by comparing the catalytic potential of CP to other CoTPP derivatives bearing different axial ligands. We aimed to assess the effect of the axial ligand, as well as the concomitant change in oxidation state of the metal, on the catalysis. More specifically in the case of the CP, we wanted to establish whether the DTDA ligand is important to the catalytic reaction.

3.2 Catalysis: Comparative study

3.2.1 Co-porphyrin catalysts

The CoTPP derivatives (aside from the CP) that were used as catalysts during the course of this study are illustrated in Figure 3.3.

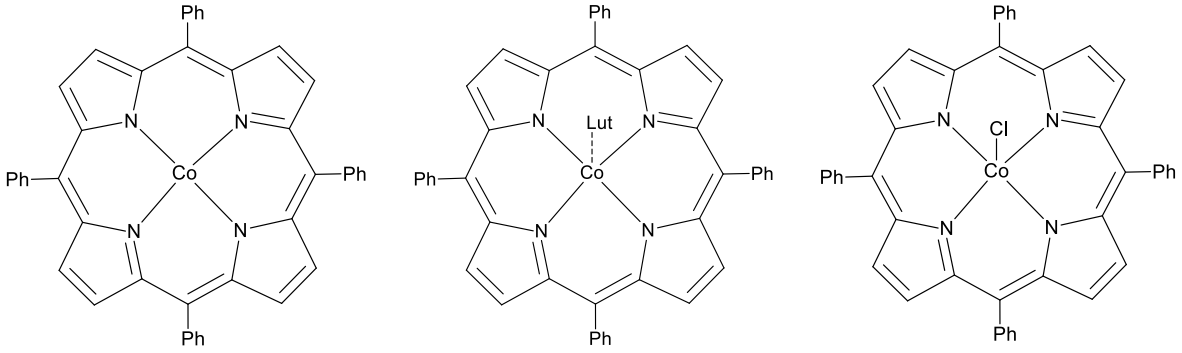

CoTPP **CoTPP-Lut** **CoTPP-Cl**

Figure 3.3: Co-porphyrin catalysts. The classic cobalt (II) *meso*-tetraphenylporphyrin (CoTPP) (left) without any axial ligand, in the middle, 3,5-dimethylpyridine cobalt (II) *meso*-tetraphenyloprphyrin (CoTPP-Lut) with 3,5-dimethylpyridine as axial ligand, and on the right, cobalt (III) *meso*-tetraphenylporphyrin chloride (CoTPP-Cl) with a chloride as axial ligand.

By comparing these catalysts to one another, we hoped to make certain conclusions: firstly, will there be an effect on the conversion of benzyl alcohol between these complexes bearing different axial ligands? If so, would be this be due to the ligand or the concomitant change in oxidant state of the Co-metal center? During the catalytic reaction, TBHP coordinates to the

Co-metal center and oxidizes it from +2 to +3, regardless of whether an axial ligand is present, and if it is already in the oxidation state +3, the valency does not change.[18] Therefore, what effect will the oxidation of the Co-metal center have if it is already in the oxidation state +3 due to another axial ligand?

All four catalysts, CP included, have the same porphyrin structure of a typical 1st generation catalyst (Chapter 1), with no additional substituents on the phenyl ring or *β*-pyrrolic positions.[5,7,9] These complexes were all prepared using literature procedures. The well-known methods developed by Adler and coworkers were used to prepare TPP and CoTPP (see Chapter 1).[19,20] CoTPP-Lut was discovered by Scheidt and Ramanuja after it unexpectedly crystallized from a solution of CoTPP dissolved in a chloroform-2,4,6-trimethylpyridine mixture where 3,5-lutidine (also known as 3,5-dimethylpyridine) was present as an impurity.[21] Therefore we attempted to prepare it by dissolving CoTPP in a chloroform-3,5-lutidine mixture. It must be noted that the even though the precipitate seems pure, when dissolved, a mixture of CoTPP and CoTPP-Lut exist in solution due to the dissociation of the 3,5-lutidine, as is evident from the UV-Vis spectroscopy data (see Appendix B – Figure B.16). The preparation and structural study of CoTPP-Cl was pioneered by Sakurai and coworkers,[22,23] but in this study a modified method from the Rieger group was used.[24,25]

CoTPP has previously been explored as catalyst, with several reports on its use in the oxidation of alkanes with molecular oxygen.[9,26–29] Similary, CoTPP-Cl has also been used in the oxidation of alkanes[30,31] and alcohols,[32] and is also able to catalyze the polymerization of carbon dioxide and epoxides.[24,25,33] CoTPP-Lut has not been explored as a catalyst, however there are reports of CoTPP with pyridine as axial ligand catalyzing oxidative polymerizations of indene and 1,1-diphenylethylene, as well as oxidative copolymerization of styrene with α-methylstyrene.[34-36]

3.2.2 Experimental notes and obstacles

A significant amount of time was spent at the start of this study optimizing the analysis of the products of the catalytic reaction. Gas chromatography was used to quantify the products, but we were plagued by instrumental and software problems. Over 50 analyses were carried out before a robust procedure for quantifying the reaction products was developed.

The catalytic experiments were carried out with TBHP as a 70% by weight solution in water instead of TBHP in decane (5 – 6 M). Initial experiments with TBHP in decane yielded several additional peaks in the chromatogram, which could be due to the formation of oxygenated

hydrocarbon products during the catalytic reaction, since decane is part of the reaction mixture and metalloporphyrins are known to oxidize aliphatic hydrocarbons. Therefore, concerned that some of these peaks might overlap with our product peaks (benzaldehyde and benzoic acid) and complicate quantitative analysis, we decided to use TBHP in water. The CP that was used for catalytic experiments in this work was previously prepared by Dr Nikita Chaudhary.

All experiments were carried out in duplicate and at the optimized reaction conditions: 0.5 mmol benzyl alcohol, 1 mmol TBHP, 4.8 mL of acetonitrile (to yield a final reaction volume of 5 mL), 70 °C, 16 hours (see Experimental section for details). The conversion of benzyl alcohol was calculated by using the internal standard method, with *p*-xylene as the internal standard. Conversion was based on the amount of benzyl alcohol that was left after the completion of the reaction. The amount of benzaldehyde and benzoic acid that formed was also calculated by using the internal standard method, with *p*-xylene as the internal standard. The selectivity of benzaldehyde over benzoic acid is the mole ratio of benzaldehyde to the total mole amount obtained for benzaldehyde and benzoic acid, expressed as a percentage. The full set of catalytic results are tabulated and can be found in Appendix B.

3.2.3 Effect on benzyl alcohol conversion

The preliminary work carried out by Dr Chaudhary indicated that some parameters make a noticeable difference in the conversion of benzyl alcohol to the corresponding aldehyde,[17] in particular the catalyst loading, type of oxidant and oxidant amount. An increase in the conversion of benzyl alcohol was observed as the catalyst loading of the CP was increased from 0.5 mol% to 1.5 mol%.[17] Furthermore, molecular oxygen and hydrogen peroxide were also employed as oxidants, but failed to result in any significant conversion, while TBHP (5.0 – 6.0 M in decane solution) resulted in very high conversions in the presence of the CP.[17] TBHP has previously been used in the oxidation of benzyl alcohol,[37–40] but it was still quite surprising how molecular oxygen and hydrogen peroxide performed so poorly, considering that they have also been shown to oxidize a variety of organic substrates[41,42] as well as alkanes and alcohols,[8] in the presence of metalloporphyrin catalysts.

Intrigued by the pronounced difference when using TBHP, we thought that it would be interesting to note the effect it would have on the catalytic reaction without a catalyst present, and so a control experiment was carried out. Even without a catalyst present, TBHP still oxidizes benzyl alcohol with just above 60% conversion, as depicted in Figure 3.4. This is possibly due to the long reaction time, as another group reported 10% conversion in 6 hours at 80 °C in acetonitrile,[43] and so allowing it to stir for 16 hours could result in high conversions.

Also shown here are the resulting conversion percentages for all four catalysts at 1.5 mol% catalyst loading at the optimized reaction conditions, all resulting in above 75% conversion. The effect of loading is depicted in Figure 3.5. All catalysts give above 70% conversion at all loadings, showing that inclusion of a catalyst results in somewhat higher conversions of benzyl alcohol.

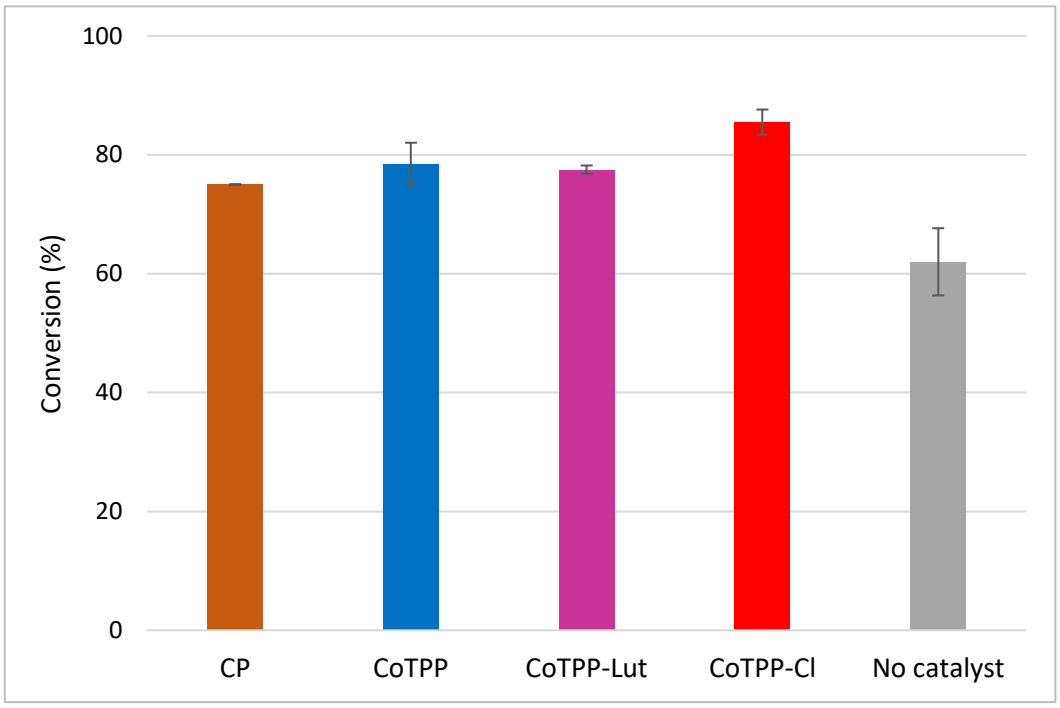

Figure 3.4: Influence of each catalyst on the conversion of benzyl alcohol at a catalyst loading of 1.5 mol%. Conversion without catalyst and only oxidant is also included for comparison. Reaction conditions: 0.5 mmol benzyl alcohol, 1 mmol TBHP, 70 °C, 16 hours, 5 mL reaction volume.

In Figure 3.5, conversion is displayed as a function of the different catalyst loadings. The experiments were carried out at the optimized reaction conditions, but changing the catalyst loading for each catalyst. For CoTPP, catalyst loadings of 0.5 mol% and 1.0 mol% essentially result in the same conversion for each catalyst at approximately 76% conversion. When the catalyst loading is increased to 1.5 mol%, there seems to be a slight increase to 78.5% conversion. The difference, however, is within error and so it appears that changing the catalyst loading for CoTPP does not really result in higher conversions. On the other hand, reactions with CoTPP-Lut also give in similar conversions at 0.5 mol% and 1.0 mol%, with approximately 73% conversion, but there seems to be a clear increase when 1.5 mol% catalyst loading is used. In this case, approximately 77.5% conversion was obtained at the highest catalyst loading.

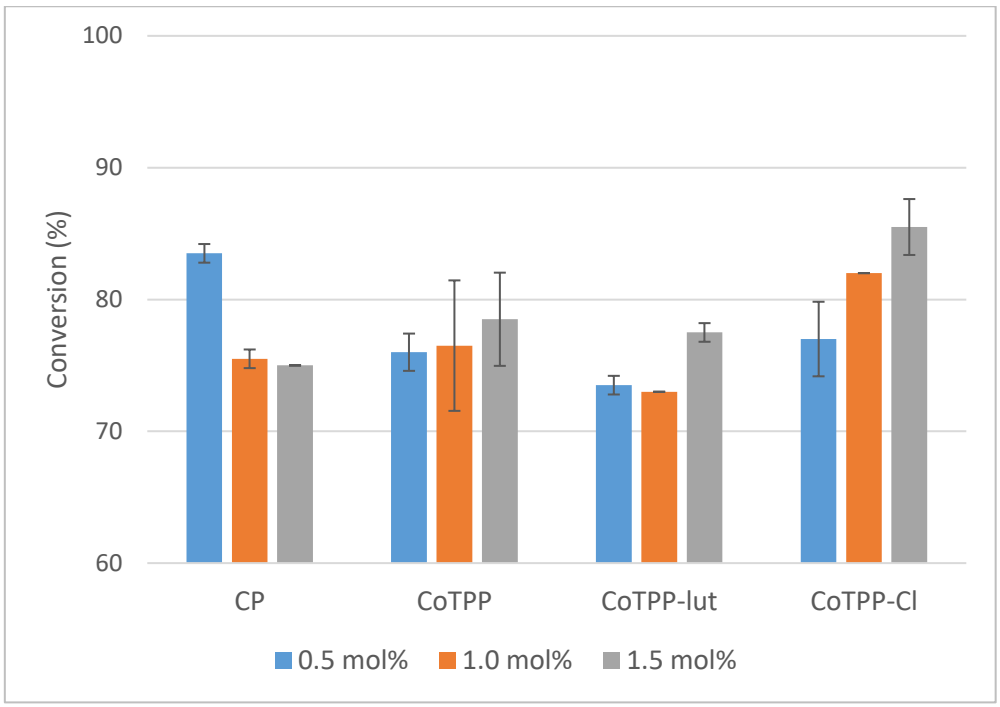

Figure 3.5: Influence of different catalyst loadings on the conversion of benzyl alcohol. Reaction conditions: 0.5 mmol benzyl alcohol, 1 mmol TBHP, 70 °C, 16 hours, 5 mL reaction volume.

The conversions obtained for CoTPP seems to be slightly higher overall in comparison to CoTPP-Lut. This was quite an interesting observation, especially considering that mixtures of both CoTPP and CoTPP-Lut are present in solution due to the dissociation of the 3,5-lutidine from CoTPP, which reveals that the 3,5-lutidine ligand could have an effect on the catalytic reaction.

With the CoTPP-Cl catalyst, there is a steady increase in conversion as more catalyst is added, which increases from 77% conversion at 0.5 mol% to 86% conversion at 1.5 mol%. Generally, higher conversions were obtained for CoTPP-Cl at all catalyst loadings in comparison to CoTPP and CoTPP-Lut. In contrast, the catalysis results of the CP present a slightly different picture. A similar conversion was obtained to that for CoTPP-Cl, but at a lower catalyst loading. A conversion of 84% was obtained at 0.5 mol% loading, after which it drops to ~ 75% for both 1.0 and 1.5 mol%. The conversion of benzyl alcohol with the CP at 0.5 mol% catalyst loading was the highest in comparison to all the other catalysts at the same catalyst loading of 0.5 mol%.

From Figure 3.4 it is evident that the inclusion of a catalyst is making a difference in the conversion, albeit not significantly. A possible explanation for the moderate increase in conversion could be that the Co-porphyrin is undergoing oxidative degradation during the reaction and so is only involved in the catalytic reaction for a short while, causing a slight increase in conversion in comparison to when no catalyst is present. The degradation involves the formation of a *meso*-hydroxyporphyrin after hydroxylation at the *meso* position (Figure

3.6), inactivating the catalyst.[5,7,18,44] According to a study by Mamardashvili, who studied the destruction processes of CoTPP in the presence of peroxides, as soon as the peroxide coordinates to the metal center, the porphyrin starts to degrade almost immediately,[18] meaning it is not in a catalytic active form for very long, which could explain the low activity.

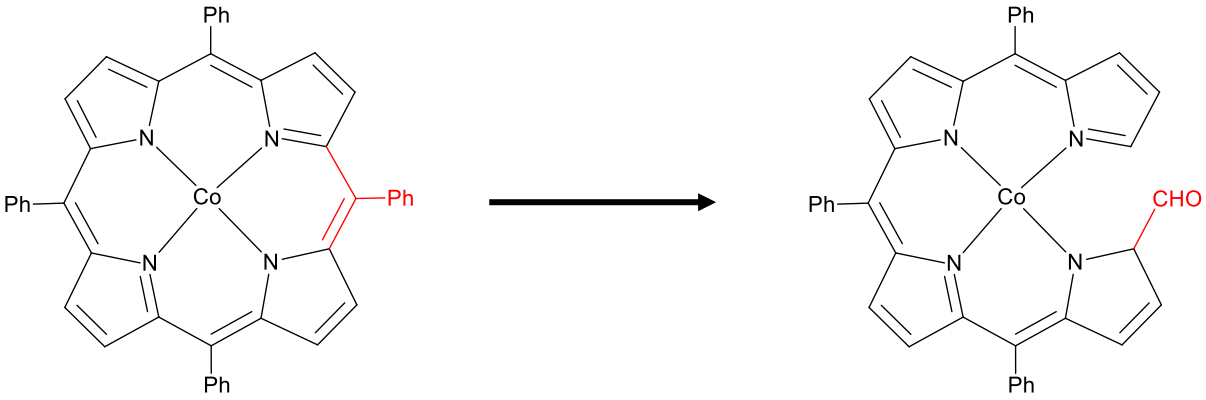

Figure 3.6: Hydroxylation at the meso position (in red) of CoTPP (as an example) to form the meso-hydroxyporphyrin.

It does seem like the majority of the Co-porphyrin catalysts achieve a higher conversion at higher catalyst loadings, which could just simply be due to there being more catalyst present, resulting in greater oxidation activity. However, the opposite is seen with the CP: lower catalyst loadings result in higher conversions, which could possibly be due to the tendency of porphyrins to aggregate in solution at certain concentrations. According to Lavallee, researchers prefer to work at 10^{-5} M concentrations of metalloporphyrin in solution to avoid aggregation.[45] In this work, Co-porphyrin concentrations ranged between $4.9 \times 10^{-4} – 1.5 \times 10^{-3}$ M, and so it is very possible that some aggregation occurred. This implies that, at higher catalyst loadings, it is possible for the CP to aggregate in solution, obstruct the binding of the peroxide and slow down catalysis, resulting in low conversion as opposed to higher conversions at lower catalyst loadings, where less aggregation is probable.[45,46] Unfortunately, this postulation does not justify the results obtained for the other three catalysts, and so if it turns out that aggregation is not likely at the concentrations we have been working with, it is possible that other characteristics of the CP is at play, such as the redox properties, which have been shown to be quite interesting,[47] but demand further investigation.

These results also show that the Co-porhyrin catalysts in the +3 oxidation state perform better, *i.e.* CoTPP-Cl and the CP result in higher conversions of benzyl alcohol than CoTPP and CoTPP-Lut, in which the cobalt metal center is in the +2 oxidation state. This will be further discussed in Section 3.2.5.

3.2.4 Effect on benzaldehyde selectivity

Preliminary work indicated that catalysis with the CP results in over-oxidation of benzyl alcohol to benzoic acid.[17] In Figure 3.7, the selectivity for benzaldehyde over benzoic acid is shown as a function of the catalyst loading for each catalyst. For instance, in the case of no catalyst used, benzaldehyde is formed in 52.5% selectivity to the benzoic acid (at 47.5%, which is not shown).

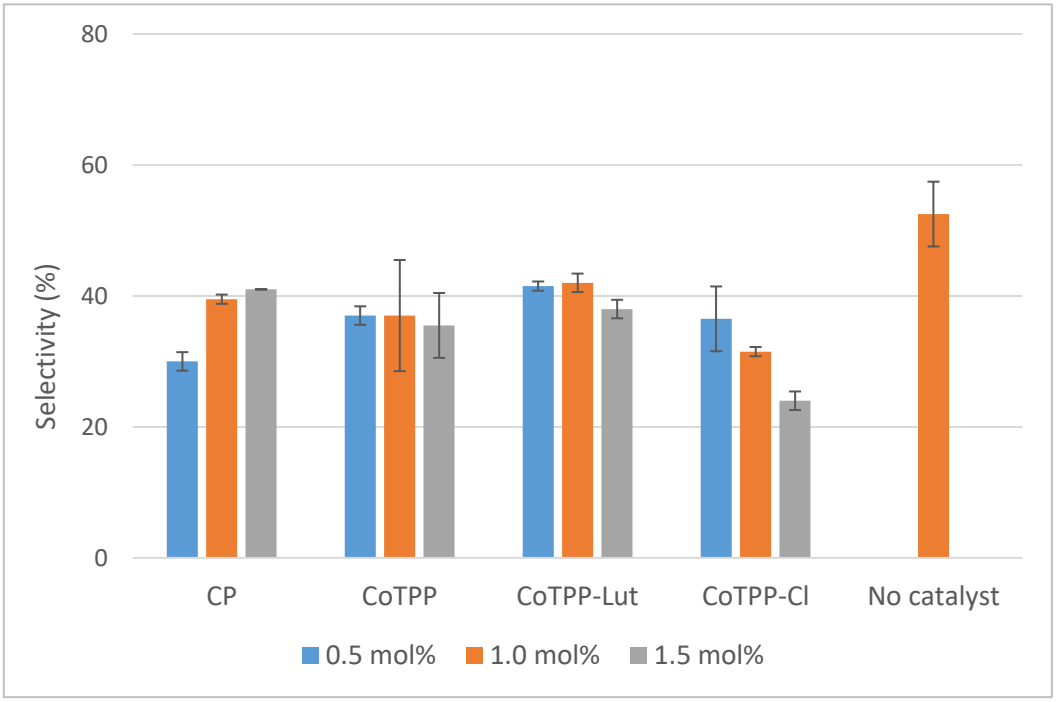

Figure 3.7: Influence of catalyst loadings on benzaldehyde selectivity, calculated as the mole ratio of benzaldehyde to the total mole obtained between benzaldehyde and benzoic acid, expressed as a percentage. Reaction conditions: 0.5 mmol benzyl alcohol, 1 mmol TBHP, 70 °C, 16 hours, 5 mL reaction volume.

From Figure 3.7, it is clear that for all the catalysts, benzoic acid is preferentially produced since not one of the catalysts produces benzaldehyde with a selectivity greater than 50%. An exception is when no catalyst is added, in which TBHP produces benzaldehyde with a slight preference (selectivity of 53%), although over-oxidation still occurs. It is clear that as the conversion of benzyl alcohol increases, more over-oxidation occurs to produce more benzoic acid.

For instance, if 0.5 mol% of CoTPP-Cl catalyst is added, 77% conversion is achieved with a selectivity of 37% for benzaldehyde, as opposed to 1.5 mol% catalyst loading in which the selectivity drops to 24%. The same is observed for the CP, even though higher conversions are achieved at lower catalyst loading. At 0.5 mol% loading, 84% conversion is obtained, with a selectivity of 30%. In addition, similar conversions result in similar selectivity, for instance, at a catalyst loading of 0.5 mol% for CoTPP and CoTPP-Cl, the conversion is 76% and 77%, respectively, with selectivity towards benzaldehyde being 37% and 36.5%, respectively.

Even though the Co-porphyrin catalysts do not increase the conversion substantially, it does seem that they promote the over-oxidation of benzaldehyde to benzoic acid. It is possible that the long reaction time allows for a lot of over-oxidation to occur, and it would be interesting to see what the selectivity would look like if the reaction time is reduced.

3.2.5 Effect of the ligand

Referring again to Figure 3.5, it is interesting to note the differences in conversion between the catalysts bearing different axial ligands. The lowest conversions overall are obtained with CoTPP and CoTPP-Lut, which also has the cobalt metal center in the +2 oxidation state, where higher conversions were observed with the CP and CoTPP-Cl, bearing the cobalt metal center in the +3 oxidation state.

Yamada and Kamiya studied the coordination of hydroperoxides to CoTPP derivatives by spectroscopic methods, and they showed that upon coordination, the cobalt metal center is oxidized from the +2 to the +3 oxidation state,[48] which was also confirmed by the studies of Mamardashvili and co-workers.[18] In the case where the CoTPP derivative is already in the +3 oxidation state, the peroxide still coordinates and the oxidation state does not change.[18] This means that eventually for all the catalysts, the cobalt metal center will end up in the +3 oxidation state as the active species, regardless of whether it was in the +2 oxidation state prior to coordination, or already in the +3 oxidation state due to another ligand. Since we are still seeing differences in the conversion, it is therefore possible that the difference is not due to the oxidation state of the metal, but rather the effect of the ligand.[18]

As mentioned before, the study of Mamardashvili and co-workers focused on the destruction of CoTPP by peroxides,[18] and they revealed the difference that the axial ligand has. If the catalysis takes place by coordination of the peroxide, the first step in an interaction of the Co-porphyrin with the peroxide is the coordination to form a 5- or 6-coordinate complex (Figure 3.8).[18]

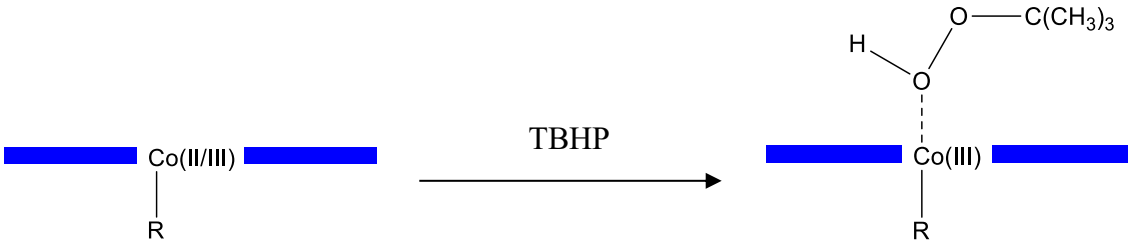

Figure 3.8: Coordination of TBHP to a Co-porphyrin.

Since the destruction of the porphyrin commences immediately after the coordination of the peroxide, it implies that the presence of available coordination sites ultimately promotes the degradation of the porphyrin.[18] When the reaction is happening in a coordinating solvent, the peroxide competes for the coordinating site with the solvent, which slows the down the destruction process slightly. In the case of already having an axial ligand (5-coordinate complex), the degradation is even slower.[18] As soon as 2 axial ligands are coordinated prior to addition of the peroxide (6-coordinate complex), a ligand exchange with the peroxide needs to occur in order for it to coordinate, which slows down the degradation even more.[18]

Examining our results, it is possible that the differences can be explained in light of the results obtained from the Mamardashvili study. Higher conversions are seen with the CP and CoTPP-Cl, possibly because of the additional axial ligand, meaning their degradation is slightly delayed in comparison to CoTPP and CoTPP-Lut, which results in higher conversions. It is interesting to note that CoTPP, bearing no axial ligand, does not result in lower conversions in comparison to CoTPP-Lut. Even though there is an equilibrium between CoTPP-Lut and CoTPP in a solution of CoTPP-Lut, one would still expect a slightly higher conversion for CoTPP-Lut. However, this turned out not to be the case. Furthermore, from these results, it does not seem like the DTDA ligand is having an effect with regards to higher conversion in comparison to CoTPP-Cl. However as mentioned before, lower catalyst loadings of CP result in higher conversions in contrast to the other catalysts. Further investigation into this will be required.

3.3 Concluding remarks

In conclusion, a series of Co-porphyrin compounds was investigated as catalysts in the oxidation of benzyl alcohol. The reaction conditions were optimized in preliminary work using the CP as model compound. Subsequently, a comparative study was carried out in order to assess what the effect of the ligand is on the catalytic reaction, in particular the DTDA ligand of the CP. The highest conversion was obtained with CoTPP-Cl, although all the catalysts increase the conversion somewhat in comparison to when no catalyst is present. The small increase in conversion on addition of catalyst could be due to the porphyrin catalyst undergoing degradation upon coordination of the peroxide, meaning it is not an active catalytic species for long. Generally, an increase in catalyst loading led to an increase in conversion, however for the CP, lower catalyst loadings resulted in higher conversion, which could be to minimal aggregation at that specific concentration. All the catalysts result in over-oxidation of benzaldehyde to benzoic acid, which was formed at a higher selectivity. This could be due to

the long reaction time. Generally, it was seen that as the conversion of benzyl alcohol increased, the more over-oxidation occurred. Finally, the effect of the ligand was assessed. The binding of peroxide to the cobalt metal center results in immediate degradation, and available coordination sites promote degradation. It is possible that higher conversions observed with CoTPP-Cl and the CP could be due to fewer accessible sites that are available for peroxide to coordinate as opposed to CoTPP and CoTPP-Lut.

3.4 Experimental section

3.4.1 General remarks and instrumentation

All catalytic reactions were carried out in a 25 mL round-bottom flask, fitted with a condenser. The reaction products were analyzed using a Varian 3900 gas chromatograph (GC) equipped with a flame ionization detector (FID) and a HP INNOWAX column with dimensions 30 m × 0.25 mm and a film thickness of 0.5 µm. Quantitative analysis was performed using internal standard method, where *p*-xylene was used as the internal standard.

3.4.2 Synthetic procedures

3.4.2.1 Synthesis of *meso*-tetraphenylporphyrin (TPP)

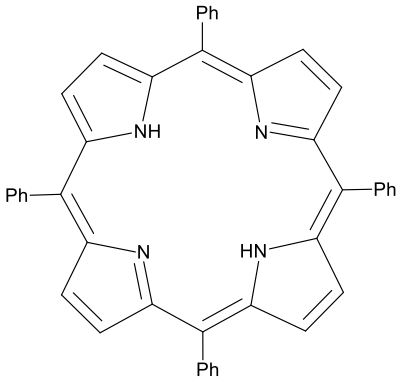

TPP

Propionic acid (250 mL) was added to a 500 mL round-bottomed flask together with boiling stones and heated to 150 °C prior to adding freshly distilled pyrrole (4 mL, 58 mmol) and benzaldehyde (5.88 mL, 58 mmol). The reaction mixture was then refluxed in air for 1 hour. After 1 hour, heating was stopped and the reaction mixture was allowed to cool to room temperature, before cooling in the refrigerator overnight. The reaction mixture was filtered the next day and washed with hot distilled water (3 × 30 mL) to yield the product as purple crystalline material (2.05 g, 23%). ^{1}H NMR (600 MHz, $CDCl_3$): δ (ppm) -2.75 (s, 2H, N-H),

7.74-7.80 (m, 12H, *para*- and *meta*- ArCH), 8.22-8.23 (m, 8H, *ortho*- ArCH), 8.85 (s, 8H, pyrrole-H).[49,50] UV-Vis (CH_2Cl_2): 420 nm, 517 nm, 552 nm, 592 nm, 648 nm.[51]

3.4.2.2 Synthesis of cobalt (II) *meso*-tetraphenylporphyrin (CoTPP)

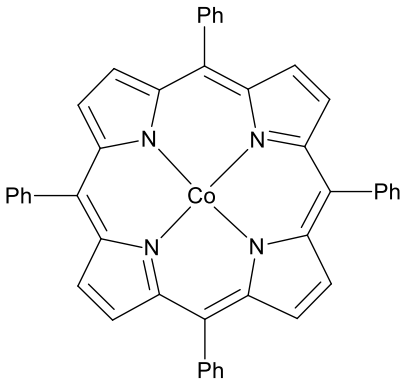

CoTPP

Degassed DMF (50 mL) was brought close to reflux under nitrogen before adding tetraphenylporphyrin (TPP, 405 mg, 0.66 mmol). After the dissolution of TPP, excess cobalt (II) acetate tetrahydrate (811 mg, 3.26 mmol) was added and the reaction mixture brought to reflux and maintained at reflux for 3 hours under nitrogen. After the allotted time, heating was stopped and the reaction mixture allowed to cool to room temperature. After it cooled, distilled water (30 mL) was added to precipitate the product, and it was kept in the refrigerator overnight. The next day, the reaction mixture was filtered and washed with distilled water (3 × 20 mL) to yield cobalt (II) tetraphenylporphyrin as a maroon powder (362 mg, 0.54 mmol, 82%). ^{1}H NMR (400 MHz, $CDCl_3$): δ (ppm) 9.73 (s, 4H, *para*- ArCH), 9.93 (s, 8H, *meta*- ArCH), (13.12 (s, 8H, *ortho*- ArCH), 15.88 (s, 8H, pyrrole-H).[49] UV-Vis (CH_2Cl_2): 410 nm, 528 nm.[51]

3.4.2.3 Synthesis of cobalt (III) *meso*-tetraphenylporphyrin chloride (CoTPP-Cl)

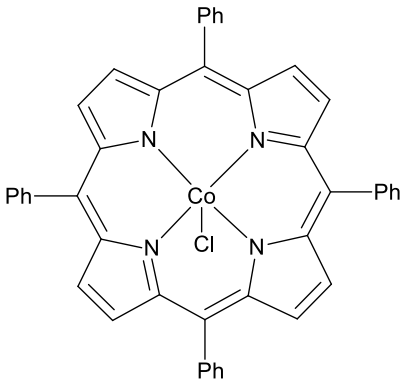

CoTPP-Cl

Cobalt (II) tetraphenylporphyrin (97 mg, 0.14 mmol) was added to methanol (250 mL) in a 500 mL round-bottomed flask. The solution was stirred for a few minutes before adding 7 mL of concentrated hydrochloric acid (0.23 mol) dropwise. The resulting dark purple colour solution was left to stir overnight. The next day methanol was removed under reduced pressure and the remaining suspension filtered. The filtration cake was then washed with water (3 × 20 mL), followed by a saturated aqueous sodium bicarbonate solution (3 × 20 mL) and then water again (5 × 20 mL). The resulting solid was air dried overnight. The crude product was redissolved in acetone (30 mL), filtered and the solvent removed under reduced pressure. This was repeated three times to yield cobalt (III) tetraphenylporphyrin chloride as a dark purple solid (44.6 mg, 0.063 mmol, 42%). ^{1}H NMR (400 MHz, $CDCl_3$): δ (ppm) 7.75 (br, 12H, *para*- and *meta*- ArCH), 8.24 (br, 8H, *ortho*- ArCH), 8.69 (br, 8H, pyrrole-H).[24,25,52] UV-Vis (CH_2Cl_2): 407 nm, 543 nm (br).[24,25]

3.4.2.4 Synthesis of 3,5-dimethylpyridine cobalt (II) *meso*-tetraphenylporphyrin (CoTPP-Lut)

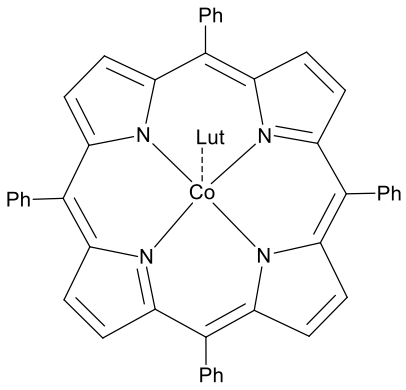

CoTPP-Lut (Lut = 3,5-lutidine)

Chloroform (5 mL) was added to cobalt (II) tetraphenylporphyrin (53 mg, 0.074 mmol), the solution heated up slightly and stirred until the solids dissolved. While stirring, 4 mL of 3,5-lutidine was added and the mixture stirred for another 5 minutes. After 5 minutes, the reaction mixture was removed from the heat and left open to air for 2 – 3 days to allow for the solvent to evaporate and the product to crystallize. After 3 days, the reaction mixture was filtered and washed with water (3 × 5 mL) and air dried overnight, or dried *in vacuo* at room temperature to yield dark purple crystals (0.028 g crude product – yield not determined due to lack of purity).[21] ^{1}H NMR (400 MHz, $CDCl_3$): δ (ppm) – 2.94 (s, 6H, ArC-C*H*, 3,5-lutidine), 7.17 (s, ArCH, 3,5-lutidine), 8.22-8.23 (m, ArCH, 3,5-lutidine), 9.07 (s, 4H, *para*- ArCH), 9.39

(s, 8H, *meta*- ArCH), 11.56 (s, 8H, *ortho*- ArCH), 14.69 (s, 8H, pyrrole-H). UV-Vis (CH_2Cl_2): 418 nm, 433 nm, 517 nm (br), 549 nm (br), 589 nm (br), 648 nm (br).

3.4.3 Catalysis procedure

A typical procedure for the oxidation of benzyl alcohol was as follows, using CoTPP as an example.

In a 25 mL round-bottom flask, CoTPP (3.4 mg, 0.005 mmol, 1.0 mol%) together with benzyl alcohol (54.1 mg, 52 µL, 0.5 mmol) was added. After the addition of acetonitrile (4.8 mL), the flask was placed in a pre-heated oil bath at 70 °C, which was maintained throughout the reaction. TBHP (138 µL, 1 mmol) was added, and subsequently the reaction mixture was stirred for 16 hours, after which the reaction mixture turned light yellow with a green precipitate. After 16 hours, heating was ceased and the reaction quenched in an ice bath, followed by the addition of a small amount of $MgSO_4$. Subsequently, the reaction mixture was filtered and analyzed by GC-FID.

It should be noted that for the CP, after the catalytic reaction, a green precipitate was not observed, but rather the solution turned light to dark brown, yielding a brown precipitate.

3.5 References

1 D. Dolphin, T. G. Traylor and L. Y. Xie, *Acc. Chem. Res.*, 1997, **30**, 251–259.

2 D. Mansuy, *C. R. Chim.*, 2007, **10**, 392–413.

3 C. M. Che and J. S. Huang, *Chem. Commun.*, 2009, 3996–4015.

4 J. T. Groves, T. E. Nemo and R. S. Myers, *J. Am. Chem. Soc.*, 1979, **101**, 1032–1033.

5 B. Meunier, *Chem. Rev.*, 1992, **92**, 1411–1456.

6 M. Costas, *Coord. Chem. Rev.*, 2011, **255**, 2912–2932.

7 J. C. Barona-Castaño, C. C. Carmona-Vargas, T. J. Brocksom and K. T. De Oliveira, *Molecules*, 2016, **21**, 1–27.

8 M. J. F. Calvete, M. Piñeiro, L. D. Dias and M. M. Pereira, *ChemCatChem*, 2018, **10**, 1–25.

9 K. Pamin, E. Tabor, S. Górecka, W. W. Kubiak, D. Rutkowska-Zbik and J. Połtowicz,

ChemSusChem, 2019, **12**, 684–691.

10 B.-Z. Zhan and A. Thompson, *Tetrahedron*, 2004, **60**, 2917–2935.

11 M. J. Schultz and M. S. Sigman, *Tetrahedron*, 2006, **62**, 8227–8241.

12 C. E. Chan-Thaw, A. Savara and A. Villa, *Catalysts*, 2018, **8**, 1–21.

13 E. B. Fleischer, *Acc. Chem. Res.*, 1970, **3**, 105–112.

14 P. D. Smith, B. R. James and D. H. Dolphin, *Coord. Chem. Rev.*, 1981, **39**, 31–75.

15 W. Nam, H. J. Han, S. Y. Oh, Y. J. Lee, M. H. Choi, S. Y. Han, C. Kim, S. K. Woo and W. Shin, *J. Am. Chem. Soc.*, 2000, **122**, 8677–8684.

16 Y. Kang, H. Chen, Y. J. Jeong, W. Lai, E. H. Bae, S. Shaik and W. Nam, *Chem. Eur. J.*, 2009, **15**, 10039–10046.

17 N. Chaudhary and D. A. Haynes, *Unpublished work*.

18 G. M. Mamardashvili, O. R. Simonova, N. V. Chizhova and N. Z. Mamardashvili, *Russ. J. Gen. Chem.*, 2018, **88**, 1154–1163.

19 A. D. Adler, F. R. Longo, J. D. Finarelli, J. Goldmacher, J. Assour and L. Korsakoff, *J. Org. Chem.*, 1967, **32**, 476.

20 A. D. Adler, F. R. Longo, F. Kampas and J. Kim, *J. Inorg. Nucl. Chem.*, 1970, **32**, 2443–2445.

21 W. R. Scheidt and J. A. Ramanuja, *Inorg. Chem.*, 1975, **14**, 2643–2648.

22 T. Sakurai, K. Yamamoto, N. Seino and M. Katsuta, *Acta Crystallogr.*, 1975, **B31**, 2514–2517.

23 T. Sakurai, K. Yamamoto, H. Naito and N. Nakamoto, *Bull. Chem. Soc. Jpn.*, 1976, **49**, 3042–3046.

24 W. Xia, S. I. Vagin and B. Rieger, *Chem. Eur. J.*, 2014, **20**, 15499–15504.

25 W. Xia, K. A. Salmeia, S. I. Vagin and B. Rieger, *Chem. Eur. J.*, 2015, **21**, 4384–4390.

26 H. Tang, C. Shen, M. Lin and A. Sen, *Inorganica Chim. Acta*, 2000, **300**–**302**, 1109–

1111.

27 C. C. Guo, Q. Liu, X. T. Wang and H. Y. Hu, *Appl. Catal. A Gen.*, 2005, **282**, 55–59.

28 X. Zhou and H. Ji, *Chinese J. Chem.*, 2012, **30**, 2103–2108.

29 X. T. Zhou, H. Y. Chen, Q. Han, M. Lv and H. B. Ji, *New J. Chem.*, 2020, **44**, 10286–10291.

30 D. Mansuy, J. F. Bartoli and M. Momenteau, *Tetrahedron Lett.*, 1982, **23**, 2781–2784.

31 C. C. Guo, M.-F. Chu, Q. Liu, Y. Liu, D.-C. Guo and X.-Q. Liu, *Appl. Catal. A Gen.*, 2003, **246**, 303–309.

32 H. B. Ji, Q. L. Yuan, X. T. Zhou, L. X. Pei and L. F. Wang, *Bioorganic Med. Chem. Lett.*, 2007, **17**, 6364–6368.

33 H. Sugimoto and K. Kuroda, *Macromolecules*, 2008, **41**, 312–317.

34 A. K. Nanda and K. Kishore, *Macromolecules*, 2001, **34**, 1600–1605.

35 A. K. Nanda and K. Kishore, *Macromolecules*, 2002, **35**, 6505–6510.

36 S. Pal, A. Vaish and P. De, *Polym. Int.*, 2015, **64**, 541–546.

37 B. K. Samra, M. Andersson and P. Adlercreutz, *Biocatal. Biotransformation*, 1999, **17**, 381–391.

38 R. Chakrabarty, P. Sarmah, B. Saha, S. Chakravorty and B. K. Das, *Inorg. Chem.*, 2009, **48**, 6371–6379.

39 V. R. Choudhary, D. K. Dumbre and S. K. Bhargava, *Ind. Eng. Chem. Res.*, 2009, **48**, 9471–9478.

40 V. R. Choudhary and D. K. Dumbre, *Appl. Catal. A Gen.*, 2010, **375**, 252–257.

41 A. K. Mandal, V. Khanna and J. Iqbal, *Tetrahedron Lett.*, 1996, **37**, 3769–3772.

42 A. K. Mandal and J. Iqbal, *Tetrahedron*, 1997, **53**, 7641–7648.

43 G. C. Behera and K. M. Parida, *Appl. Catal. A Gen.*, 2012, **413**–**414**, 245–253.

44 C. K. Chang and M.-S. Kuo, *J. Am. Chem. Soc.*, 1979, **101**, 3413–3415.

45 D. K. Lavallee, *Coord. Chem. Rev.*, 1985, **61**, 55–96.

46 J. Turay, P. Hambright and N. Datta-Gupta, *J. Inorg. Nucl. Chem.*, 1978, **40**, 1687–1688.

47 D. A. Haynes, L. J. Van Laeren and O. Q. Munro, *J. Am. Chem. Soc.*, 2017, **139**, 14620–14637.

48 T. Yamada and Y. Kamiya, *Bull. Chem. Soc. Jpn.*, 1980, **53**, 1077–1080.

49 R. J. Abraham, I. Marsden and L. Xiujing, *Magn. Reson. Chem.*, 1990, **28**, 1051–1057.

50 R. E. Falvo, L. M. Mink and D. F. Marsh, *J. Chem. Educ.*, 1999, **78**, 237–239.

51 M. Gouterman, *J. Mol. Spectrosc.*, 1961, **6**, 138–163.

52 G. Mamardashvili, E. Kaigorodova, O. Simonova and N. Mamardashvili, *J. Coord. Chem.*, 2018, **71**, 4194–4209.

Chapter 4

Catalysis by mechanochemistry – oxidation of benzyl alcohol with Co-porphyrin catalysts

4.1 Introduction

Mechanochemistry, albeit a non-classical method, has become a very effective technique for chemical transformations in the solid state, and its potential in several fields of chemistry has already been recognized. For instance, in supramolecular chemistry and the field of crystal engineering, mechanochemistry has been used to control which crystal form (polymorph, solvate) is the outcome of a particular reaction. It is often not possible, or much harder, to control crystal form in solution.[1–3] Materials science has also reaped the benefits of mechanochemistry, which allows for the functionalization of complex structures such as cages and rings,[4,5] but also provides an alternative, milder synthetic route to metal-organic frameworks (MOFs),[6–8] which still rely on the traditional solvothermal methods that require high temperatures and pressures, and could take days or weeks. Mechanochemistry is becoming important in various other fields, such as medicinal chemistry,[9] coordination chemistry,[10] organic chemistry and synthesis,[4,5,11–16] inorganic chemistry[17,18] and organometallic chemistry,[19] but of particular interest are the advancements made in metal-catalyzed reactions.[20,21] It has been shown that using mechanochemistry in catalytic reactions can have advantages over solution-based methods in terms of reduced reaction times, yield and selectivity enhancement.[16] For example, Jiang *et al* reported the Suzuki-Miyaura reaction of aryl chlorides and aryl boronic acids under mechanochemical conditions, in which they were able to achieve yields as high as 97% in 99 minutes of ball milling.[22] The same reaction in solution at reflux temperature only gives a maximum yield of 63% after 6 hours,[22] showing a clear distinction between the two methods with regards to yields and reaction time. Furthermore, even though there are clear differences between mechanochemistry and solution-based chemistry, it has been shown that it is not always necessary to modify the catalysts originally designed for solution-based methods in order for them to achieve similar (or even better) activity in mechanochemical catalysis. For example, this is the case for the Suzuki-Miyaura reaction described above,[22] and the Friščić group has used the commercially available

Grubbs catalysts to achieve high-yielding olefin metathesis of solid and liquid olefins at a high rate under mechanochemical conditions.[23]

With the nature of mechanochemical reactions differing quite significantly from solution-based reactions,[14] modification and optimization of reaction parameters has a different focus. Changing reagent stoichiometry and reaction time is conventional for both methods, however, instead of changing the temperature as with solution-based reactions, one would change the frequency at which the reaction vessels are shaken to increase the input of mechanical energy (as opposed to increasing the input of thermal energy).[16] Other parameters that could be changed include the size, amount and material of the milling balls, material of the milling vessels[24] and the addition of a small amounts of solvent in a technique known as liquid-assisted grinding (LAG).[25]

As discussed in the previous chapter, we are interested in the catalytic oxidation of alcohols by metal catalysts, specifically metalloporphyrins. Although numerous metal-catalyzed organic reactions have been carried out by mechanochemistry, for example Heck and Sonogashira reactions,[26,27] oxidation of alcohols has been shown to proceed mechanochemically both with and without a metal-based catalyst present,[28–33] meaning the oxidant used can act as both the catalyst and oxidant. For instance, Porcheddu *et al* reported the mechanochemical oxidation of primary and secondary alcohols within 15 minutes with a copper complex $[Cu(MeCN)_4](OTf)$, using catalytic amounts of 2,2,6,6-tetramethylpiperidine-1-yl(oxyl) (TEMPO) as oxidant.[28] In contrast, Achar *et al* were able to oxidize a diverse range of aromatic alcohols to carbonyl compounds in the presence of a stoichiometric amount of 2-iodoxybenzoic acid (IBX) over a period of 45 min – 3 h with no metal catalysts present.[30]

Based on the results reported in Chapter 3, we wanted to investigate whether metalloporphyrins are also able to catalyze the oxidation of alcohols in the solid state by mechanochemistry (Figure 4.1). Even though some metal catalysts can perform in either solution or mechanochemical conditions, there is not necessarily a correlation. Porphyrins and their metallated analogues have previously been synthesized by mechanochemistry,[34–36] however reports of their ability to catalyze reactions in the solid state by mechanochemistry remain limited.

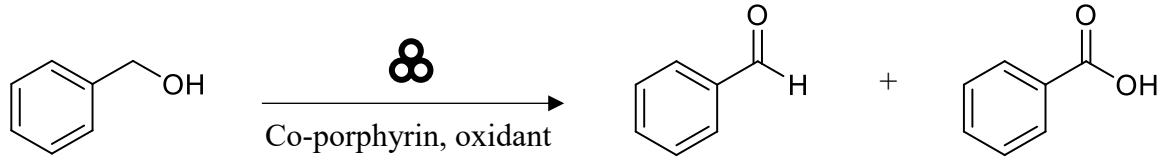

Figure 4.1: Typical oxidation of benzyl alcohol by mechanochemistry with cobalt porphyrins. Triangular symbol (proposed by the Hanusa group[19]) designates a mechanochemical reaction.

4.2 Model system for the oxidation of benzyl alcohol

Before testing the metalloporphyrin catalysts, it was important to establish that a known mechanochemical oxidation could be efficiently carried out using the equipment available in our research labs. This is because some parameters depend on the availability of equipment, such as the size and material of grinding balls and vessels. For instance, carrying out a mechanical reaction in a Teflon jar versus a stainless steel jar will not necessarily result in the same outcome: because of the difference in material density, the energy transference during the reaction is not the same.[24] We therefore carried out a preliminary study to validate our equipment.

The work from the Mal group was of interest. They carried out the multicomponent Biginelli reaction that involves the oxidation of an alcohol as part of a subcomponent synthesis in the first step.[32] Prior to optimizing the reaction conditions for the full reaction, they attempted to use *N*-bromosuccinimide (NBS) to oxidize the alcohol (Figure 4.2). This worked extremely well (> 98% conversion), but failed to produce an efficient by-product catalyst for the subsequent reaction, and low yields of dihydropyrimidones were obtained in the second step, so this procedure was discarded.[32] According to them, this was the first report of using NBS to oxidize alcohols by mechanochemistry.[32] This seemed an ideal oxidation reaction with which to test our equipment.

The reaction conditions entailed milling benzyl alcohol in the presence of NBS for 30 minutes at 1260 rpm.[32] Even though the material of our jars and grinding balls were different to those used my Mal *et al* (we used Teflon-lined grinding jars and zirconium oxide balls as opposed to stainless steel jars and balls), we were able to reproduce this reaction with a conversion of more than 99% and a slight increase in selectivity of 96% for benzaldehyde‡. This result confirms that known reactions can be effectively carried out in our apparatus, allowing us to proceed with the catalytic oxidation of benzyl alcohol with Co-porphyrins.

‡ Percentage conversion refers to the amount of substrate that has been converted to products, while the selectivity refers to how much benzaldehyde formed in relation to benzoic acid.

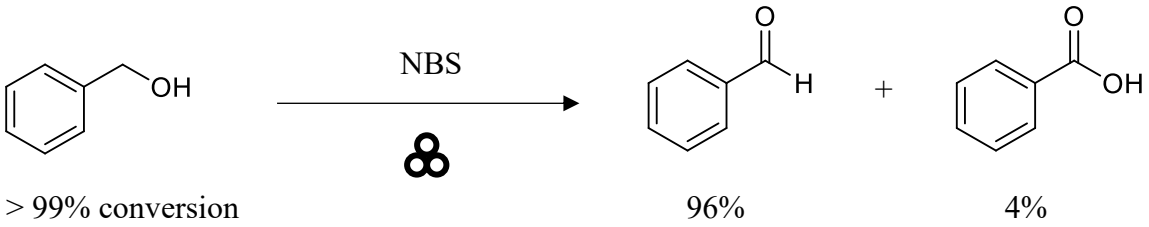

Figure 4.2: Oxidation of benzyl alcohol by mechanochemistry using NBS as oxidant. Conversions of more than 99% were obtained, with a 96% selectivity towards benzaldehyde.

4.3 Preliminary reaction conditions for the oxidation of benzyl alcohol

Since metalloporphyrins have not been used as catalysts in mechanochemistry, there are no guidelines on appropriate preliminary reaction conditions to use for the oxidation of benzyl alcohol. In the work described in the previous chapter, TBHP was used as the oxidant in the oxidation of benzyl alcohol. Initially, TBHP was considered as an oxidant under mechanochemical conditions to enable a direct comparison to the solution-based catalytic experiments. However, due to the shock sensitive nature of this compound,[37] an alternative oxidant needed to be identified, preferably a solid. In the review by Meunier on the use of metalloporphyrins in oxidation catalysis,[38] several other (solid) oxidants have been employed for oxidation reactions with metalloporphyrins in solution, and some of them have also found use in other mechanochemical reactions. For example, sodium periodate ($NaIO_4$), *meta*-chloroperbenzoic acid (*m*-CPBA) and sodium hypochlorite (NaOCl) have all been used with metalloporphyrins in oxidation catalysis, and in turn have found use in mechanochemistry in the dehydrogenation of γ-terpinene ($NaIO_4$),[39] Baeyer-Villiger oxidation of ketones (*m*-CPBA)[40] and oxidation of alcohols (NaOCl),[33] respectively.

Although all of these are good candidates to test the catalytic potential of metalloporphyrins by mechanochemistry, results in solution suggested that a peroxide would be a better choice. A colleague from McGill University in Canada suggested the solid form of hydrogen peroxide, complexed with urea (urea-H_2O_2-adduct, UHP), which then seemed like an appropriate candidate.

The structure of UHP was determined in 1941, and the hydrogen peroxide shows strong hydrogen-bonding to the urea.[41] UHP essentially serves as a hydrogen peroxide carrier, which, upon dissolution in water, releases hydrogen peroxide.[42,43] It is also not sensitive to impact and friction, and so appears to be a safer option than TBHP for mechanochemistry. Considering that UHP has been previously used in mechanochemistry,[39,44] this seemed like a good starting point for the current investigation.

4.4 Optimization

As mentioned previously, it is not uncommon for oxidation reactions to proceed without a catalyst present. So initially, reaction conditions were chosen based on published protocols, starting with 0.5 mmol benzyl alcohol, 1 equivalent of UHP, 25 µL water (η = 0.25 µL/mg)[§], 900 rpm milling frequency, 5 mL Teflon jars, 1 ZrO_2 ball in each jar (5 mm) and 4 hours reaction time (Figure 4.3).

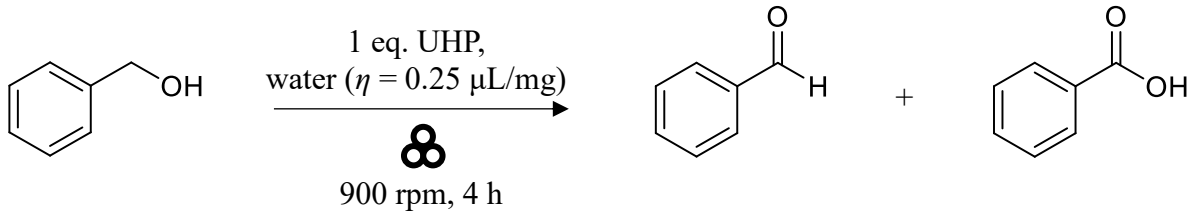

Figure 4.3: Initial reaction conditions employed for the oxidation of benzyl alcohol in the presence of UHP.

The reaction conditions were subsequently optimized by varying one parameter at a time while keeping the others constant. The parameters varied in this study were the milling frequency, reaction time, oxidant amount and the solvent amount in utilizing the LAG technique. Optimization was carried out without a metal catalyst. Each reaction was analyzed to assess how each factor influences both the conversion of benzyl alcohol and the selectivity for the product carbonyl compounds. All reactions were carried out in duplicate. The conversion of benzyl alcohol was calculated by using the internal standard method, with *p*-xylene as the internal standard. Conversion was based on the amount of benzyl alcohol that was left after the allotted reaction time. The amount of benzaldehyde and benzoic acid that formed was also calculated by using the internal standard method, with *p*-xylene as the internal standard. The selectivity of benzaldehyde over benzoic acid is the ratio of moles of benzaldehyde to the total mole amount obtained for benzaldehyde and benzoic acid, expressed as a percentage.

4.4.1 Effect of frequency

The first parameter to be varied was the milling frequency, as it has previously been shown in literature to make a difference to yield and selectivity.[16,24] Analogous to increasing the temperature in solution-based reactions, increasing the milling frequency will increase the mechanical energy entering the system. In our system, starting with 900 rpm, there is a 4% conversion of the benzyl alcohol to benzaldehyde, which drops slightly to 3% conversion at 1200 rpm and then increases slightly to 5% conversion at 1500 rpm (Figure 4.4). In all these

[§] η refers to the quantification of liquids in mechanochemistry experiments. See Section 4.4.4 for more information.

reactions, only benzaldehyde was detected after 4 hours of reaction time. Since a higher conversion was obtained at a frequency of 1500 rpm, this was used in the remaining optimization experiments.

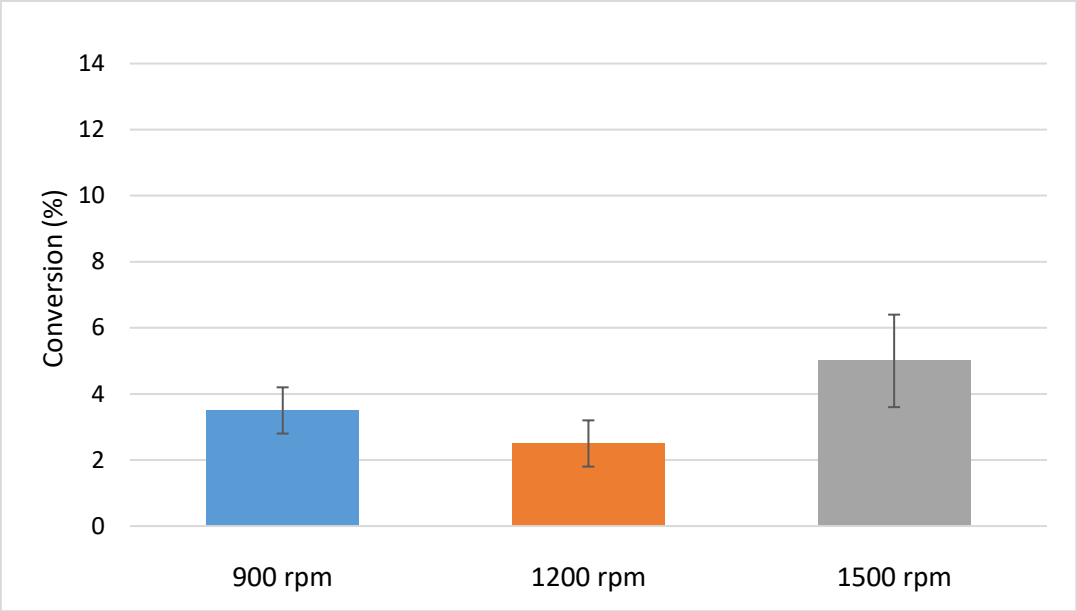

Figure 4.4: Influence of the milling frequency on the conversion of benzyl alcohol and selectivity of benzaldehyde. Reaction conditions: 0.5 mmol benzyl alcohol, 1 mmol UHP, 4 hours, 25 µL water (η = 0.25 µL/mg).

4.4.2 Effect of reaction time

Once the milling frequency was optimized, the effect of reaction time was investigated next. The reaction conditions were still the same as the initial chosen reaction conditions, except for the frequency being changed to 1500 rpm. When the reaction was milled for 4 hours, 5% conversion was obtained, and, within error, no noteworthy increase was seen as the milling time was extended to 6 and 8 hours of milling, respectively (Figure 4.5). Only benzaldehyde was detected during analysis. In general, it does not seem that additional reaction time has an effect on the conversion of benzyl alcohol, and so it was decided to continue with a milling time of 4 hours as this is more energy efficient.

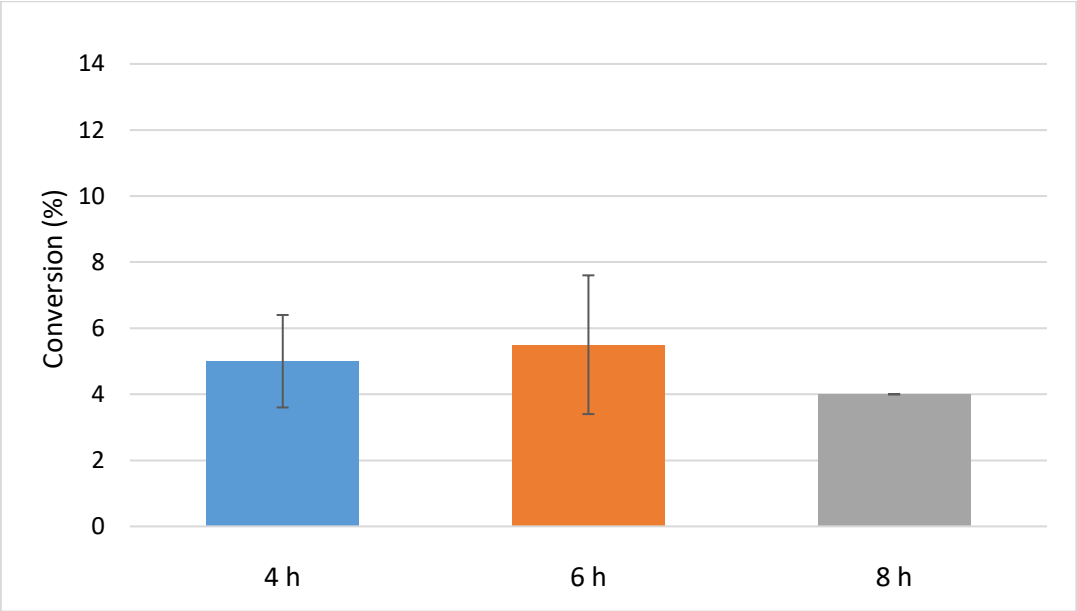

Figure 4.5: Influence of the milling time on conversion of benzyl alcohol and selectivity of benzaldehyde. Reaction conditions: 0.5 mmol benzyl alcohol, 1 mmol UHP, 1500 rpm, 25 µL water (η = 0.25 µL/mg). No benzoic acid detected.

4.4.3 Effect of oxidant amount

Next, we were interested in how the conversion of benzyl alcohol would be affected by additional amounts of the oxidant in the reaction mixture. Using the same reaction conditions, but changing the amount of oxidant from 1 equivalent (0.5 mmol), to 2 equivalents (1.0 mmol) or 3 equivalents (1.5 mmol), the following was observed, as illustrated in Figure 4.6: with the addition of 1 equivalent of UHP, we only see a conversion of 5%, which increased to 6% when 2 equivalents were added. Using 3 equivalents of UHP resulted in 7.5% conversion of benzyl alcohol to benzaldehyde. Again, only benzaldehyde was detected after the analysis of these reactions, and with higher conversions being obtained with 3 equivalents of UHP, this was used in subsequent experiments.

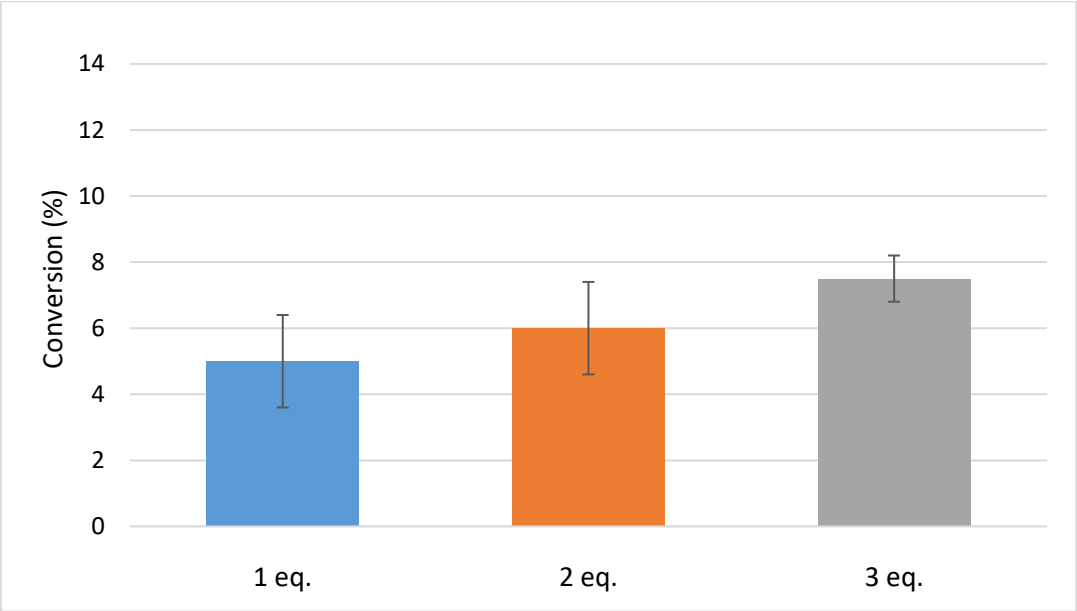

Figure 4.6: Influence of different oxidant amounts on the conversion of benzyl alcohol and selectivity of benzaldehyde. Reaction conditions: 0.5 mmol benzyl alcohol, 1500 rpm, 4 hours, 25 – 49 µL (η = 0.25 µL/mg). No benzoic acid detected.

4.4.4 Liquid-Assisted Grinding (LAG)

The effects of LAG has been known since the early 2000s. Work was pioneered by the Jones group, who showed for the first time that a minute amount of solvent (MeOH) improves the co-crystal formation between cyclohexane-1,3,5-tricarboxylic acid and 4,4'-bypiridine during grinding.[45] Aside from its importance in crystal engineering, LAG has also been found to have an effect in metal-catalyzed reactions.[22,23,46–49] Friščić and Jones defined a parameter to allow comparison of the amount of liquid added across different LAG reactions[50] This parameter η, is defined as the ratio of solvent (in µL) to sample weight (in mg),[50] as illustrated in Equation 1.

$$\eta = \frac{\text{V (liquid,µL)}}{\text{m (sample,mg)}} \quad \ldots(1)$$

For instance, in the experiments described above, the addition of 54 mg of benzyl alcohol (52 µL) plus 1 equivalent of UHP (47 mg, 0.5 mmol) results in a total reagent weight of 101 mg, and so 25 µL of water results in an η value of approximately 0.25 µL/mg. If no solvent is added, this is known as neat grinding (η = 0), while reactions in the range η = 2 – 12 µL/mg and > 12 µL/mg are slurry and solution type reactions, respectively.[4,5,50] Increasing the amount of water added increases the η value, which is the parameter that was varied next in the optimization process, as illustrated in Figure 4.7.

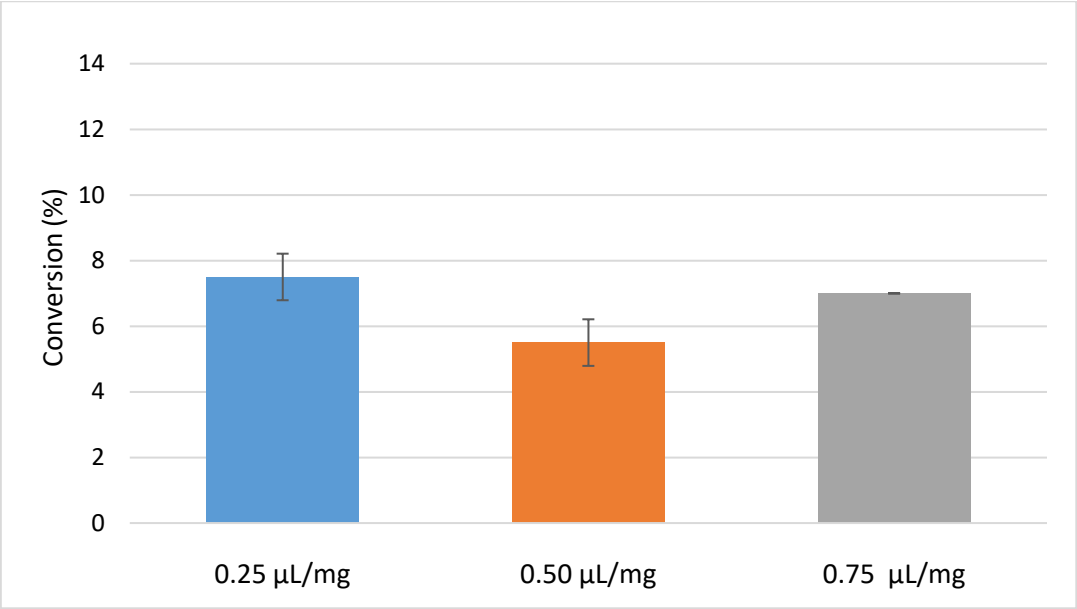

Figure 4.7: Influence of the amount of water (LAG) on the conversion of benzyl alcohol and selectivity of benzaldehyde. The η values of 0.25 µL/mg, 0.50 µL/mg and 0.75 µL/mg refer to the addition of 49 µL, 98 µL and 147 µL of water, respectively. Reaction conditions: 0.5 mmol benzyl alcohol, 1.5 mmol UHP, 1500 rpm, 4 hours. No benzoic acid detected.

No increase in conversion was observed upon increasing the amount of water added. This was quite a surprising result, since UHP dissolves in water to release hydrogen peroxide, and so the addition of more water should make more hydrogen peroxide available for oxidation. An η value of 0.50 µL/mg resulted in a conversion of 5.5% conversion, whereas 0.75 µL/mg η value resulted in a slightly higher conversion of 7%, but lower than that of 0.25 µL/mg at 7.5% conversion. As with previous experiments, only benzaldehyde was detected during the analysis. Therefore, an η value of 0.25 µL/mg was used for subsequent experiments, since a higher conversion was obtained with this value.

4.5 Comparative study: Co-porphyrins as catalysts

After the optimization study, the optimized reaction conditions were as follows: 0.5 mmol benzyl alcohol, 1.5 mmol UHP, 1500 rpm, 4 hours, 25 µL water (η = 0.25 µL/mg). The Co-porphyrins that were used as catalyst in this work are illustrated in Figure 4.8.

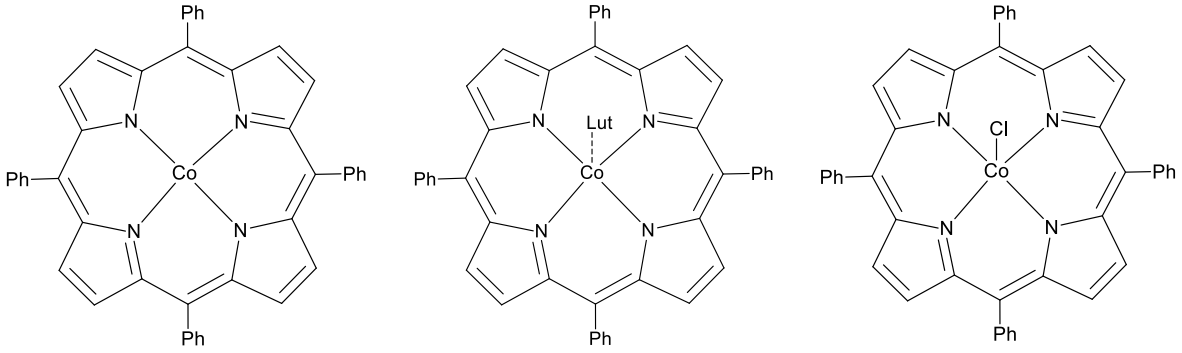

CoTPP **CoTPP-Lut** **CoTPP-Cl**

Figure 4.8: The Co-porphyrins that were used in this mechanochemical catalysis study.

Next, we firstly wanted to find out whether these metalloporphyrin catalysts actually catalyze the oxidation of benzyl alcohol under mechanochemical conditions, and secondly, with reference to Chapter 3, whether the ligand (and the concomitant change in oxidation state) also have an effect on the conversion of benzyl alcohol and selectivity towards benzaldehyde.

4.5.1 CoTPP

CoTPP without any axial ligands was tested first (Figure 4.9).

The first thing to notice is that CoTPP does not increase the conversion compared to using UHP without any catalyst. At a low catalyst loading of 0.5 mol%, the conversion is actually slightly lower at 6%, while an increase to 1.0 mol% and 1.5 mol% lead to conversions of 7.0 and 7.5%, which is similar to what is obtained with UHP solely. However, a difference is seen with the selectivity, where less benzaldehyde was detected due to over-oxidation occurring, which was not observed in the case of using UHP exclusively. At a low catalyst loading of 0.5 mol%, only benzaldehyde was detected, however as soon as the catalyst loading was increased to 1.0 mol% and 1.5 mol%, less benzaldehyde was detected. At 1.0 mol% catalyst loading, benzaldehyde was still formed with a slightly higher selectively of 56%, however in the case of 1.5 mol% catalyst loading, more over-oxidation was observed and so the selectivity for benzaldehyde decreased to 42%. Looking at Figure 4.9, it is clear that that an increase in catalyst loading does not increase the conversion of benzyl alcohol, but a steady decrease in the ratio of benzaldehyde to benzoic acid is observed instead, and so it seems that CoTPP prefers to oxidize the benzaldehyde that forms to benzoic acid, as opposed to oxidizing the benzyl alcohol.

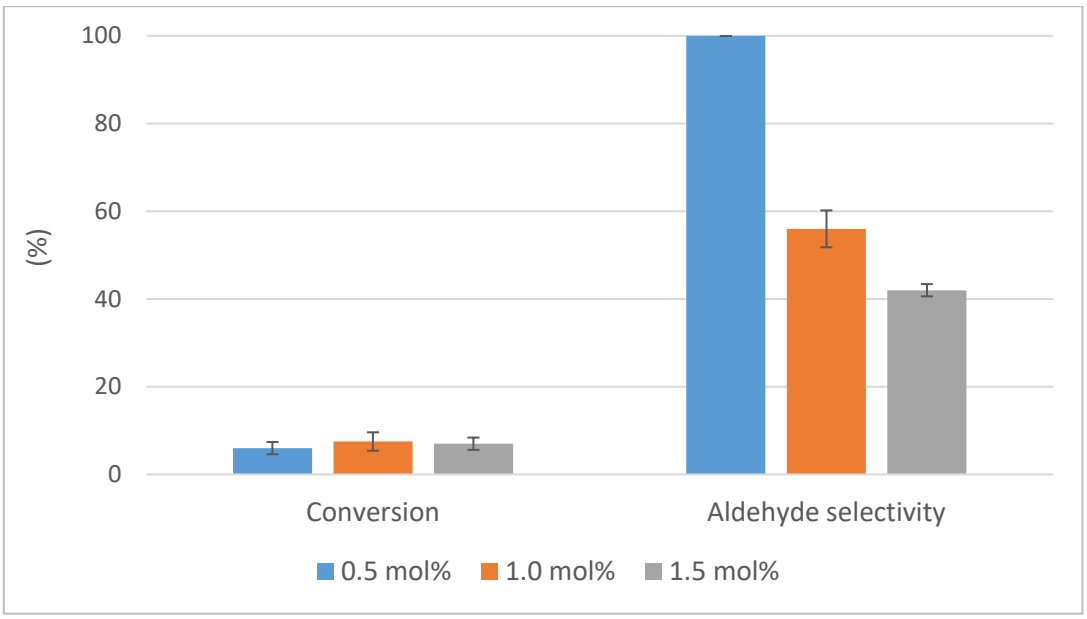

Figure 4.9: Catalytic activity and selectivity towards benzaldehyde of the CoTPP catalyst as a function of different catalyst loadings 0.5 mol%, 1.0 mol% and 1.5 mol%. Reaction conditions: 0.5 mmol benzyl alcohol, 1.5 mmol UHP, 25 uL water (η = 0.25 µL/mg) in 5 mL Teflon jar with 1 ZrO2 grinding ball (Ø = 5 mm). Ball milling conditions: 4 hours at 1500 rpm (25 Hz).

4.5.2 CoTPP-Lut

The next catalyst to be tested was the CoTPP derivative containing a 3,5-lutidine as axial ligand, as illustrated in Figure 4.10.

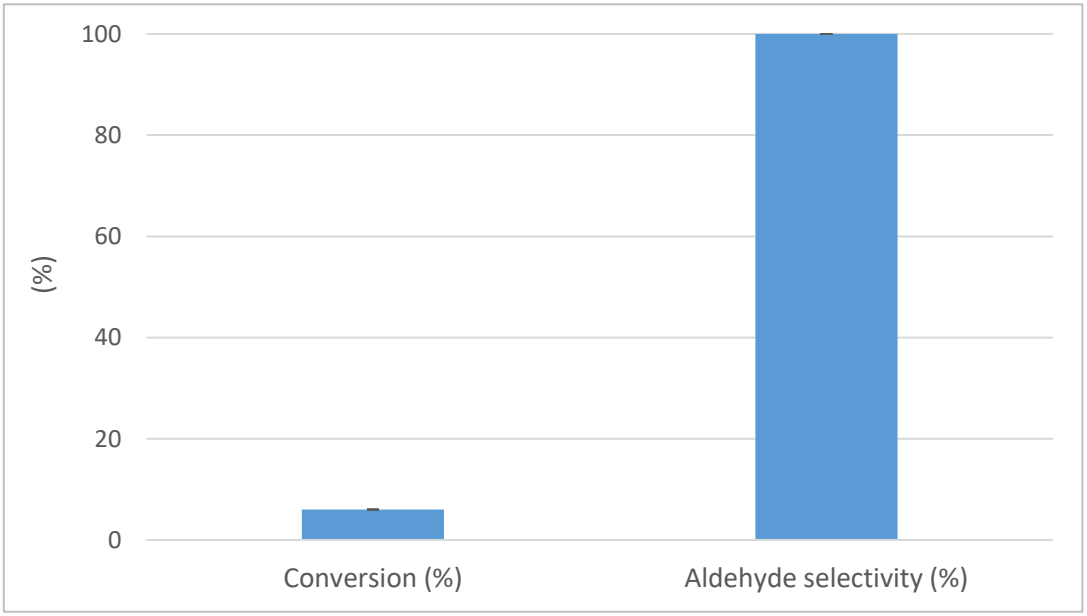

Figure 4.10: Catalytic activity and selectivity towards benzaldehyde of the CoTPP-Lut catalyst as a function of the catalyst loading 0.5 mol%. Reaction conditions: 0.5 mmol benzyl alcohol, 1.5 mmol UHP, 25 uL water (η = 0.25 µL/mg) in 5 mL Teflon jar with 1 ZrO_2 grinding ball (Ø = 5 mm). Ball milling conditions: 4 hours at 1500 rpm (25 Hz).

The graph shows the percentage conversion and selectivity towards benzaldehyde as a function of 0.5 mol% catalyst loading only. Experiments of catalyst loading 1.0 mol% and 1.5 mol%

were also carried out, as with the previous CoTPP catalyst, but spurious results were obtained and these experiments must be repeated in order for reliable conclusions to be drawn. Nevertheless, the results obtained from 0.5 mol% catalyst loading give similar results to those observed with 0.5 mol% CoTPP (Figure 4.9). The same conversion of 6% was obtained, and only benzaldehyde was detected during the analysis. It would be interesting to see what results are obtained with 1.0 mol% and 1.5 mol% catalyst loadings. The coordination chemistry of aromatic amines to Co-porphyrins has been investigated previously,[51] and an equilibrium exists between the bound and dissociated complexes. It might be possible for the 3,5-lutidine to dissociate during the reaction, and play a role in the catalysis almost like an added liquid, which is a phenomenon discussed by Bowmaker in his review of solvent-assisted mechanochemistry.[25] For instance, when one reactant is a hydrate, water could be generated during the reaction, or other reactions could produce water (or other liquids) as by products that could aid the progress of the reaction.[25] Of course, the reactions would need to be carried out before the effect of 3,5-lutidine can be analyzed. Because it is a challenge to obtain pure compound, as alluded to in Chapter 3, the minute amount of 3,5-lutidine present may not make a difference at all.

4.5.3 CoTPP-Cl

Finally, the CoTPP catalyst derivative with a chloride axial ligand was evaluated next to see whether it could catalyze oxidation under mechanochemical conditions, and the results are shown in Figure 4.11.

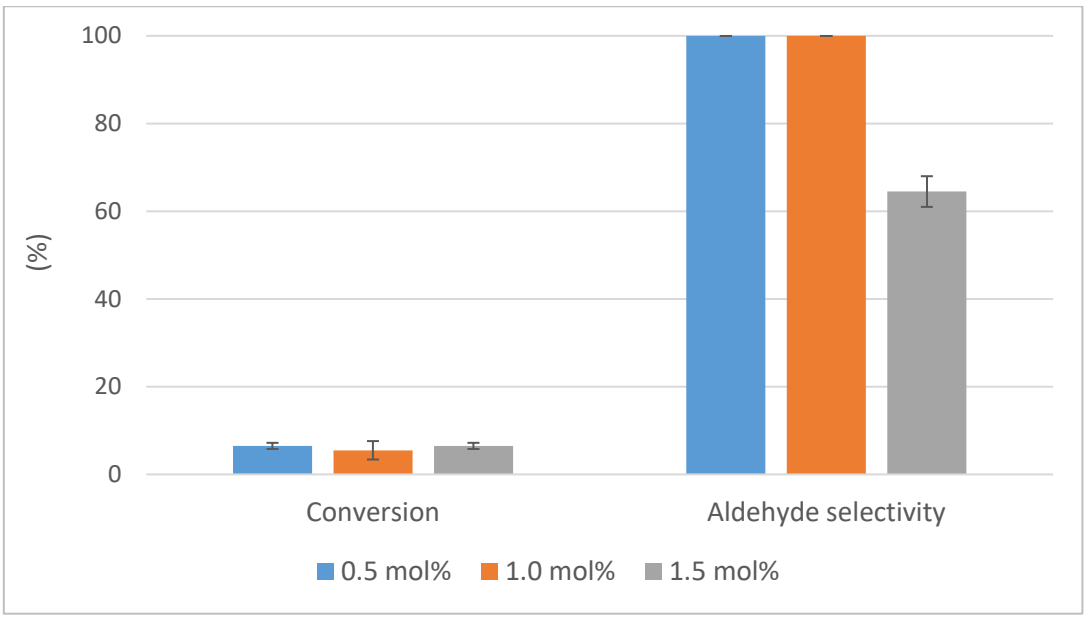

Figure 4.11: Catalytic activity and selectivity towards benzaldehyde of the CoTPP-Cl catalyst as a function of different catalyst loadings 0.5 mol%, 1.0 mol% and 1.5 mol%. Reaction conditions: 0.5 mmol benzyl alcohol, 1.5 mmol UHP, 25 uL water (η = 0.25 µL/mg) in 5 mL Teflon jar with 1 ZrO2 grinding ball (Ø = 5 mm). Ball milling conditions: 4 hours at 1500 rpm (25 Hz).

The graph in Figure 4.11 illustrates the percentage conversion and selectivity towards benzaldehyde as a function of the catalyst loadings of 0.5 mol%, 1.0 mol% and 1.5 mol%. There was also no increase in the conversion of benzyl alcohol with this catalyst, only a slight decrease with 0.5 mol% and 1.5 mol% giving the same conversion of 6.5%, whereas 1.0 mol% resulted in a conversion of 5.5%. Interestingly, 0.5 mol% and 1.0 mol% catalyst loading did not result in any over-oxidation of benzaldehyde, as seen with CoTPP. Instead, only at the highest catalyst loading of 1.5 mol% do we detected less benzaldehyde, but with a moderate selectivity of 64.5%. It seems like in this case, the benzaldehyde was also preferentially oxidized over the benzyl alcohol, albeit at a higher catalyst loading.

4.5.4 Comparison between CoTPP and CoTPP-Cl

Since the catalytic reactions of CoTPP-Lut were not completed, these will not be included in this discussion of the comparison between the catalysts. Figure 4.12 illustrates the data for the catalytic reactions using 1.5 mol% catalyst loadings for both catalysts (CoTPP and CoTPP-Cl), the only case where over-oxidation of benzaldehyde was detected in both reactions.

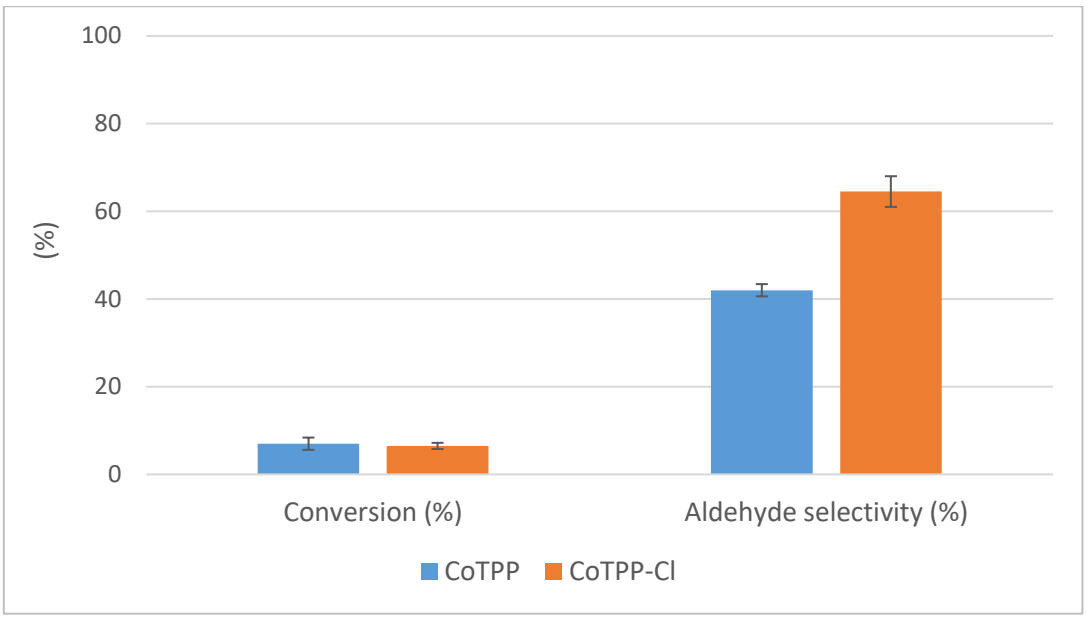

Figure 4.12: Comparison of the activity and selectivity towards benzaldehyde of CoTPP and CoTPP-Cl at a catalyst loading of 1.5 mol%. Reaction conditions: 0.5 mmol benzyl alcohol, 1.5 mmol UHP, 25 uL water (η = 0.25 µL/mg) in 5 mL Teflon jar with 1 ZrO2 grinding ball (Ø = 5 mm). Ball milling conditions: 4 hours at 1500 rpm (25 Hz).

Notably, it seems that neither catalyst resulted in any substantial increase in conversion compared to no catalyst, however it was shown that they both preferentially oxidize the benzaldehyde to benzoic acid. This only occurs for CoTPP-Cl at a higher loading. Furthermore, for the same catalyst loading, CoTPP results in more over-oxidation than CoTPP-Cl, as is evident from Figure 4.12 in which more benzaldehyde was detected at a selectivity of 64.5% for the CoTPP-Cl catalyst as opposed to 42% selectivity for CoTPP. This is quite an intriguing result, and differs from what is seen in solution catalysis, discussed in Chapter 3. CoTPP-Cl achieves higher yields and lower selectivity of benzaldehyde in solution than CoTPP, while in the mechanochemistry experiments, the conversions are similar, but a higher selectivity is seen for CoTPP-Cl. A possible explanation could be the structure of CoTPP-Cl and the nature of mechanochemical reactions. CoTPP-Cl has an axial ligand that does not dissociate, leaving only one side of the metalloporphyrin open for coordination of the peroxide to progress with catalysis. The right orientation for coordination of the peroxide may be occurring on fewer occasions than with CoTPP, which has two available sites and thus a higher probability of coordination, implying higher activity. With this in mind, one could possibly predict the outcome of using CoTPP-Lut as catalyst, in which there exists an equilibrium of bound and dissociated complexes. The activity performance will probably be in between CoTPP and CoTPP-Cl, due to more complexes with accessible sites being available in comparison to CoTPP-Cl. A direct comparison to the solution experiments done in Chapter 3 cannot be made with confidence since the same oxidant could not be used due to safety considerations.

4.6 Concluding remarks

In conclusion, three Co-porphyrin catalysts in the form of CoTPP, CoTPP-Lut and CoTPP-Cl were evaluated as catalysts for the oxidation of benzyl alcohol under mechanochemical conditions, which has not previously been explored. The shock-sensitive nature of TBHP, which was used in the solution-based reactions, was considered and UHP was chosen as the safer option to the test the catalytic performance of Co-porphyrins. The reaction conditions were optimized with UHP solely, varying reaction parameters that included the milling frequency, reaction time, oxidant amount and LAG. After the optimized reaction conditions were established, catalytic reactions with the three Co-porphyrin catalysts were carried out subsequently. For all the catalysts, no increase in conversion was observed at the respective catalyst loadings that were investigated, however preferential oxidation of benzaldehyde to benzoic acid was detected for catalysts CoTPP and CoTPP-Cl. It was observed that CoTPP seemed to be slightly more active in the benzaldehyde oxidation, over-oxidizing at catalyst loadings of 1.0 and 1.5 mol%, while CoTPP-Cl oxidized benzaldehyde only at a high catalyst loading of 1.5 mol%. A possible explanation could be due to the nature of the mechanochemical reactions, with CoTPP having a higher probability of binding peroxide due to more accessible sites, thereby displaying higher activity.

4.7 Experimental section

4.7.1 General remarks and instrumentation

All mechanochemical reactions were carried out in a FTS-1000 Shaker Mill® (Form-Tech Scientific, Canada), using Teflon milling jars, also obtained from Form-Tech Scientific. The jar volume was 5 mL, grinding balls used were made of zirconium oxide (ZrO_2, 1 × 5 mm Ø), milling frequency up to 1500 rpm and milling time up to 8 hours. The reaction products were analyzed using a Varian 3900 gas chromatograph (GC) equipped with a flame ionization detector (FID) and a HP INNOWAX column with dimensions 30 m × 0.25 mm and a film thickness of 0.5 µm. Quantitative analysis was performed using the internal standard method, where *p*-xylene was used as the internal standard.

4.7.2 Catalysis procedure

A typical mechanochemical procedure for the catalysis of benzyl alcohol was carried out as follows, using CoTPP as an example.

CoTPP (3.4 mg, 0.005 mmol, 1.0 mol%), urea-hydrogen peroxide (141.1 mg, 1.5 mmol) and benzyl alcohol (54.1 mg, 52 µL, 0.5 mmol) were placed in a Teflon jar (5 mL). After the addition of 50 µL water (η = 0.25), one ZrO_2 ball (5 mm Ø) was added to each jar, after which the jars were clamped and milled at 1500 rpm (25 Hz) for 4 hours. After the allotted time, the jars were collected and sample was washed out with 4.888 mL acetonitrile (to yield a total sample volume of 5 mL). Subsequently, a small amount of $MgSO_4$ was added to the acetonitrile mixture, it was then filtered and analyzed by GC-FID.

4.8 References

1 A. V. Trask, W. D. S. Motherwell and W. Jones, *Chem. Commun.*, 2004, 890–891.

2 A. V Trask, N. Shan, W. D. S. Motherwell, W. Jones, S. Feng, R. B. H. Tan and K. J. Carpenter, *Chem. Commun.*, 2005, 880–882.

3 A. V Trask, J. van de Streek, W. D. S. Motherwell and W. Jones, *Cryst. Growth Des.*, 2005, **5**, 2233–2241.

4 D. Tan and T. Friščić, *European J. Org. Chem.*, 2018, **2018**, 18–33.

5 C. Mottillo and H. M. Titi, *Angew. Chemie - Int. Ed.*, 2020, **59**, 1018–1029.

6 T. Friščić, *J. Mater. Chem.*, 2010, **20**, 7599–7605.

7 P. Li, F. Cheng, W.-W. Xiong and Q. Zhang, *Inorg. Chem. Front.*, 2018, **5**, 2693–2708.

8 T. Stolar and K. Užarević, *CrystEngComm*, 2020, **22**, 4511–4525.

9 D. Tan, L. Loots and T. Friščić, *Chem. Commun.*, 2016, **52**, 7760–7781.

10 C. Mottillo and T. Friščić, *Molecules*, 2017, **22**, 1–38.

11 S. L. James, C. J. Adams, C. Bolm, D. Braga, P. Collier, T. Friščic, F. Grepioni, K. D. M. Harris, G. Hyett, W. Jones, A. Krebs, J. Mack, L. Maini, A. G. Orpen, I. P. Parkin, W. C. Shearouse, J. W. Steed and D. C. Waddell, *Chem. Soc. Rev.*, 2012, **41**, 413–447.

12 G. Wang, *Chem. Soc. Rev.*, 2013, **42**, 7668–7700.

13 T. K. Achar, A. Bose and P. Mal, *Beilstein J. Org. Chem.*, 2017, **13**, 1907–1931.

14 J. L. Do and T. Friščić, *Synlett*, 2017, **28**, 2066–2092.

15 J. Andersen and J. Mack, *Green Chem.*, 2018, **20**, 1435–1443.

16 J. L. Howard, Q. Cao and D. L. Browne, *Chem. Sci.*, 2018, **9**, 3080–3094.

17 V. V. Boldyrev and E. G. Avvakumov, *Russ. Chem. Rev.*, 1971, **40**, 847–859.

18 E. Boldyreva, *Chem. Soc. Rev.*, 2013, **42**, 7719–7738.

19 N. R. Rightmire and T. P. Hanusa, *Dalt. Trans.*, 2016, **45**, 2352–2362.

20 J. G. Hernández and T. Friščić, *Tetrahedron Lett.*, 2015, **56**, 4253–4265.

21 A. Porcheddu, E. Colacino, L. De Luca and F. Delogu, *ACS Catal.*, 2020, **10**, 8344–8394.

22 Z. J. Jiang, Z. H. Li, J. B. Yu and W. K. Su, *J. Org. Chem.*, 2016, **81**, 10049–10055.

23 J. L. Do, C. Mottillo, D. Tan, V. Štrukil and T. Friščić, *J. Am. Chem. Soc.*, 2015, **137**, 2476–2479.

24 A. Stolle, T. Szuppa, S. E. S. Leonhardt and B. Ondruschka, *Chem. Soc. Rev.*, 2011, **40**, 2317–2329.

25 G. A. Bowmaker, *Chem. Commun.*, 2013, **49**, 334–348.

26 E. Tullberg, D. Peters and T. Frejd, *J. Organomet. Chem.*, 2004, **689**, 3778–3781.

27 R. Thorwirth, A. Stolle and B. Ondruschka, *Green Chem.*, 2010, **12**, 985–991.

28 A. Porcheddu, E. Colacino, G. Cravotto, F. Delogu and L. De Luca, *Beilstein J. Org. Chem.*, 2017, **13**, 2049–2055.

29 Z. Y. Zhang, D. Ji, W. Mao, Y. Cui, Q. Wang, L. Han, H. Zhong, Z. Wei, Y. Zhao, K. Nørgaard and T. Li, *Angew. Chemie - Int. Ed.*, 2018, **57**, 10949–10953.

30 T. K. Achar, S. Maiti and P. Mal, *RSC Adv.*, 2014, **4**, 12834–12839.

31 G. Cravotto and E. C. Gaudino, *RSC Green Chem.*, 2015, **2015**, 58–80.

32 P. K. Sahoo, A. Bose and P. Mal, *European J. Org. Chem.*, 2015, **2015**, 6994–6998.

33 A. Porcheddu, F. Delogu, L. De Luca, C. Fattuoni and E. Colacino, *Beilstein J. Org. Chem.*, 2019, **15**, 1786–1794.

34 H. Shy, P. Mackin, A. S. Orvieto, D. Gharbharan, G. R. Peterson, N. Bampos and T. D. Hamilton, *Faraday Discuss.*, 2014, **170**, 59–69.

35 K. Ralphs, C. Zhang and S. L. James, *Green Chem.*, 2017, **19**, 102–105.

36 D. Damunupola, N. Chaudhri, A. O. Atoyebi and C. Brückner, *Green Chem.*, 2020, **22**, 3643–3652.

37 T. K. Achar and P. Mal, *J. Org. Chem.*, 2015, **80**, 666–672.

38 B. Meunier, *Chem. Rev.*, 1992, **92**, 1411–1456.

39 T. Szuppa, A. Stolle, B. Ondruschka and W. Hopfe, *Green Chem.*, 2010, **12**, 1288–1294.

40 F. Toda, M. Yagi and K. Kiyoshige, *J. Chem. Soc. Chem. Commun.*, 1988, 958–959.

41 C.-S. Lu, W. Hughes and P. A. Giguére, *J. Am. Chem. Soc.*, 1941, **63**, 1507–1513.

42 P. Lulinski, A. Kryska, M. Sosnowski and L. Skulski, *Synthesis*, 2004, 441–445.

43 R. Matyáš, J. Selesovsky, V. Pelikán, M. Szala, S. Cudziło, W. A. Trzciński and M. Gozin, *Propellants, Explos. Pyrotech.*, 2017, **42**, 198–203.

44 R. Thorwirth, F. Bernhardt, A. Stolle, B. Ondruschka and J. Asghari, *Chem. Eur. J.*, 2010, **16**, 13236–13242.

45 N. Shan, F. Toda and W. Jones, *Chem. Commun.*, 2002, **2**, 2372–2373.

46 D. Tan, C. Mottillo, A. D. Katsenis, V. Štrukil and T. Friščič, *Angew. Chemie - Int. Ed.*, 2014, **53**, 9321–9324.

47 D. Tan, V. Štrukil, C. Mottillo and T. Friščić, *Chem. Commun.*, 2014, **50**, 5248–5250.

48 J. G. Hernández and C. Bolm, *Chem. Commun.*, 2015, **51**, 12582–12584.

49 K. Y. Jia, J. B. Yu, Z. J. Jiang and W. K. Su, *J. Org. Chem.*, 2016, **81**, 6049–6055.

50 T. Friščić, S. L. Childs, S. A. A. Rizvi and W. Jones, *CrystEngComm*, 2009, **11**, 418–426.

51 F. A. Walker, *J. Am. Chem. Soc.*, 1973, **95**, 1150–1153.

Chapter 5

Concluding remarks and future work

5.1 Concluding remarks

This thesis describes the use of Co-porphyrins in the catalytic oxidation of benzyl alcohol in solution, but also in the solid state by mechanochemistry.

Chapter one describes the structure and synthesis of porphyrins and their metallated analogues. Structural aspects on the periphery of the porphyrin, as well as the coordination chemistry of metalloporhyrins, were introduced since these aspects are crucial in understanding their chemistry. This then led to a discussion of their catalytic applications and how the abovementioned structural aspects and coordination chemistry can influence their catalytic activity. Subsequently, mechanochemistry as a non-classical technique was introduced through a brief historical outline. Hereafter, equipment and techniques were presented, before expanding into redox and metal-catalyzed reactions by mechanochemistry.

Chapter two describes the synthetic investigation into 4-(4'-pyridyl)-1,2,3,5-dithiadiazolyl (pyrDTDA), which forms part of a CoTPP coordination polymer (CP) of interest as a bridging ligand in the solid state. A report from the Oakley group described a structural change that occurs during synthesis, giving rise to two pyrDTDA radicals (neutral and charged). We decided to investigate the synthesis and purification of these two materials, in the hope that better yields of the CP could be obtained by using one or the other. The structures of the two pyrDTDA radicals were confirmed based on numerous analytical methods that included IR spectroscopy, PXRD, solid-state UV-Vis spectroscopy and CHNS analysis. Subsequently, they were used in CP synthesis and no significant difference in yields were observed.

Chapter three describes the investigation of Co-porphyrins as catalysts in the oxidation of benzyl alcohol in solution. Specifically, we wanted to compare different CoTPP derivatives, bearing different axial ligands, to the newly-discovered CP, which has been shown previously to oxidize benzyl alcohol in solution in the presence of TBHP as oxidant. Overall, the catalysts showed only moderate activity compared to when no catalyst was present, which could be due to the degradation of the Co-porphyrins by the peroxide. Generally, an increase in catalyst

loading results in a steady increase in benzyl alcohol conversion, except for the CP, where maximum conversion was achieved at the lowest catalyst loading. The effect of the axial ligand was assessed, showing that it had an influence on the catalytic reaction by slowing down the degradation. Co-porphyrins that were already in oxidation +3 due to the presence of axial ligands performed better as catalysts.

Lastly, in **Chapter four** an investigation of whether the abovementioned Co-porphyrins can catalyze the oxidation of benzyl alcohol in the solid state by mechanochemistry was described. Urea-hydrogen peroxide (UHP) was chosen as the oxidant over TBHP due to the latter being shock sensitive. The reaction conditions were optimized with UHP without a metal catalyst, by varying milling frequency, reaction time, oxidant amount and the amount of water (LAG). After the optimized reaction conditions was established, three Co-porphyrin catalysts (CoTPP, CoTPP-Lut and CoTPP-Cl) was used to catalyze the oxidation of benzyl alcohol. No increase in conversion was observed with any of the catalysts, however it seems that CoTPP and CoTPP-Cl preferentially oxidized the benzaldehyde formed to benzoic acid, which was not detected without a catalyst present.

5.2 Future work

It is perplexing how two different pyrDTDA radicals can result in similar yields of the CP. This raises the question of whether there truly are two different radicals that are structurally different once in solution, and in what form are they reacting in solution. Structural data of these two radicals need to be obtained in order to confirm the presence of an additional hydrogen atom on the nitrogen and a chloride counter ion. This can only happen if good single crystals can be obtained, which can hopefully be attained through several re-sublimations. Due to the insolubility of both radicals in common organic solvents, solution crystallization is not really an option. Furthermore, in the second step of the synthesis after condensation with SCl_2, it is likely that mixtures of charged and neutral pyrDTDA radicals are obtained. By deprotonating, we can ensure that solely neutral radical is obtained. In the future, it might be worthwhile adding acid (maybe HCl) purposely, instead of base, to ensure that only charged pyrDTDA radical is obtained for further structural analysis. However, the acid stability of these radicals might be an issue and needs to be evaluated first.

With regards to the synthesis of the CP, if we are able synthesize it with both pyrDTDA radicals, how is this affecting its redox behavior in the solid and solution state? This is something that could be revisited, even though Haynes and Munro did a thorough investigation.[1] Furthermore,

how do the different radicals used to make the CP affect its behavior in solution regarding catalysis?

In terms of catalysis by Co-porphyrins, a number of aspects could be followed up in the future. According to the study by Mamardashvili, cobalt (II) *meso*-tetraphenylporphyrin degrades quite easily in the presence of peroxides.[2] This is quite a challenging issue, since the phenyl rings were a strategy employed to slow down degradation, but it still happens quite readily. Based on their work, it might be worthwhile using a derivative of CoTPP with two axial ligands as a catalyst, in which the peroxide would need to compete and exchange with the axial ligand. Figure 5.1 illustrates an example of a CoTPP catalyst derivative that could be used instead, first synthesized by Belghith and co-workers.[3] One would expect that the peroxide will only be able to exchange with the pyridine, and so with only one site available, degradation might be slowed down. Will this then in turn affect the efficiency and rate of the catalytic reaction? In addition, more substituents on the phenyl rings and pyrrolic β-positions could be added to prolong the lifetime of the catalyst.

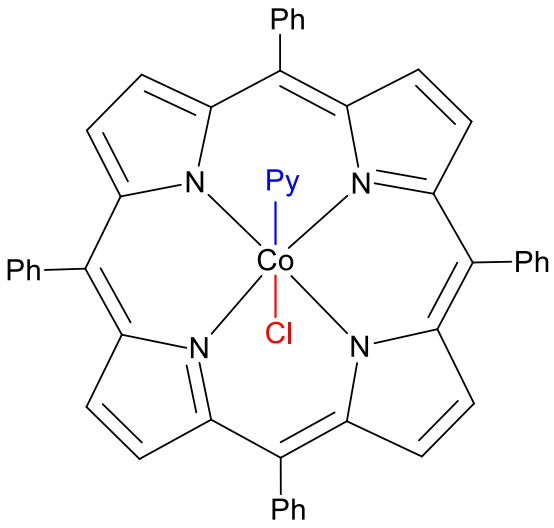

Figure 5.1: Pyridine cobalt (III) meso-tetraphenylporphyrin chloride.

Investigating the catalytic potential of metalloporphyrins under mechanochemical conditions is an avenue we are only now beginning to venture into. After repeating the mechanochemistry experiments with CoTPP-Lut, it might be worthwhile attempting to use TBHP as oxidant, since Co-porphyrins and UHP did not work very well and TBHP has been shown to work better with Co-porphyrins (Chapter 3). Even though it is a shock-sensitive chemical, if the necessary safety measures are taken into consideration, it might be still be possible to do those experiments that eluded us in this initial study. Furthermore, a peculiar observation that was made is that it seems that the Co-porphyrin catalysts prefer to oxidize benzaldehyde over benzyl alcohol. This is

something that needs to be revisited and verified. Another interesting avenue could be to investigate solvent-assisted grinding with 3,5-lutidine. Once CoTPP-Lut can be made pure, a thorough investigation of this can commence, which could entail grinding with CoTPP-Lut solely, and in a separate reaction, grind CoTPP with 3,5-lutidine added separately, and evaluate what role it plays in the catalytic reaction. Moreover, several other oxidants, as mentioned in the main text, could also be utilized. Specifically, using molecular oxygen, which has been shown to work very well with Co-porphyrins, should be investigated. Even though milling with gases has previously been carried out,[4] it is by no means an established method and could well be a challenging venture since numerous modifications will need to be made on the jars and ball mill. It would also be worthwhile to consider whether metalloporphyrins are not degrading under mechanochemical conditions, which could shed light on why the activity of our systems is so poor. Furthermore, a well-known phenomenon in mechanochemistry, called mechanical activation, is also an interesting endeavor.[5] This technique works by creating defects in the structure of the catalyst, thereby improving its catalytic activity. This could potentially improve the catalytic activity of metalloporphyrins in solution and by mechanochemistry. Even though Co-porphyrins with UHP did not work very well, numerous other metalloporphyrins, especially Fe-, Mn- and Ru-porphyrins could be used instead, since their catalytic activity are more superior to that of cobalt.

5.3 References

1 D. A. Haynes, L. J. Van Laeren and O. Q. Munro, *J. Am. Chem. Soc.*, 2017, **139**, 14620-14637.

2 G. M. Mamardashvili, O. R. Simonova, N. V. Chizhova and N. Z. Mamardashvili, *Russ. J. Gen. Chem.*, 2018, **88**, 1154–1163.

3 Y. Belghith, J. C. Daran and H. Nasri, *Acta Crystallogr. Sect. E Struct. Reports Online*, 2012, **E68**, m1104–m1105.

4 C. Bolm and J. G. Hernández, *Angew. Chemie - Int. Ed.*, 2019, **58**, 3285–3299.

5 R. A. Buyanov, V. V. Molchanov and V. V. Boldyrev, *KONA Powder Part. J.*, 2009, 38–54.

Appendix A

Experimental procedures and instrumentation

A.1 Chemicals, solvents and experimental procedures

All the chemicals that were used during the course of this study were purchased from Sigma-Aldrich and were used as received, except for pyrrole, which was distilled prior to use in porphyrin synthesis. The solvents were purchased from Alfa Aesar and Kimix Chemicals and were used as received. Diethyl ether, acetonitrile, tetrahydrofuran, *n*-hexane and dichloromethane were dried over activated 3 Å molecular sieves for at least 24 hours prior to use.

All glassware was dried in an oven at 150 °C for at least an hour before use. Standard Schlenk techniques were employed for reactions needing inert conditions. When low temperatures were required, a Dewar was used to prepare slurries of dry ice in acetone (−78 °C) and ice in water (0 °C).

A.2 Instrumentation

A.1.1. Electron paramagnetic resonance (EPR) spectroscopy

All EPR spectroscopy experiments were carried out at room temperature (~ 298 K) on a Bruker EMXplus X-band spectrometer – 8-inch ER 072 magnet, 2.7 kW power supply, EMX-m40X microwave bridge operating from 9.3 – 9.9 GHz – with a high-sensitivity continuous-wave resonator. Spectra were recorded in the solution state by diluting the material in dry dichloromethane (DCM).

A.1.2. Gas chromatography (GC)

A Varian 3800 gas chromatograph, equipped with a flame ionization detector (FID), was used for GC analyses. A cross-linked polyethylene glycol (PEG) column (HP INNOWAX) was used with dimensions 30 m × 0.25 mm and film thickness of 0.5 μm. Helium was used as the carrier gas.

A.1.3. Infrared (IR) spectroscopy

IR spectra were obtained by using a Bruker Alpha FT-IR spectrometer, employing a Platinum ATR attachment. A preliminary background scan was collected before each sample scan. All spectra were processed and generated using the KnowItAll® Informatics System (2018) software.

A.1.4. Mass spectrometry (MS)

The Central Analytical Facility (CAF) Institute of Stellenbosch University carried out the high resolution mass spectrometric analysis. A Waters Synapt G2 instrument was used to record the spectra for solution and solid-state samples. For solution samples, materials were dissolved in DCM and were subsequently introduced by direct injection, operating in the ESI positive mode using a Cone Voltage of 15 V.

For solid samples, the ASAP probe was used to introduce samples. This entails operating the instrument in the APCI positive mode using a Cone Voltage of 15 V, and the compounds are ionized from the tip of a melting-point tube. A single mass analysis was carried out, as well as tandem mass analysis (MSMS).

A.1.5. Nuclear magnetic resonance (NMR) spectroscopy

The recording of all ^{1}H NMR spectra were carried out at room temperature (298 K) using either a 300 MHz, 400 MHz or 600 MHz Agilent spectrometer. All samples, ranging from 5 – 25 mg, were dissolved in either deuterated chloroform ($CDCl_3$) or deuterated dimethylsulfoxide (DMSO-d6). Processing and analysis of spectra were performed using MestReNova Version 6.0.2,[1] in which chemical shifts (δ) are expressed in parts per million (ppm) relative to the residual solvent peak.

A.1.6. Powder X-ray diffraction

Powder patterns were collected at ambient temperature using a Bruker D2 phaser X-ray diffractometer equipped with a Lynxeye 1-D detector. The diffractometer operates at 10 mA current and 30 kV voltage, producing radiation from a CuKα source with wavelength of 1.54283 Å. Data were collected from 2θ = 4 – 40 °with a scan rate of either 0.500, 0.750 or 1.000 seconds per step (step size 0.0161°). The compounds were usually obtained as powders, and so sampling consisted of compressing a small amount on a zero-background holder with a glass slide. In the case of larger crystals, these were first ground with a mortar and pestle before

adding onto the zero-background holder. Analysis of powder patterns was performed with the X'Pert HighScore Plus (version 2.2e) software. Diffractograms were generated also using X'Pert HighScore Plus (version 2.2e) software.

A.1.7. Ultraviolet visible (UV-Vis) spectroscopy

UV-Vis spectra of solid and liquid samples were recorded using the Analytic Jena Specord® Plus 210. Liquid samples were recorded in the spectral range of 200 – 800 nm. Samples were dissolved in dry DCM or dry DMSO and a blank reference measurement were carried out before each sample measurement. Spectra were generated using Microsoft Excel 2016.

A diffuse reflectance accessory fitted with an integrating sphere was used to record spectra of solid samples. Spectra were recorded in the range of 380 – 1100 nm. Spectra were generated using Microsoft Excel 2016.

A.1.8. Elemental analysis: CHNS analysis

The Central Analytical Facility (CAF) Institute of Stellenbosch University carried out the elemental analysis. A Vario EL Cube Elemental Analyzer was used to carry out the CHNS analysis. Argon was used as the carrier gas and oxygen as the dosing gas for combustion. Samples were combusted in the temperature range of 1050 – 1150 °C.

A.3 References

1 *MestReNova*, version 6.0.2-5475, Mestrelab Research S. L., 2009.

Appendix B

Experimental data

B.1 Chapter 2

B.1.1 Infrared Spectroscopy

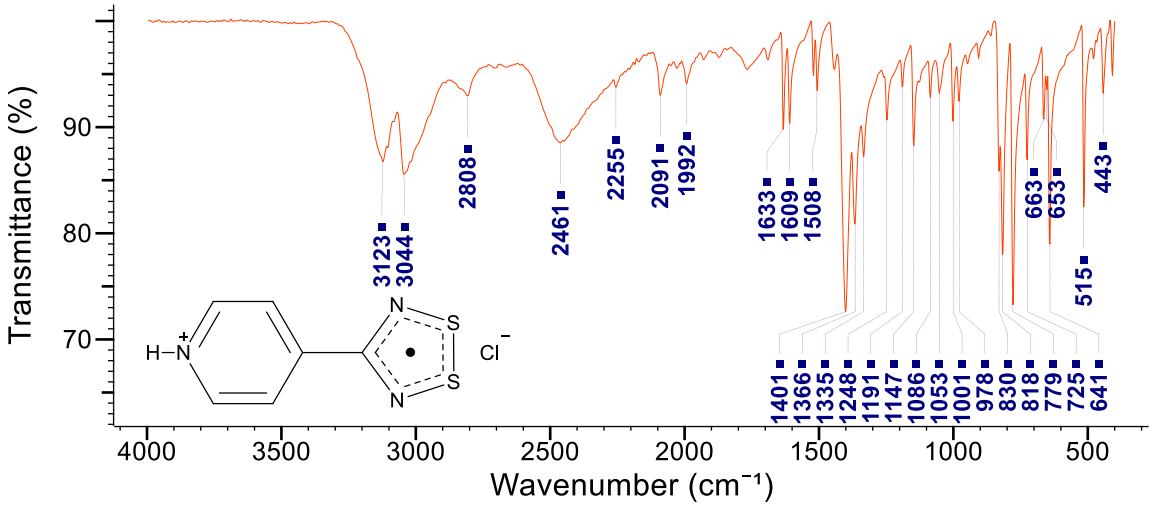

Figure B.1: IR spectrum (400 – 4000 cm^{-1}) of the charged pyrDTDA radical **4**.

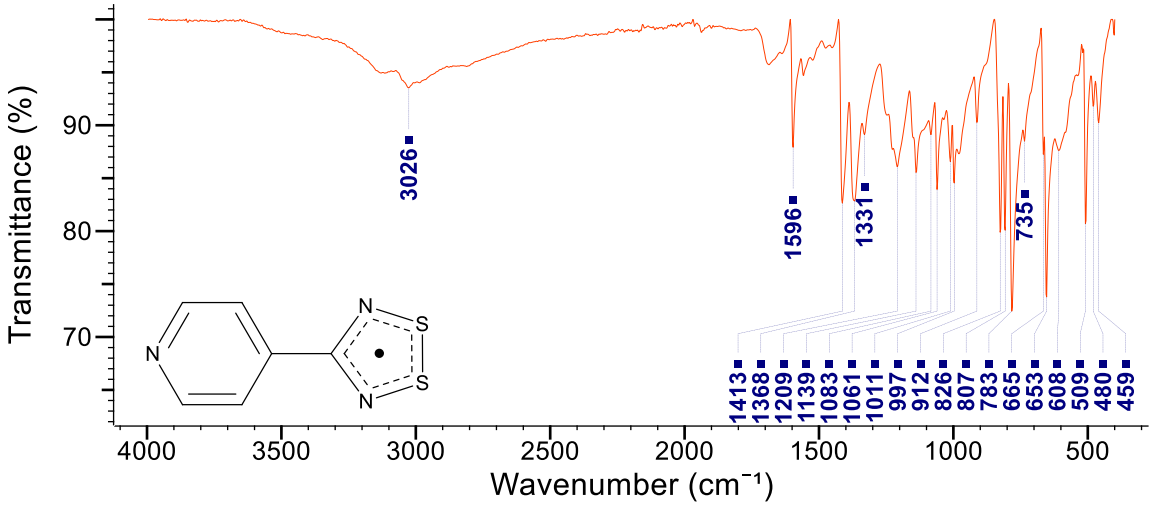

Figure B.2: IR spectrum (400 – 4000 cm^{-1}) of the neutral pyrDTDA radical **5**.

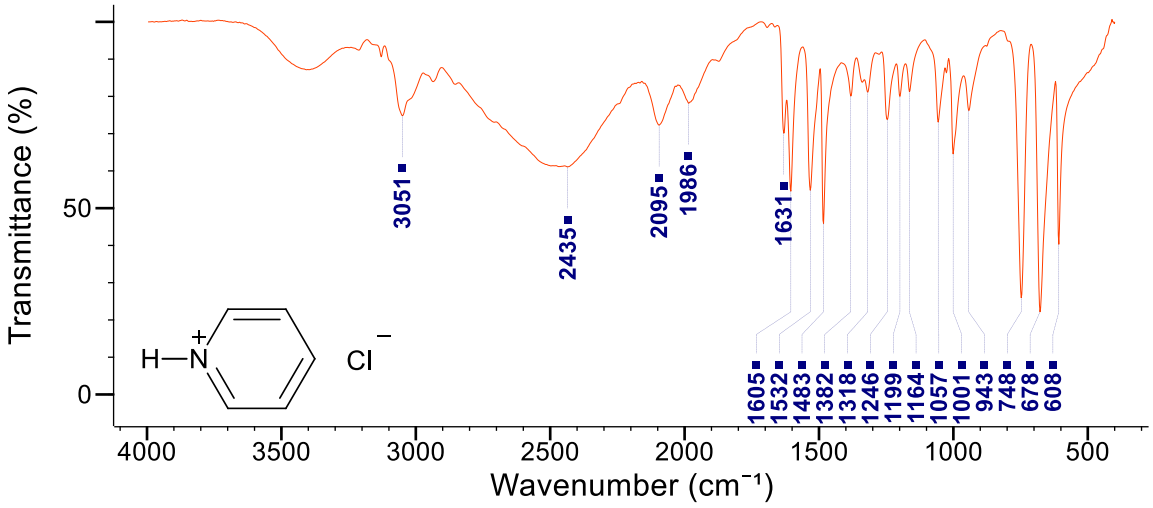

Figure B.3: IR spectrum (400 – 4000 cm^{-1}) of pyridine hydrochloride.

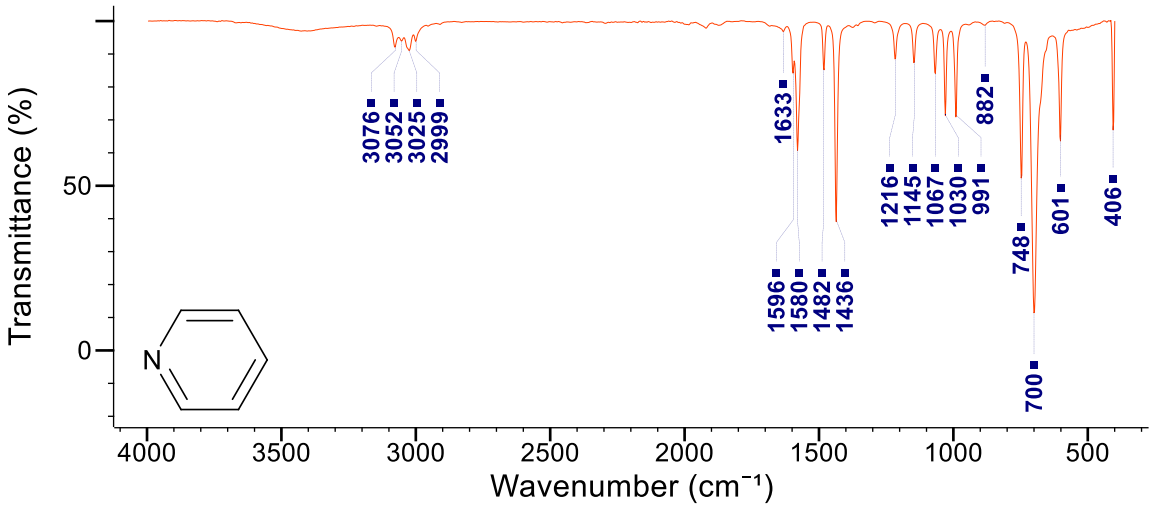

Figure B.4: IR spectrum (400 – 4000 cm^{-1}) of pyridine.

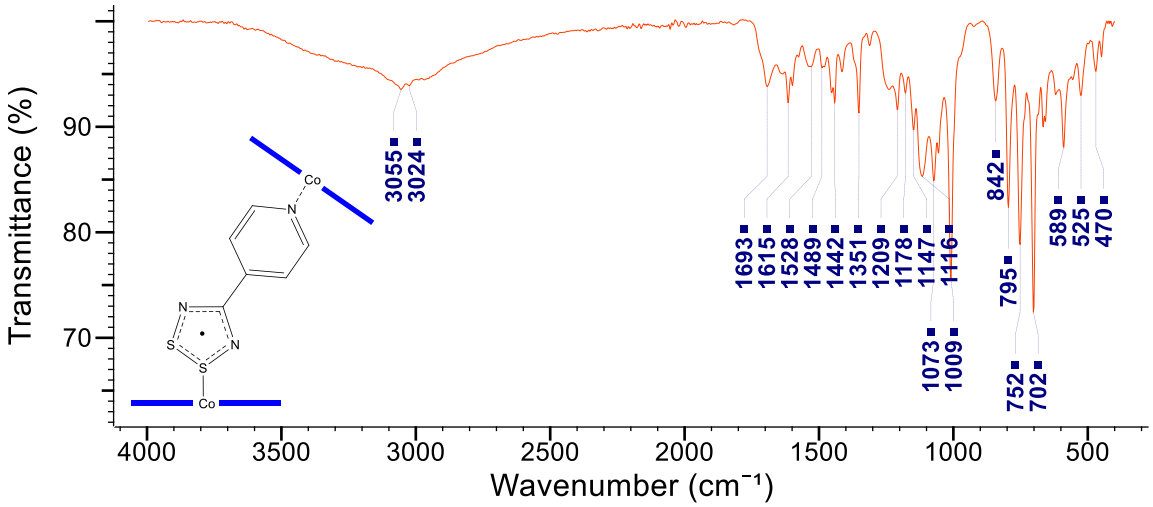

Figure B.5: IR spectrum (400 – 4000 cm^{-1}) of the CP.

B.1.2 Mass Spectrometry

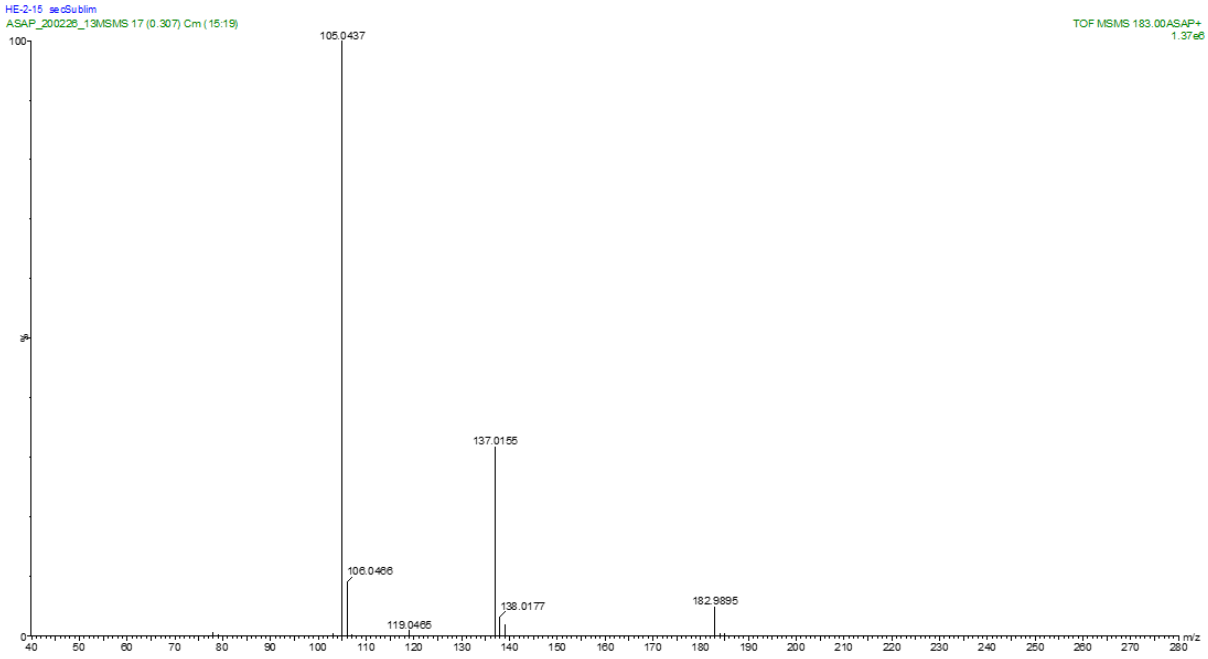

Figure B.6: Tandem mass analysis (MS/MS) of the charged pyrDTDA **4**.

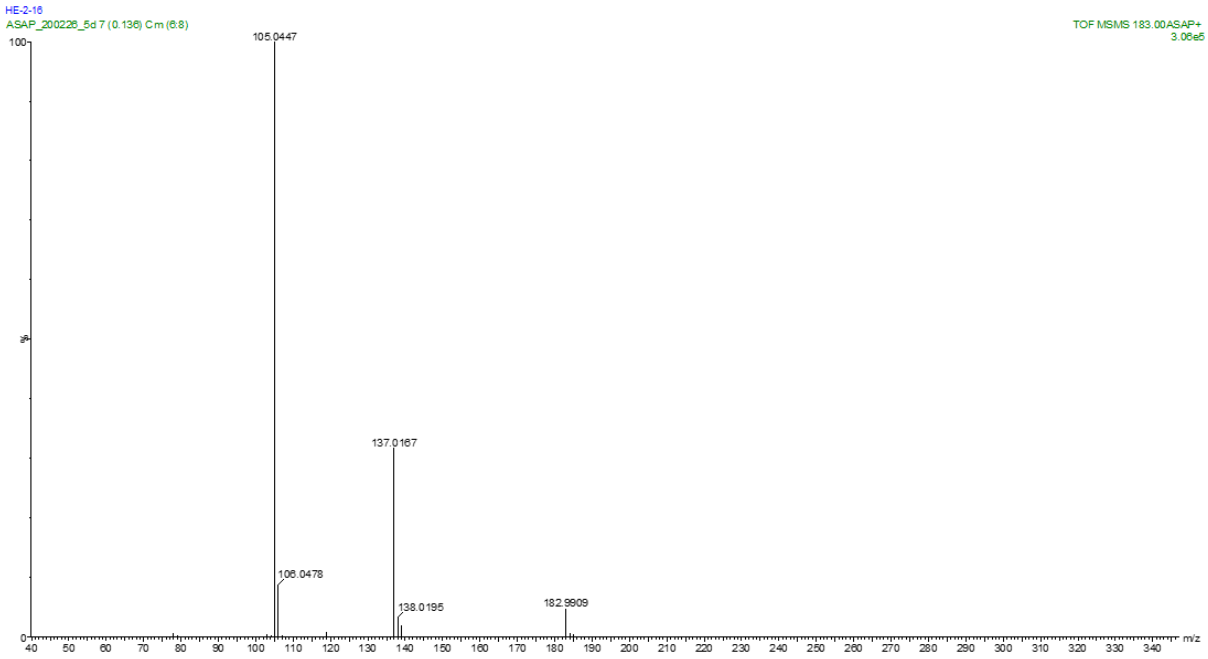

Figure B.7: Tandem mass analysis (MS/MS) of the neutral pyrDTDA radical **5**.

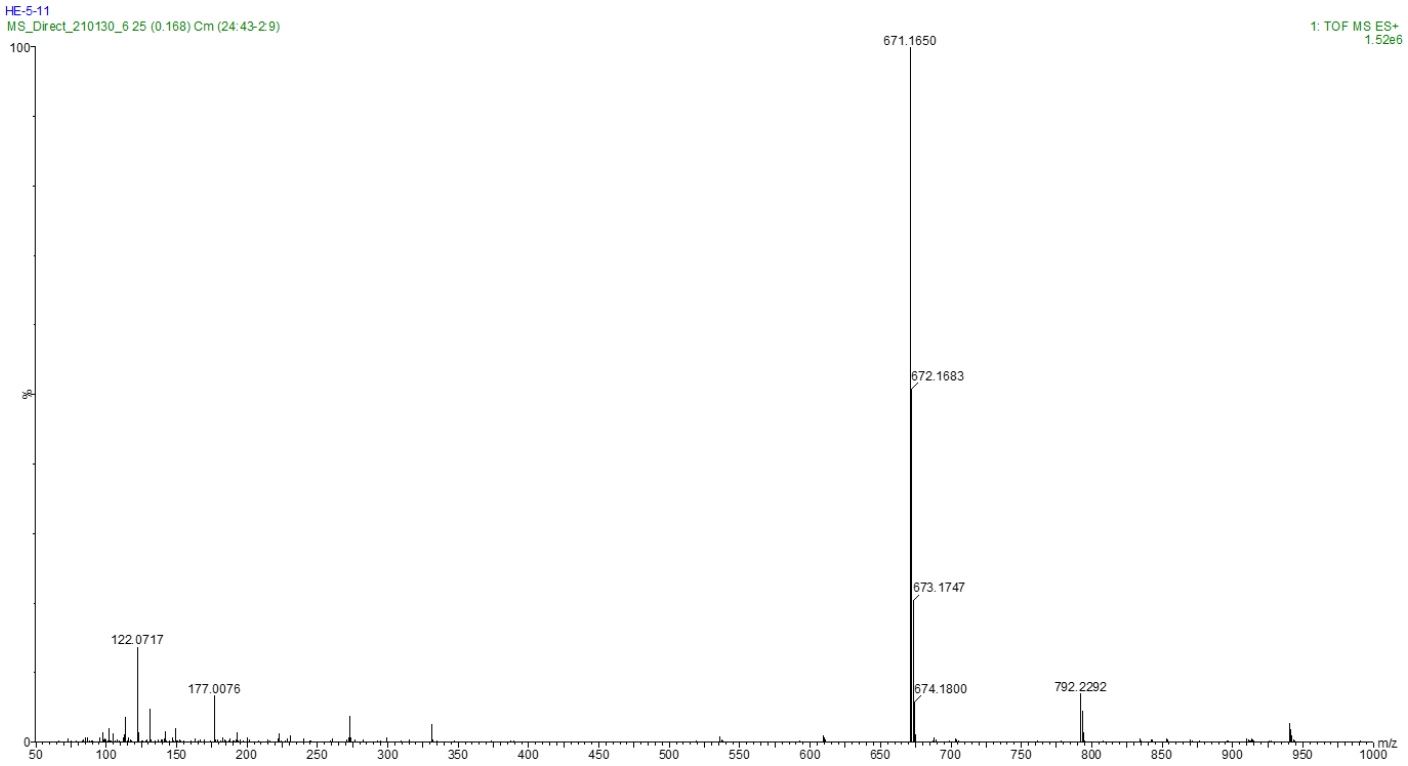

Figure B.8: Mass spectrum of the CP (charged pyrDTDA **4** preparation).

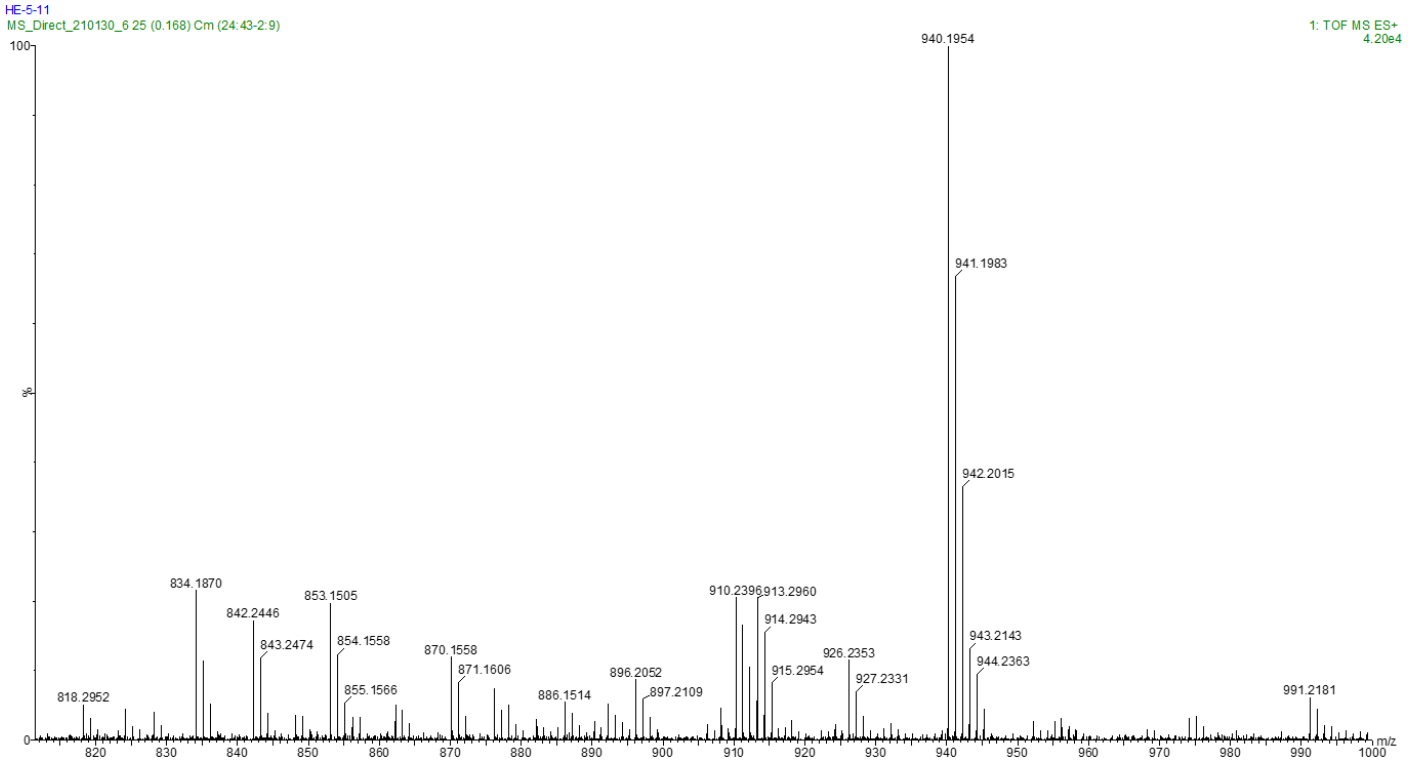

Figure B.9: Mass spectrum of the CP (charged pyrDTDA **4** preparation) in the range of 810 - 1000 m/z.

Figure B.10: Mass spectrum of the CP (neutral pyrDTDA radical **5** preparation).

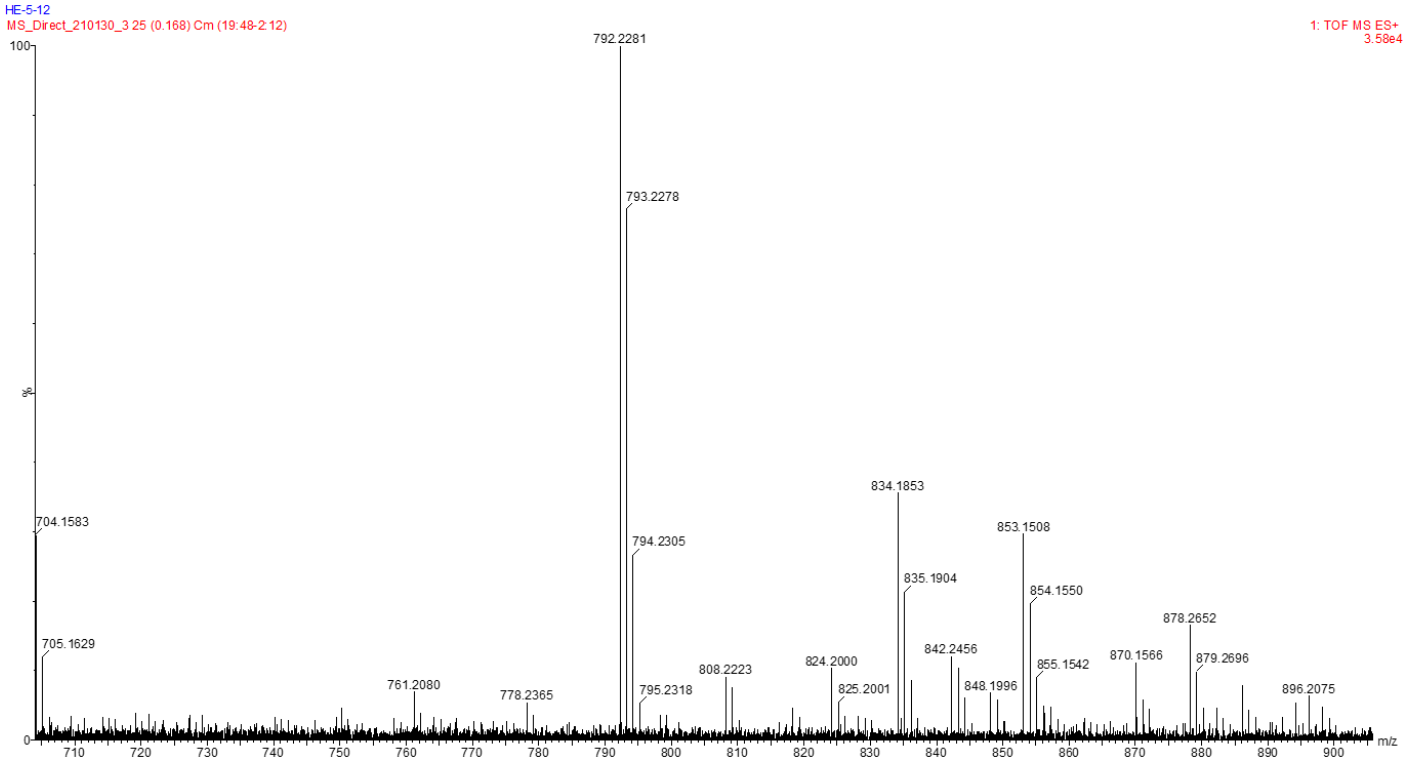

Figure B.11: Mass spectrum of the CP (neutral pyrDTDA **5** preparation) in the range 700 - 900 m/z.

B.1.3 Nuclear Magnetic Resonance (NMR) Spectroscopy

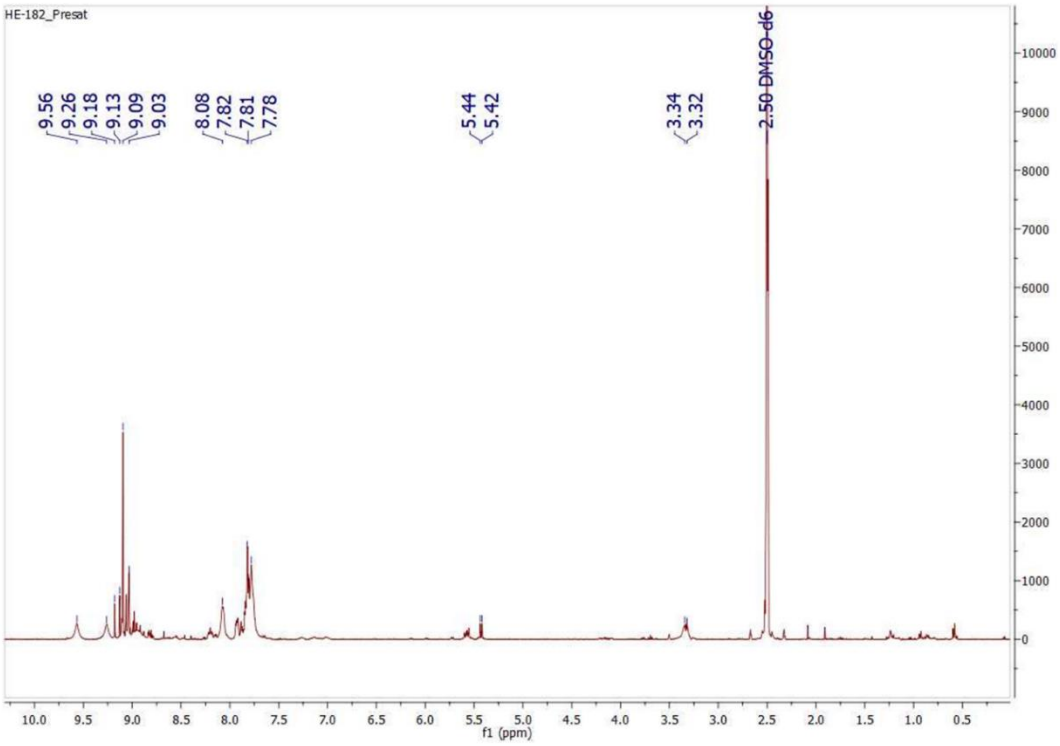

Figure B.12: NMR spectrum of CP (pyrDTDA radical **4** used in preparation).

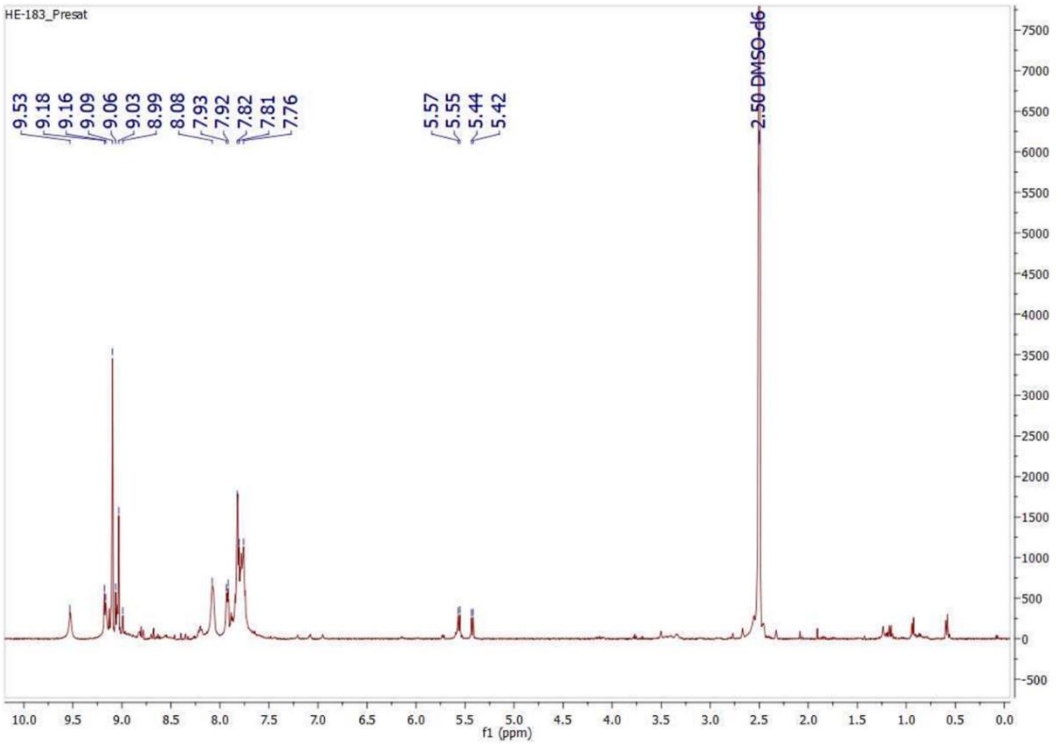

Figure B.13:NMR spectrum of CP (pyrDTDA radical **5** used in preparation).

B.1.4 UV-Vis spectroscopy

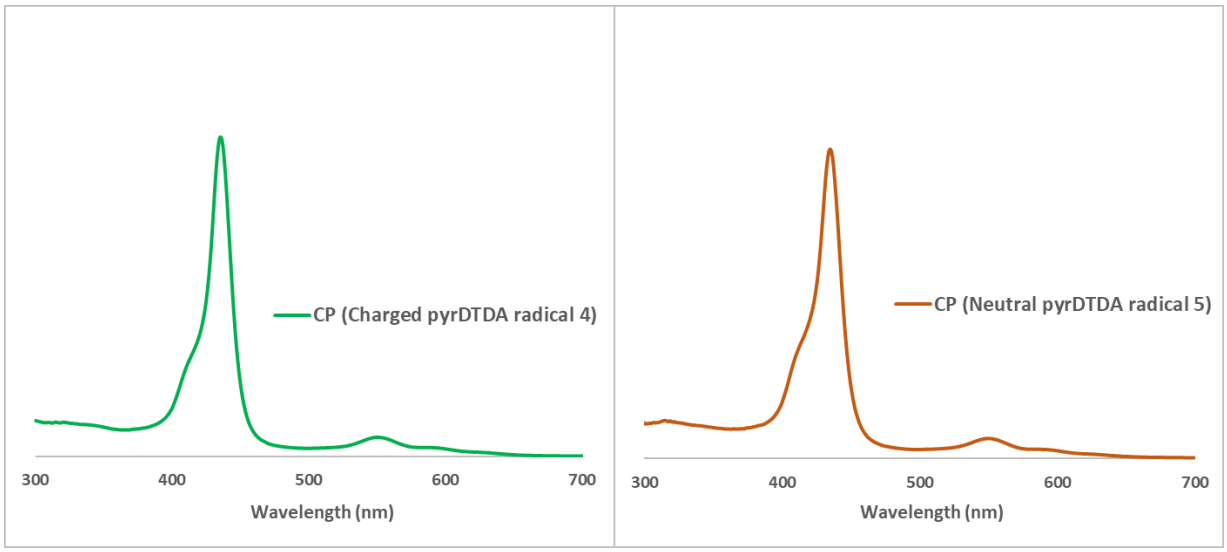

Figure B.14: UV-Vis spectra of the CP (DMSO). Spectrum in green designates the CP synthesized with the charged pyrDTDA radical **4**, whereas the spectrum in brown refers to the CP synthesized with the neutral pyrDTDA radical **5**.

B.2 Chapter 3

B.2.1 UV-Vis spectroscopy

For the UV-Vis spectra of TPP and CoTPP, see Chapter 1. The spectra of the remaining porphyrin catalysts will be presented here. All spectra were recorded at room temperature in DCM, except for the CP, which was done in DMSO.

Figure B.15 illustrate the spectrum of CoTPP-Cl. The soret band shift slightly to a shorter wavelength (~ 407 nm), while the Q-band becomes broad and also shifts to ~543 nm.[1,2]

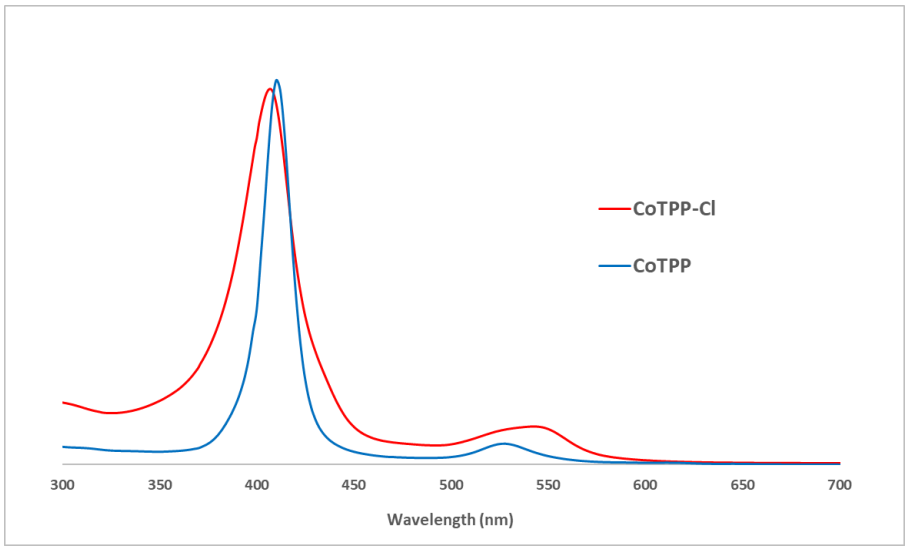

Figure B.15: UV-vis spectrum of CoTPP-Cl, with the spectrum of CoTPP overlayed for comparison.

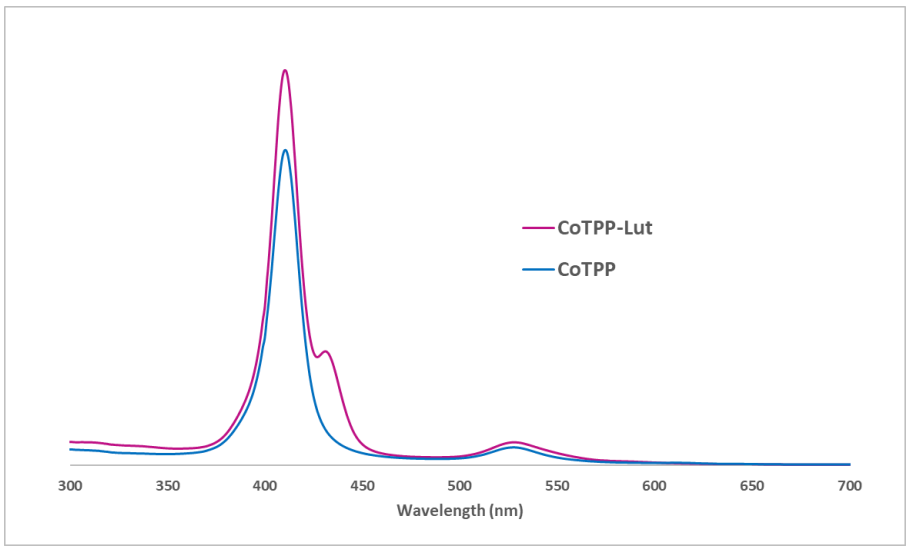

Figure B.16: UV-vis spectrum of CoTPP-Lut (purple) overlayed by CoTPP (blue) for comparison.

B.2.2 Powder X-ray diffraction patterns

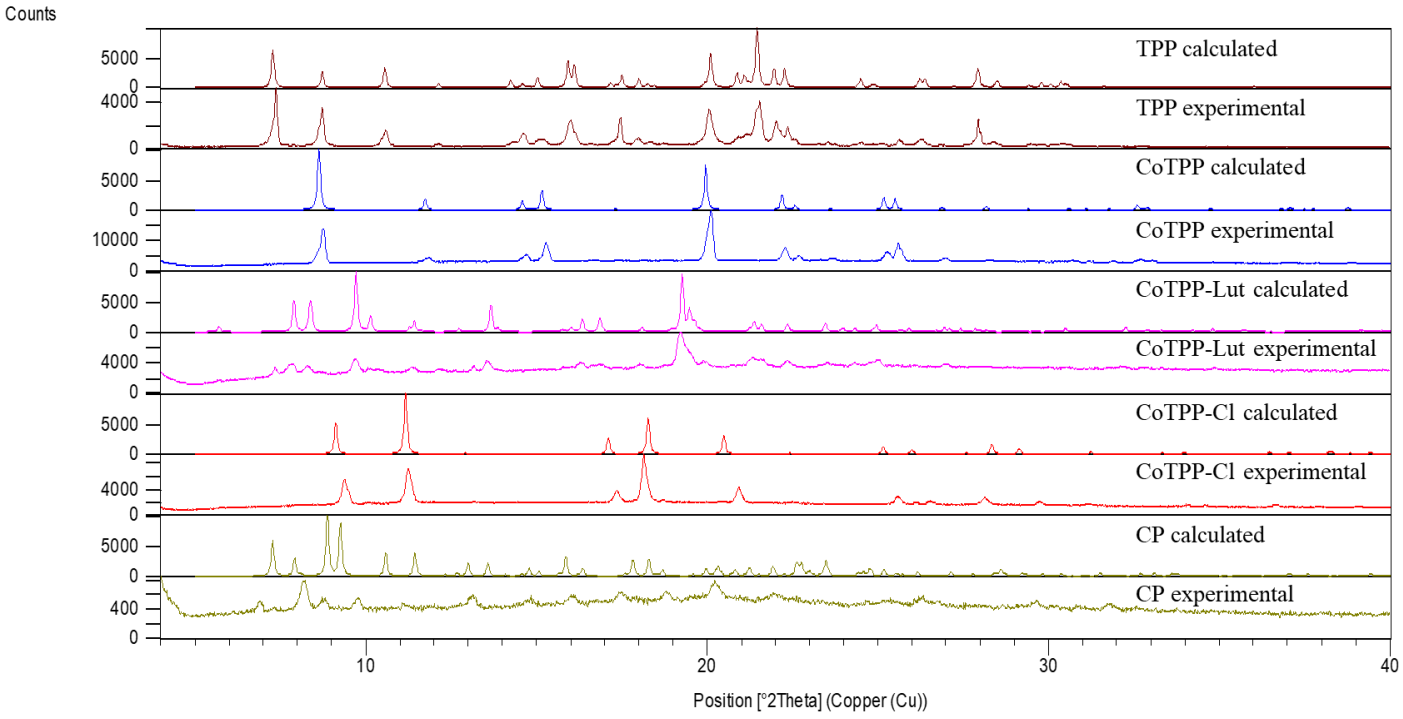

Figure B.17: PXRD patterns of the porphyrin catalysts used in this study, and for comparison, the calculated patterns are included.

B.2.3 IR spectroscopy

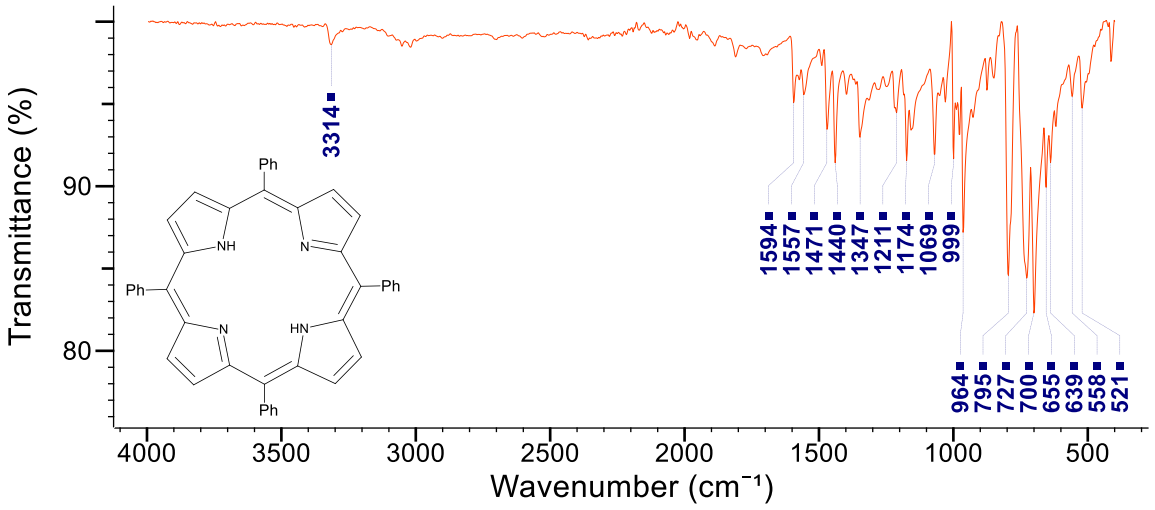

Figure B.18: IR spectrum (400 – 4000 cm^{-1}) of TPP.

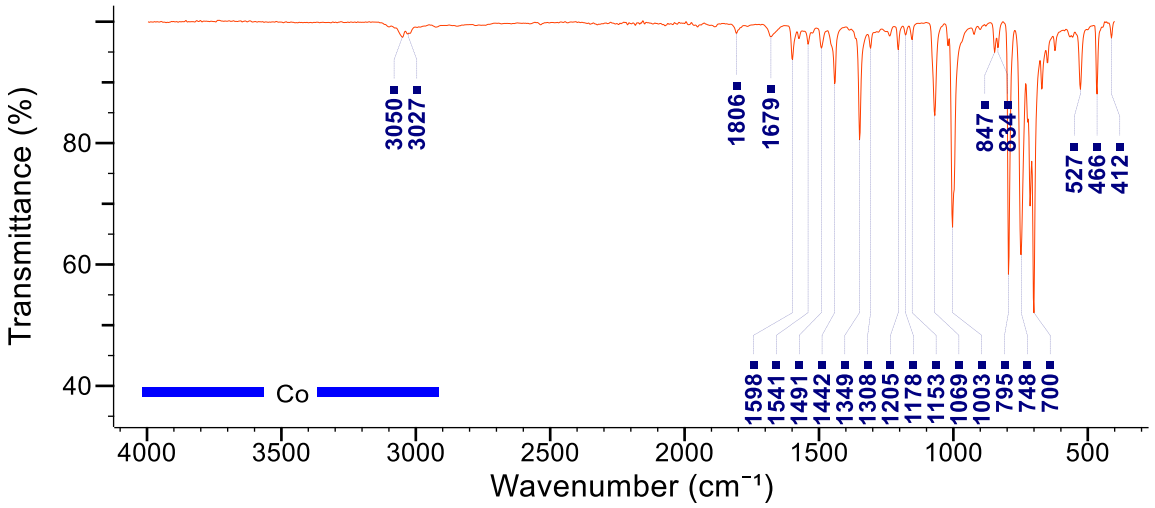

Figure B.19: IR spectrum (400 – 4000 cm^{-1}) of CoTPP.

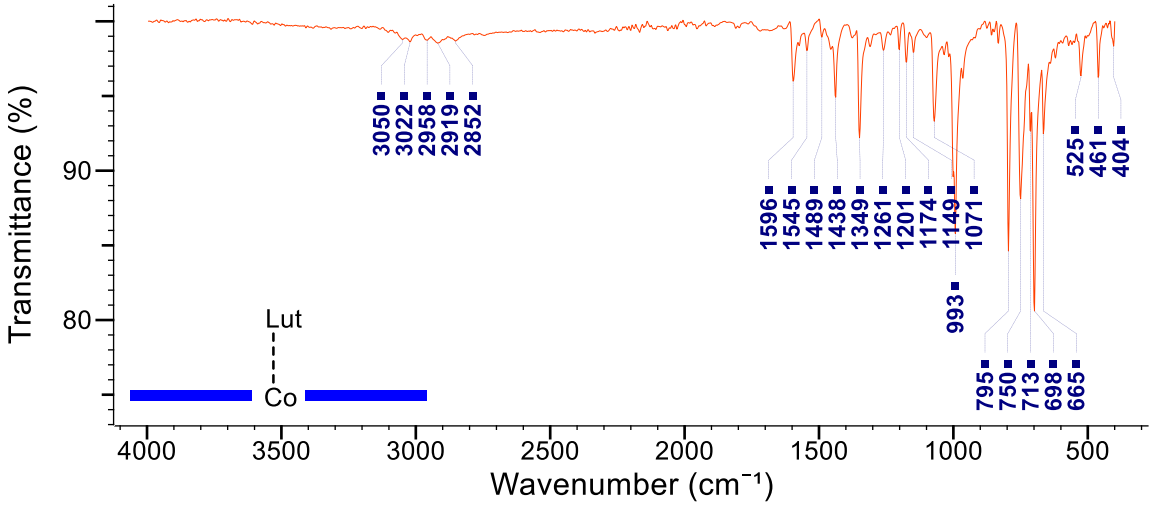

Figure B.20: IR spectrum (400 – 4000 cm^{-1}) of CoTPP-Lut.

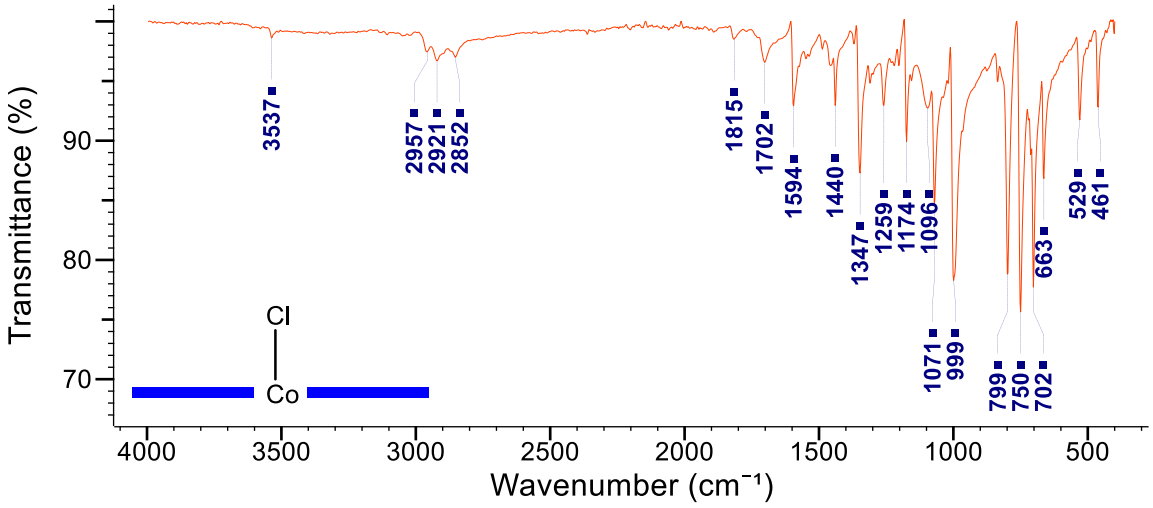

Figure B.21: IR spectrum (400 – 4000 cm^{-1}) of CoTPP-Cl.

B.2.4 NMR spectroscopy

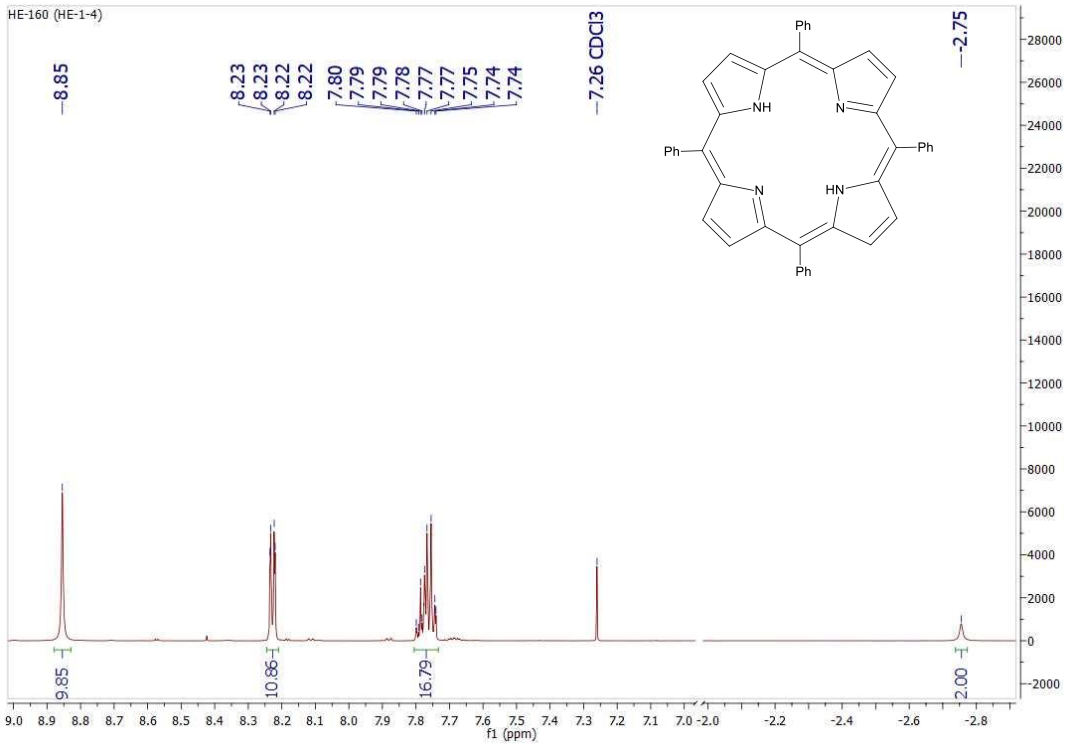

Figure B.22: NMR spectrum of TPP.

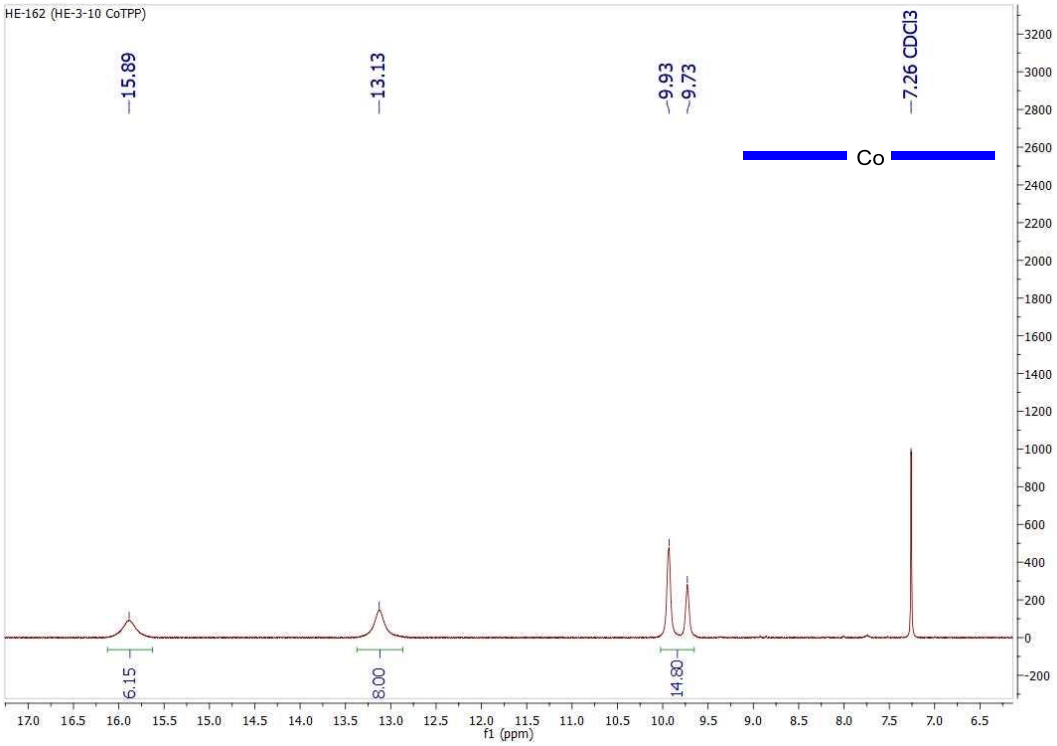

Figure B.23: NMR spectrum of CoTPP.

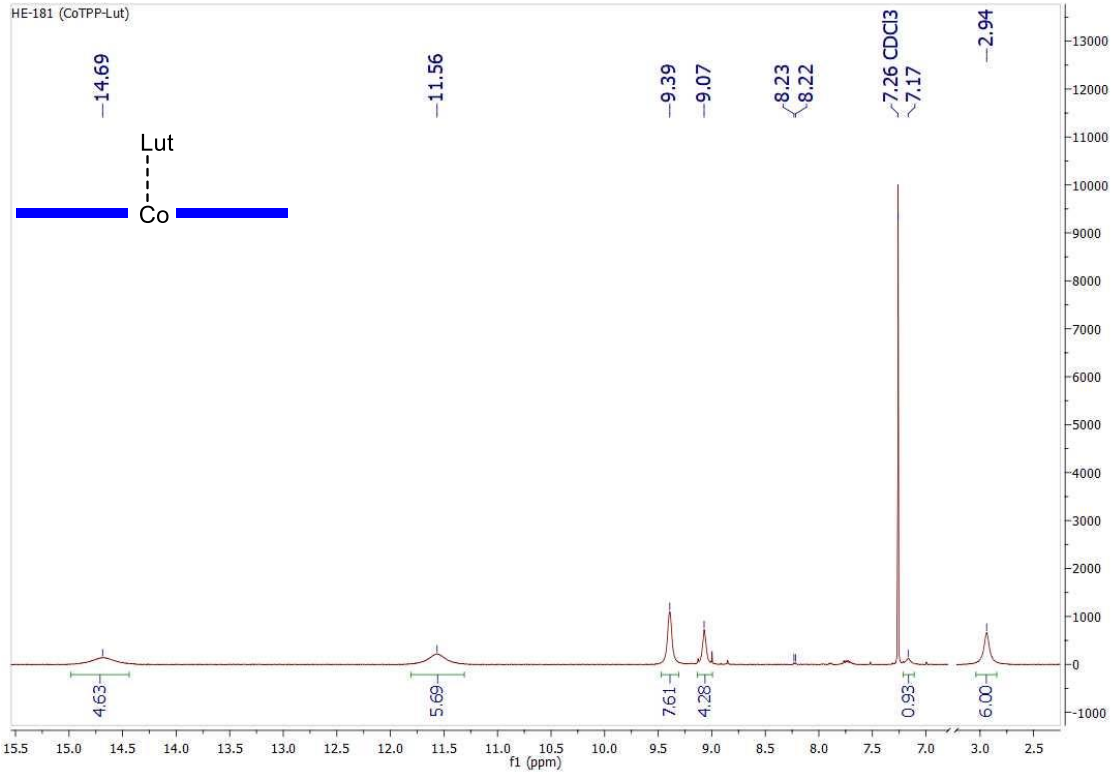

Figure B.24: NMR spectrum of CoTPP-Lut.

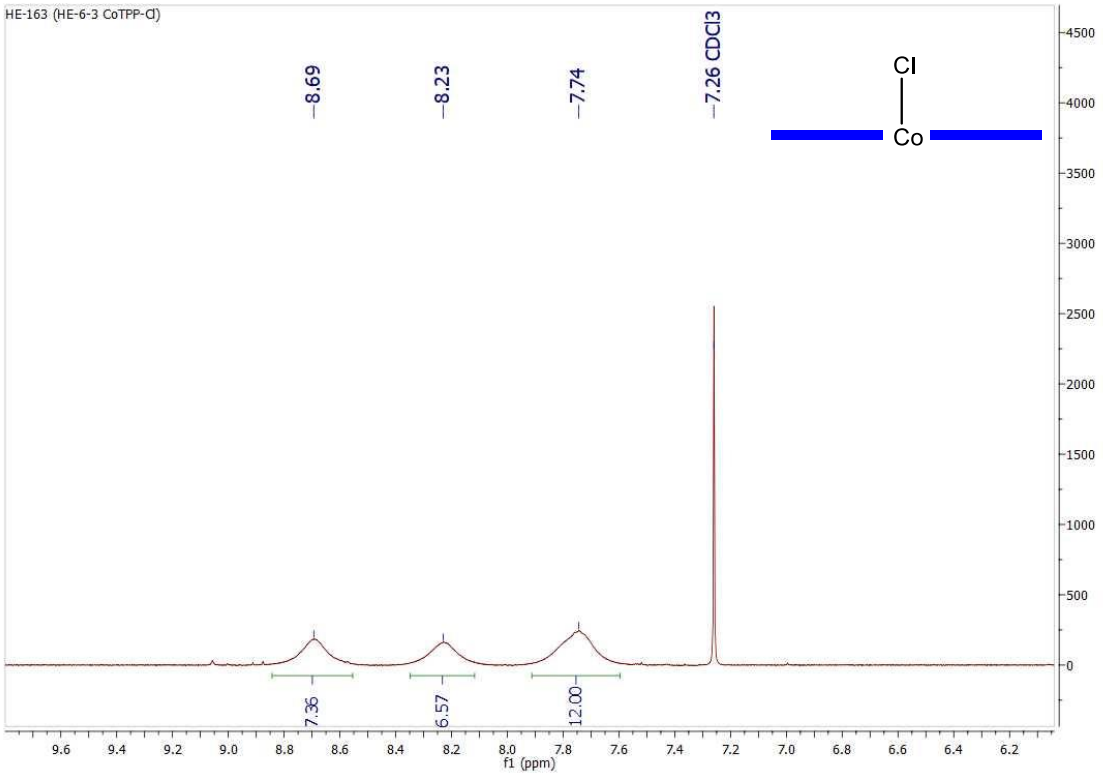

Figure B.25: NMR spectrum of CoTPP-Cl.

B.2.5 Mass spectrometry

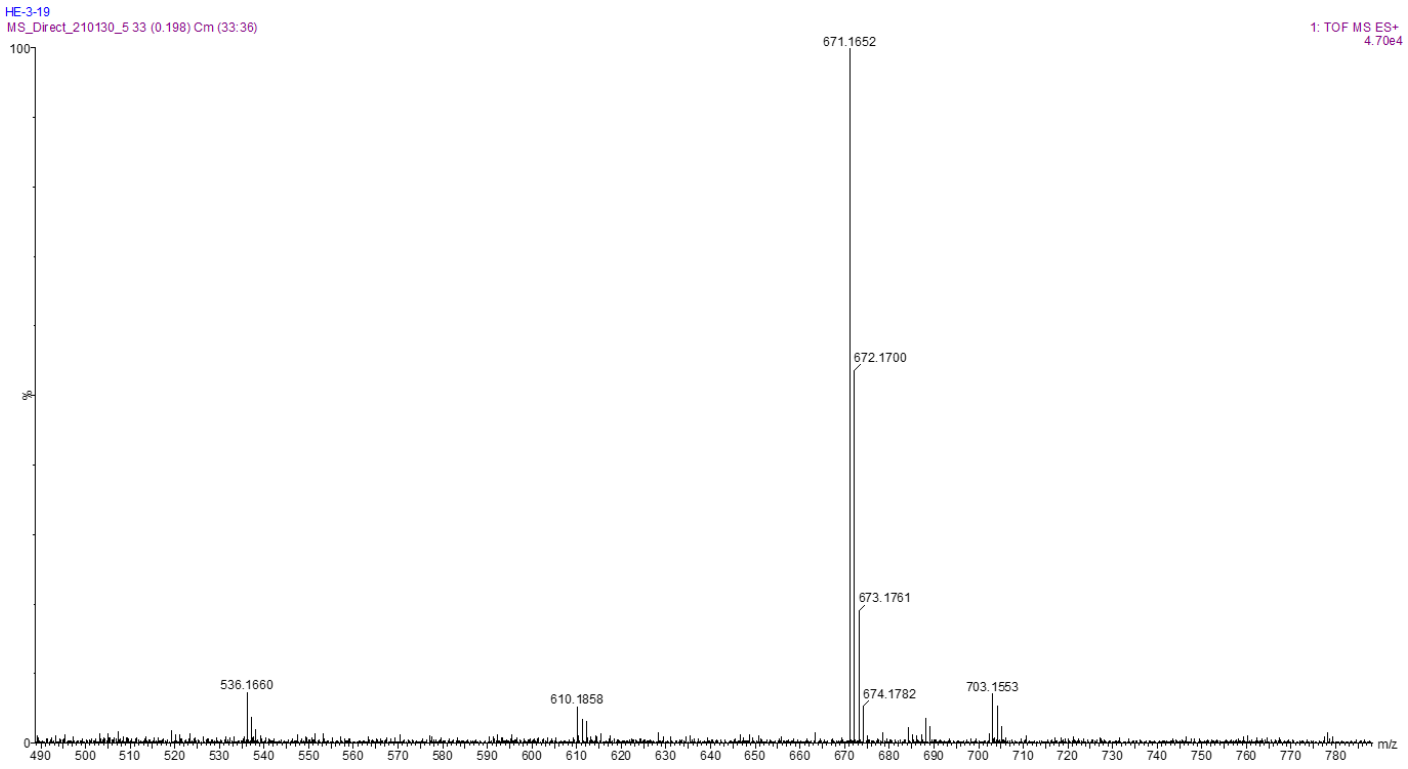

Figure B.26: Mass spectrum of CoTPP.

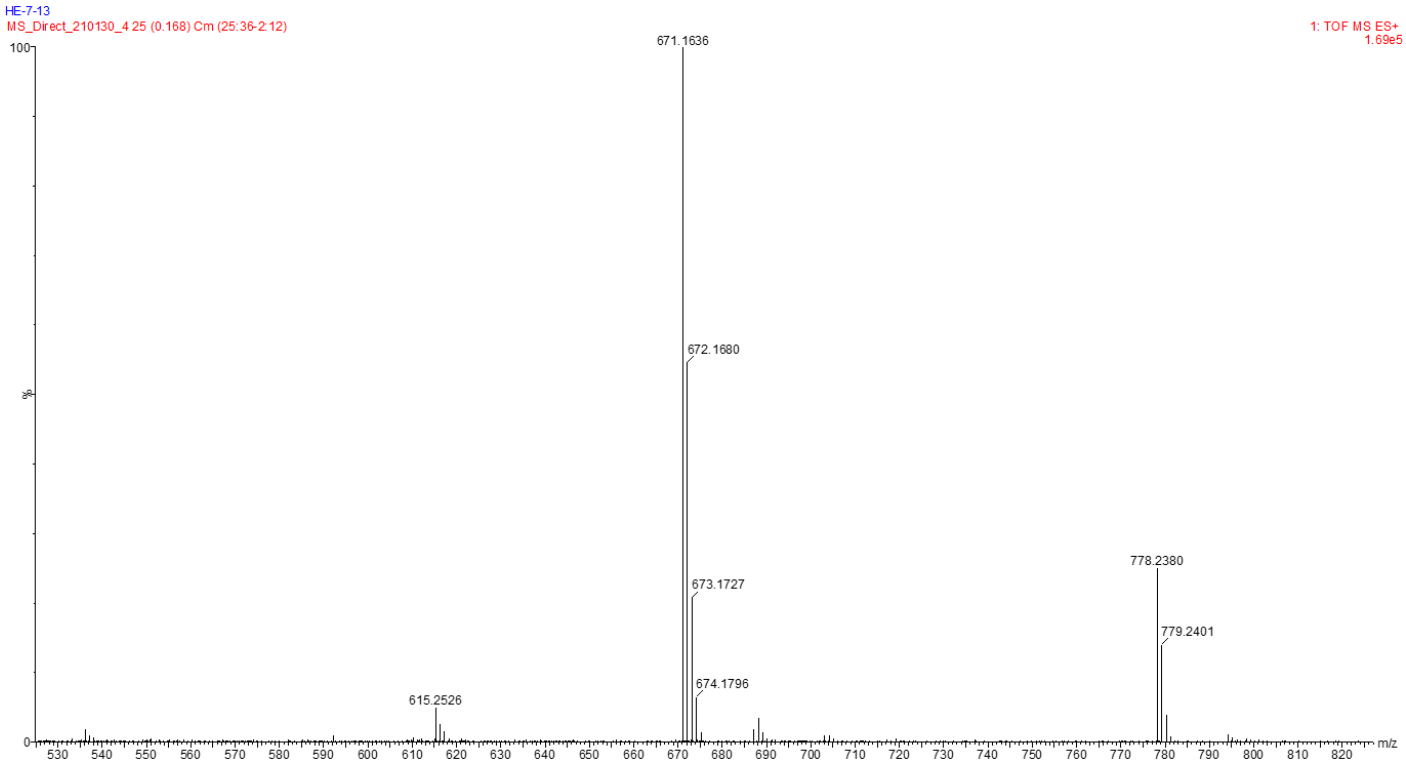

Figure B.27: Mass spectrum of CoTPP-Lut.

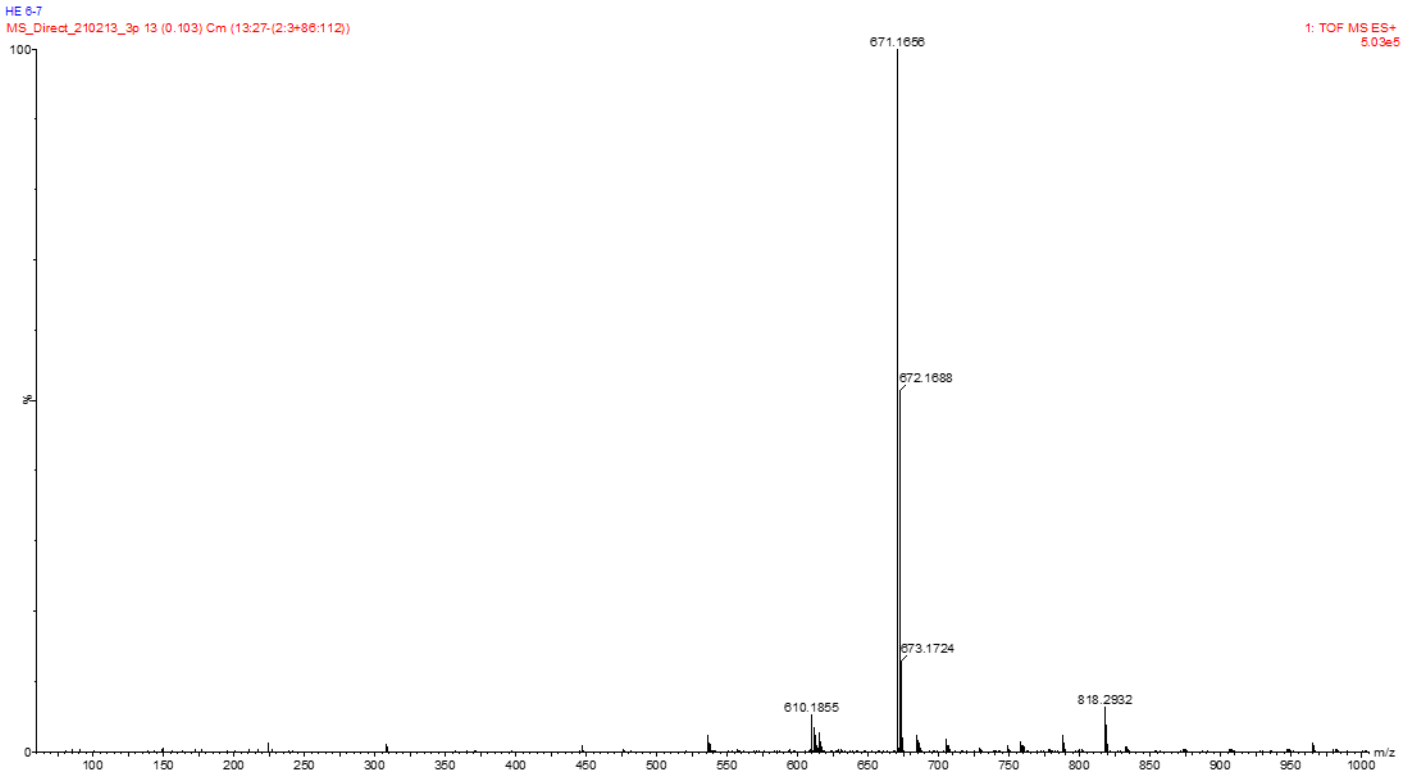

Figure B.28: Mass spectrum of CoTPP-Cl.

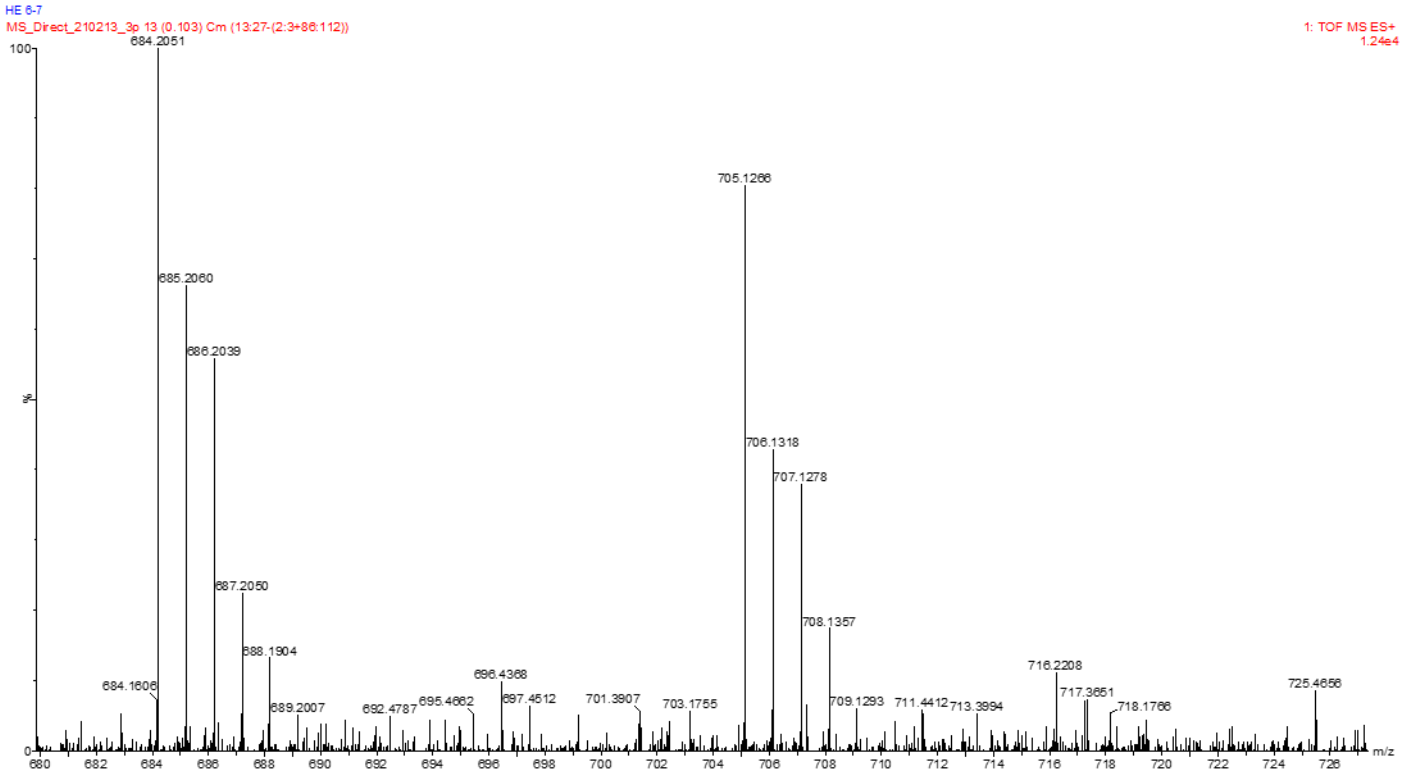

Figure B.29: Mass spectrum of CoTPP-Cl in the range 680 - 730 m/z.

B.2.6 Solution catalysis data

Table B.1: Solution catalysis data. Data that were accumulated at the optimized reaction conditions: 0.5 mmol benzyl alcohol, 1 mmol TBHP, 70 °C, 16 h, MeCN.

Entry	Catalyst	Catalyst loading (mol%)	Conversion (%)	Product selectivity (%)	
				Benzaldehyde	Benzoic acid
1	No catalyst - control		66	49	51
2			58	56	44
3	CoTPP	0.5	75	38	62
4			77	36	64
5		1.0	73	43	57

Entry	Catalyst	Catalyst loading (mol%)	Conversion (%)	Product selectivity (%)	
				Benzaldehyde	Benzoic acid
6			80	31	69
7		1.5	76	39	61
8			81	32	68
9	CoTPP-Lut	0.5	73	42	58
10			74	41	59
11		1.0	73	41	59
12			73	43	57
13		1.5	78	37	63
14			77	39	61

15	CoTPP-Cl	0.5	75	40	60
16			79	33	67
17		1.0	82	32	68
18			82	31	69
19		1.5	87	23	77
20			84	25	75
21	CP	0.5	84	29	71
22			83	31	69
23		1.0	75	40	60
24			76	39	61
25		1.5	75	41	59

B.3 Chapter 4

B.3.1 Mechanochemistry catalysis: Optimization

Table B.2: Mechanochemistry catalysis: Optimization. Reactions carried out with UHP as oxidant without a metal catalyst present. No benzoic acid was detected.

Entry	Oxidant (equiv)	Frequency (rpm)	Reaction time (hr)	LAG (μL/mg)	Conversion (%)
1	1	900	4	0.25	3
2					4
3	1	1200	4	0.25	2
4					3
5	1	1500	4	0.25	4
6					6
7	1	1500	6	0.25	4
8					7
9	1	1500	8	0.25	4
10					4
11	2	1500	4	0.25	7
12					5
13	3	1500	4	0.25	7
14					8
15	3	1500	4	0.50	5
16					6
17	3	1500	4	0.75	7
18					7

B.3.2 Mechanochemistry catalysis: Comparative study.

Table B.3: Mechanochemistry catalysis: Comparative study of Co-porphyrin catalysts. Reactions were carried out at the optimized reaction conditions: 0.5 mmol benzyl alcohol, 1.5 mmol UHP, 1500 rpm, 4 h, 0.25 µL/mg (LAG).

Entry	Catalyst	Catalyst loading (mol%)	Conversion (%)	Product selectivity (%)	
				Benzaldehyde	Benzoic acid
1	CoTPP	0.5	7	100	0
2			5	100	0
3		1.0	6	59	41
4			9	53	47
5		1.5	8	41	59
6			6	43	57
7	CoTPP-Cl	0.5	6	100	0
8			7	100	0
9		1.0	7	100	0
10			4	100	0
11		1.5	6	62	38
12			7	67	33
13	CoTPP-Lut	0.5	6	100	0
14			6	100	0

B.4 References

1 W. Xia, S. I. Vagin and B. Rieger, *Chem. Eur. J.*, 2014, **20**, 15499–15504.

2 W. Xia, K. A. Salmeia, S. I. Vagin and B. Rieger, *Chem. Eur. J.*, 2015, **21**, 4384–4390.